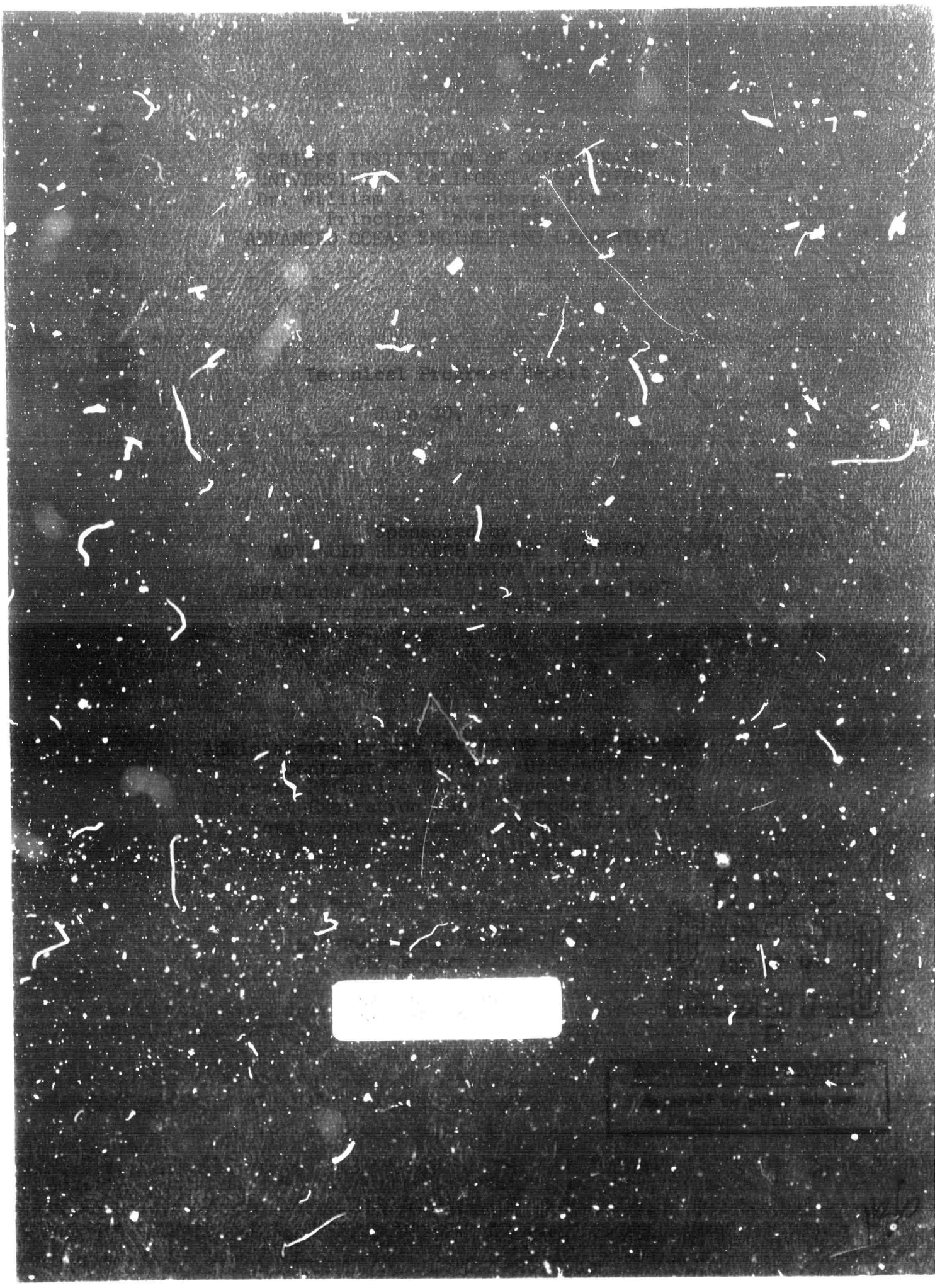

Unclassified

Security Classification

DOCUMENT CONTROL DATA - R & D

(Security classification of title, body of abstract and indexing annotation must be entered when the overall report is classified)

1. ORIGINATING ACTIVITY (Corporate author) The Regents of the University of California University of California, San Diego La Jolla, California 92037	2a. REPORT SECURITY CLASSIFICATION Unclassified 2b. GROUP Not Applicable

3. REPORT TITLE

Technical Progress Report
Advanced Ocean Engineering Laboratory

4. DESCRIPTIVE NOTES (Type of report and inclusive dates) January 1, 1971 to June 30, 1971	Dr. William A. Prothero
5. AUTHOR(S) (First name, middle initial, last name) Dr. William A. Nierenberg Dr. Fred N. Spiess Dr. Walter H. Munk Dr. Robert D. Moore	Dr. Hugh Bradner Prof. John D. Isaacs Dr. Douglas L. Inman Dr. William G. Van Dorn

6. REPORT DATE June 30, 1971	7a. TOTAL NO. OF PAGES 137	7b. NO. OF REFS 22
8a. CONTRACT OR GRANT NO. N00014-69-A-0200-6012 b. PROJECT NO. c. d.	9a. ORIGINATOR'S REPORT NUMBER(S) SIO Reference No. 71-22 9b. OTHER REPORT NO(S) (Any other numbers that may be assigned this report) AOEL Report # 23	

10. DISTRIBUTION STATEMENT

Distribution of this document is unlimited

11. SUPPLEMENTARY NOTES	12. SPONSORING MILITARY ACTIVITY Advanced Research Projects Agency c/o Office of Naval Research Arlington, Virginia 22217

13. ABSTRACT

This annual report reflects the technical status of projects conducted within the Advanced Ocean Engineering Laboratory at the Scripps Institution of Oceanography. These projects are: (1) Stable Floating Platform - to conceive, design, build and demonstrate the feasibility of large stable floating platforms in the open sea. (2) Benthic Array - a program to develop and construct a quartz vertical accelerometer appropriately packaged and adapted for long term ocean bottom or perhaps sub-bottom use. (3) Overpressures Due to Earthquakes a study of earthquakes, seaquakes and resultant overpressures as they may effect subsurface vehicles and structures. (4) Advanced Studies in Nearshore Engineering - field studies of the water-sediment interface under wave action in and near the breaker zone; and laboratory investigation of the velocity field of breaking waves. (5) Electromagnetic Roughness of the Ocean Surface - utilization of radio signals scattered from the sea surface to determine the directional spectrum of ocean waves.

DD FORM 1473 (PAGE 1)

0102-014-6600

Unclassified

Security Classification

14. KEY WORDS	LINK A		LINK B		LINK C	
	ROLE	WT	ROLE	WT	ROLE	WT
Advanced Ocean Engineering						
Stable Floating Platform						
FLIP						
Postensioned concrete						
Benthic Array						
Quartz Vertical Accelerometer						
Digital Data Logging System						
Oceanbottom Seismometer						
Acoustic Command and Control System						
SQUIB Explosive Cable Cutter						
Voltage to Frequency Converter						
Nearshore Engineering						
Crater-Sink Sand Transfer System						
Water-Sediment Interface						
Breaking Waves						
Quartz Hot-Film Velocity Probes						
Hot-Film Anenometers						
Digital Wave Staff						
Vortex-sublayer						
Electromagnetic Flowmeter						
Electromagnetic Roughness of the Ocean Surface						
Radar Cross Section						
Ocean Wave Spectrum						
Overpressures Due to Earthquakes						
Earthquakes						
Seaquakes						
Seismic Activity						

Disclaimer

The views and conclusions contained in this document are those of the authors and should not be interpreted as necessarily representing the official policies, either expressed or implied, of the Advanced Research Projects Agency or the U. S. Government

Advanced Ocean Engineering Laboratory

Technical Progress Report

Table of Contents

Part I

STABLE FLOATING PLATFORM

Principal Investigator
Dr. Fred N. Spiess
Phone (714) 453-2000, Extension 2476

ADVANCED OCEAN ENGINEERING LABORATORY
Sponsored by
ADVANCED RESEARCH PROJECTS AGENCY
ADVANCED ENGINEERING DIVISION

ONR Contract N00014-69-A-0200-6012

Part I

Stable Floating Platform

Table of Contents

List of Figures

I. Project Summary

The Stable Floating Platform Program was initiated for the purpose of advancing the technology by designing, building, and demonstrating the feasibility of large stable floating platforms in the open sea.

During the prior reporting periods, efforts involved the exploration of a number of ocean platform concepts. Before the end of 1970 a general configuration for the platform was selected and broad design specifications were set forth.

Now, the preliminary design study has been essentially completed. A subcontract for the design of the platform has been awarded to the naval architectual firm of L. R. Glosten and Associates, Inc. A review of the design concepts was held during June 1971 (see detailed report) and activities are now directed towards the preparation of the final design and specifications.

The basic concept will be comprised of a four-legged platform made up at sea from two two-legged modules, each module consisting of a pair of FLIP-type legs rigidly connected to each other and supporting a superstructure platform on a trunnion so that it (the platform) remains essentially horizontal as the legs are changed from the horizontal to the vertical attitude.

The design package for bidding purposes will be completed during the next reporting period with contract award for the construction due in January or February 1972.

II. Technical Report

A. History - The Stable Floating Platform design work until late in 1970 involved the exploration of a number of ocean platform concepts. In November 1970, a general configuration

for the platform was selected and broad design specifications were set forth. The preliminary design study is now essentially completed.

B. Design Review - A design review and critique of the Stable Floating Platform Program was held at Scripps Institution of Oceanography on June 8 and 9, 1971. Selected to serve on the panel were members with expertise in the fields of naval architecture, structures, concrete, and marine engineering. The program history, concepts, and design were presented by Scripps personnel and the Scripps' contracted naval architect along with his associates for concrete and mechanics. The review panel members were:

Mr. J.N. Donhaiser	Private Consulting Engineer	Structures and Sea Operations
Dr. C.E. Grosch	ARPA Consultant	Hydrodynamics
Dr. L.R. Hafstad	Vice President-Research, General Motors, (Retired)	General Science & Engineering
Prof. P. Mandel	Massachusetts Institute of Technology	Naval Architect
Prof. D. Pirtz	University of California Berkeley	Concrete Specialist
Admiral C.D. Wheelock	USN (Retired)	Naval Architect

A report on this review and critique is currently being prepared and will be published in the near future.

C. Design Specifications

1. The basic concept would comprise a four-legged platform (Figure 1) made up at sea from two two-legged modules, each module consisting of a pair of FLIP-type legs rigidly connected to each

other and supporting a superstructure platform on a trunnion so that it remains essentially level as the legs are changed from the horizontal to the vertical attitude.

2. Draft on station to be about 280 feet.
3. Overall breadth to be 100 feet.
4. Module "pitch" (distance between pairs of legs) to be about 100 feet.
5. Total payload for complete platform to be 500 tons. Payload to include all scientific equipment but not the basic ship machinery, outfit, and "hotel" equipment.
6. Total cost of two modules and connection devices not to exceed $4,000,000. The cost consideration has been considered to be overriding. It has been recognized as being extremely tight and restrictive on the one hand, but of value in demanding engineering discipline on the other.
7. Platform to have a capability of operating with 40-foot clearance above still water to permit the passage of an 80-foot wave.

D. Use of Concrete for Leg Structure - In addition to the specifications listed, it was understood that the already established objective of using postensioned concrete to the greatest extent possible as the structural material for the legs would prevail.

At the beginning of the preliminary design study, certain specific and challenging engineering problems were recognized:

1. The optimization of leg size and proportions.
2. The design of a linkage system to connect the modules.
3. The design of the superstructure trunnion bearings.

4. The calculation of responses of the platform modules to sea conditions in both horizontal and vertical modes.

E. Design Responsibility - In approaching these problems, it was recognized that expertise was needed in addition to that within Scripps and at L. R. Glosten & Associates, Inc. Accordingly, the firm of Skilling, Helle, Christiansen, Robertson was retained as a consultant in concrete technology and structures, and the firm of Harold West was retained as a consultant in mechanical engineering.

Scripps Institution has continued to provide the expertise with regard to the ocean environment and has continued under the direction of Dr. P. Rudnick to make the analyses of responses, forces, and moments.

F. Design Considerations - The first of the problems to be attacked was the optimization of leg size and proportions. Given the past experience with FLIP, it might be expected that this question could be quickly disposed of. However, always bearing in mind the overriding constrainst of our monetary budget, it was found that as compared to FLIP, the following factors complicated the problem:

1. The use of concrete resulted in a weight of primary structure roughly twice as great as could be achieved using steel.
2. The combined weight of payload and superstructure was large.
3. The center of gravity of the combined superstructure and payload was quite high above the waterline in the vertical mode.

The functional requirements of the legs in the vertical mode are in conflict with the necessity that they operate as a catamaran hull

while travelling across the ocean in the horizontal mode. The desired vertical characteristics of motion stability and resistance to external heeling forces would indicate a relatively long slender leg with a concentration of solid ballast in the bottom. When travelling in the horizontal mode the legs must be able to resist the longitudinal bending moments and torsions imposed by waves, and here great length and concentrated ballast tend to increase the loads while slenderness decreases the ability to resist them. The weight of the concrete structure limits the extent to which liquid ballast can be used to modify loads or increased structure can be provided to absorb them.

The design process has consisted of examining various combinations of drafts, diameters, diameter ratios, and shoulder heights within limits established on the one hand by the Scripps computer analyses of motion, and on the other by engineering feasibility within the budget. A major breakthrough to the solution of this problem came with the development, at a design conference at Scripps, of the concept of two operating drafts and movable solid ballast. Even with the easing of the structural problem which the movable ballast provides, it has been necessary to modify the cross sectional shape of the legs to increase the section modulus.

The design of suitable trunnion bearings posed technical problems, not so much because of the great size of the journal or the magnitude of the loads, but because the bearings will be loaded for long periods during which the amplitude of motion will be very small resulting in lubrication problems. Several solutions have been investigated and a tentative selection has been made of a Messinger biaxial roller bearing which is a catalogue item. Other solutions are being studied

before finalizing the selection.

As anticipated, the design of a workable and effective linkage to connect two modules into a platform has proved to be the most difficult problem. At the present time it is this design area which is farthest from satisfactory completion. This lag is due to the necessity of delaying detail consideration of the problem until other design areas were far enough along to define the linkage problem. This has now been done and details of possible arrangements are being developed.

A wide variety of combinations and degrees of rigidity, elasticity, constraint, and freedom have been considered. At the present time, study is being concentrated on a linkage system in which the two superstructures end up rigidly connected in the station-keeping mode with freedom of rotation permitted at the trunnions. Hydraulic cylinders are used in the linkage to control the connection operation and to gradually "harden" the system after preliminary hookup.

G. Model Testing - Considerable progress has been made with the 1/8 scale models of the platform. Fabrication of the first module has been completed. The module has been tested extensively in San Diego Bay. To date 26 flipping operations have been made with perfect reliability. Construction of the second module is well along. It is planned that testing of the two modules coupled together will commence during late July 1971.

Detailed tests of a 1/100 scale model of the platform have been made in the wave channel at Scripps Institution. The tests covered one module in the horizontal mode, one module with legs flipped and hull in the water, one module in the station-keeping mode, two

modules in close proximity, and two modules coupled. Measured responses are in close agreement with theory. A technical report on the 1/100 scale model tests is in preparation.

H. Platform Utilization - Numerous discussions and panel meetings have been held to consider various utilizations of the Stable Floating Platform. The efforts were directed toward:

1. Identifying research programs in ocean engineering that could benefit from the use of the platform and hardware.
2. Describing specific hardware configurations that would be useful in ocean engineering work.
3. Considering the impact of these hardware items on the platform design.

As one panel report said, "It was nearly a foregone concensus of the Panel that the proposed platform would have a number of attractive features for support of ocean engineering work. The large deck area would be useful for assembling and stowing experimental equipment. Lowering and raising these items of equipment through the air/sea interface and on down to desired depth would be a useful application for a number of programs. The availability, in a stable platform at sea, of additional important support features such as living and working spaces for a scientific party, a general purpose computer, and a moderately large source of power would be of great importance to a number of programs."

Two such panel reports are combined into one document entitled, "Reports of Application of ARPA Platform", SIO Reference #71-20, dated 15 July 1971, which is currently being prepared for publication.

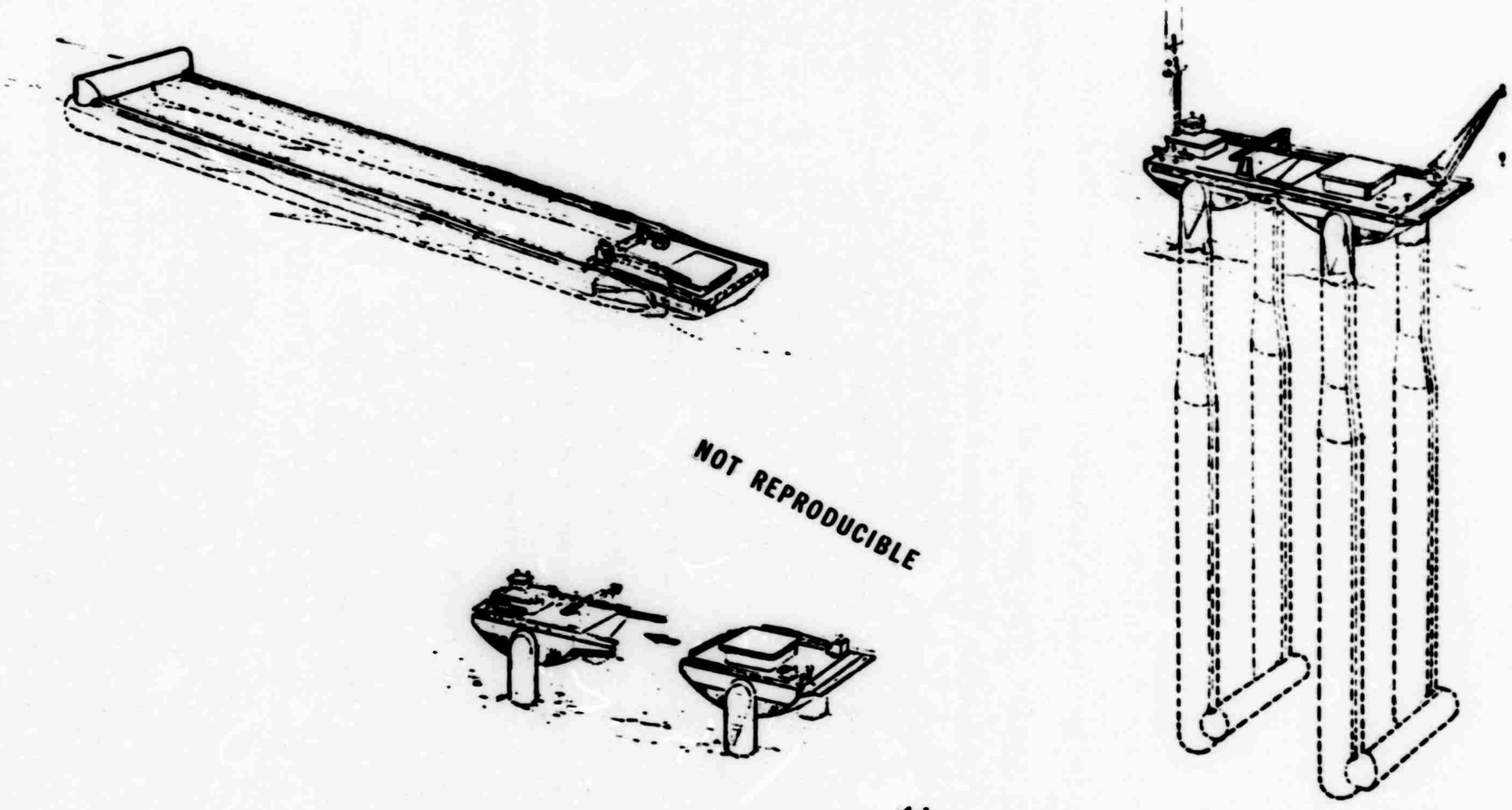

Figure 1. Engineering sketches of proposed stable floating platform.

Part II

BENTHIC ARRAY

Co-Principal Investigators

Dr. Walter H. Munk
Phone (714) 453-2000, Extension 1741

Dr. Robert D. Moore
Phone (714) 453-2000, Extension 1759

Dr. William A. Prothero
Phone (714) 453-2000, Extension 1688

ADVANCED OCEAN ENGINEERING LABORATORY

Sponsored by

ADVANCED RESEARCH PROJECTS AGENCY

ADVANCED ENGINEERING DIVISION

ONR Contract N00014-69-A-0200-6012

Part II

Benthic Array

Table of Contents

List of Figures

List of Appendices

I. PROJECT SUMMARY

The goal of this project[1] is to adapt the high performance quartz vertical accelerometer developed by Block and Moore[2] at IGPP for use on the ocean bottom, thereby increasing the technology of ocean bottom instrumentation as well as providing an increased scientific understanding of the properties of the earth below. Specifically an instrument package is being constructed which will enable the quartz accelerometer to be operated on the ocean bottom to depths of 20,000 feet. The package will be completely self-contained, including all necessary power supplies, electronics, data recording acoustical control and telemetry systems. It will be capable of operation without surface support for periods of 7 to 30 days.

The package is entering the final assembly stages with most of the problems of design now solved. During the last six months we have worked in the following areas:

A. Acoustic command and control system. The commerically available portion has been sent out for bids (see Appendix I) and the remaining control logic has been designed and partially tested.

B. Accelerometer temperature regulation. Good temperature control of the quartz accelerometer is essential to its proper operation. This has been a difficult and time consuming problem and should be solved soon. It is discussed in detail in Section II,B.

C. Installation and testing of the Honeywell low power data logging system. See Appendix II.

D. Modification of a commercial explosive cable cutter to meet our requirements for deep ocean operation.

We plan to test the complete package in the IGPP vault in September or early October, 1971. It should be ready for sea trials by January 1, 1972.

18

II. Technical Report

Specific areas of progress during the last six months are discussed in detail in the following pages. A brief discussion of each item follows. The acoustic command and control system has been designed and some very preliminary testing has been done. The design is straightforward and no problems are anticipated in this area. The problem of temperature control of the accelerometer has proved to be an extremely time consuming one. Each test takes several days and a fair amount of testing has been necessary. Work on other phases of the project is occurring in parallel, however, and we hope to have the temperature control problem solved soon. The data logging system has been received from Honeywell and is now installed in the package for testing.

An unexpected developmental task occurred when we decided to use an explosive cable cutter to release the package from its ballast which holds it on the ocean bottom. The materials used in commercially available cable cutters were not satisfactory for deep ocean work, so a modified design of a device manufactured by Hollex, Incorporated, Hollister, California was produced in cooperation with them.

A detailed discussion of each item follows:

A. Acoustic Command and Control System

This system provides the control and diagnostic functions for the capsule. Communication between the surface and capsule is accomplished by sonar transmissions. The details are described in Appendix I. Figure 1 shows a functional diagram of the entire system. When a command is received or completed, a corresponding alert code will be transmitted. Voltage levels will be converted to frequency by the voltage to frequency converter which has been designed here (Figure 2). The variable frequency output will then trigger pings on the capsule pinger. Ping intervals will then be measured at the surface to provide the voltage measurement. A description of the various command sequences follows.

1. Automatic begin: The automatic begin cycle consists of:
   a. unclamp gravimeter support gimbals so that pendulous level occurs.
   b. clamp gimbals
   c. unclamp tilt-meter and gravimeter mass clamps.
2. Gravimeter level: adjust tilt of gravimeter to its vertical or tilt-insensitive position.
3. Gravimeter diagnostics: transmit gravimeter output voltage to surface (ping rate).
4. Secondary diagnostics: transmit tilt-meter output, gravimeter temperature, and capsule temperature to surface.
5. Engineering diagnostics: transmit engineering data to surface. This will consist of battery voltages and other parameters to check on the state of capsule systems.
6. Record azimuth: record the orientation of the capsule.
7. Clamp for release: clamp tilt-meter and gravimeter masses in preparation for capsule recall.

8. Release: fire the explosive cable cutter for capsule release. There will also be a separate backup release circuit and cable cutter.
9. Reset: reset all command hold flip flops.
10. Automatic release: a separate timer will be set to release the capsule a specified time after the planned recovery time.
11. Automatic diagnostics: the diagnostic cycles will be energized automatically, and at certain intervals thereafter, a specified time after the planned recovery time.
12. Leak detector: the leak detector will automatically release the capsule if a leak occurs.

The Acoustic Command System as described in the specifications of Appendix I is presently out for bid. The other items described above have been designed and are now in the construction and testing stage.

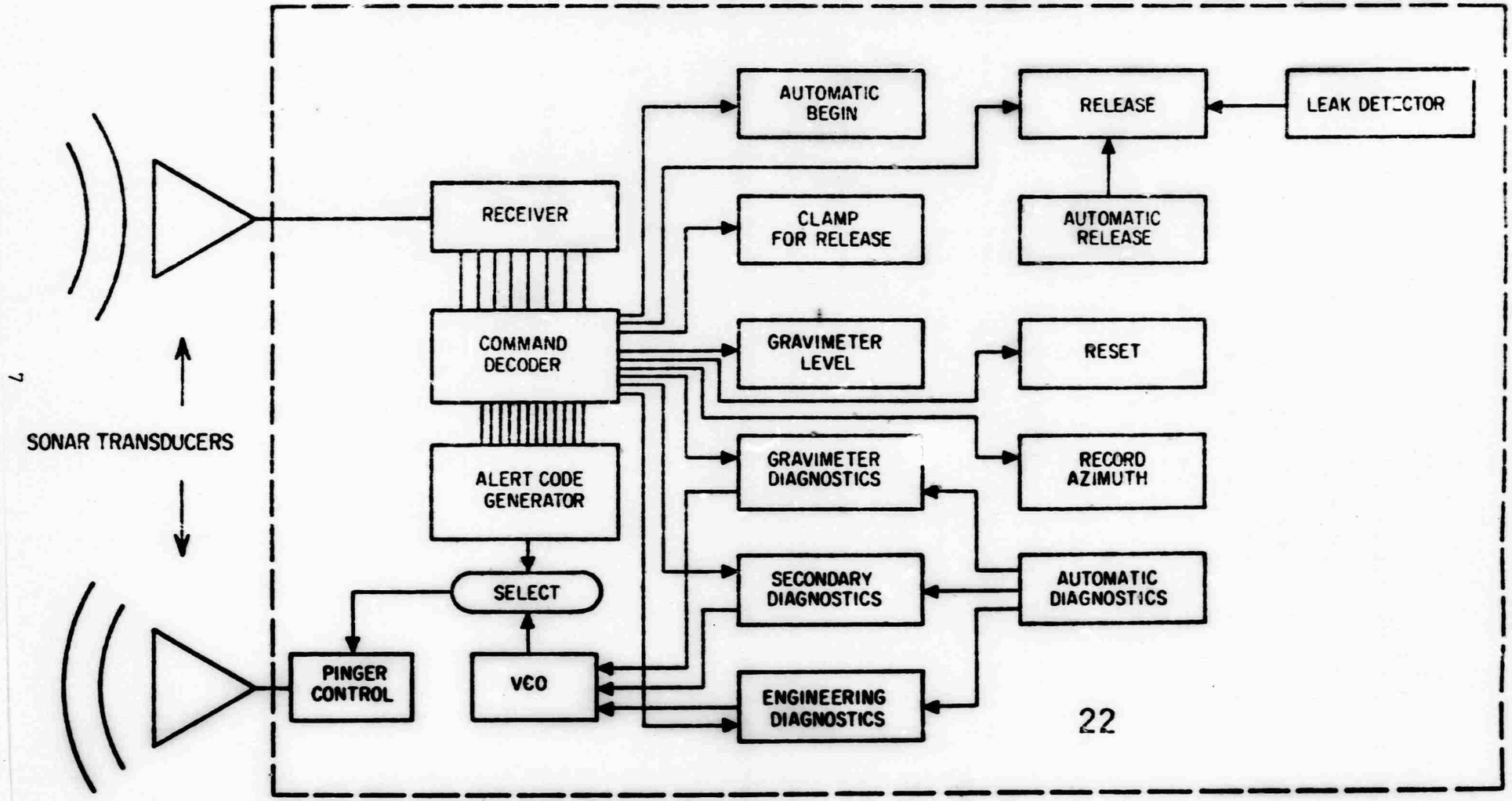

Figure 1. Acoustic Command and Control System

Figure 2. Voltage to Frequency Converter

VFC Specifications

Power:	**± 12V @ 13 ma max. The use of low power operational amplifiers will reduce this value considerably.**
Input range:	**0 to +10V**
Output range:	**0 to 1.6 KHZ**
Linearity:	**0.1%**
Short Term Stability:	**0.01%**

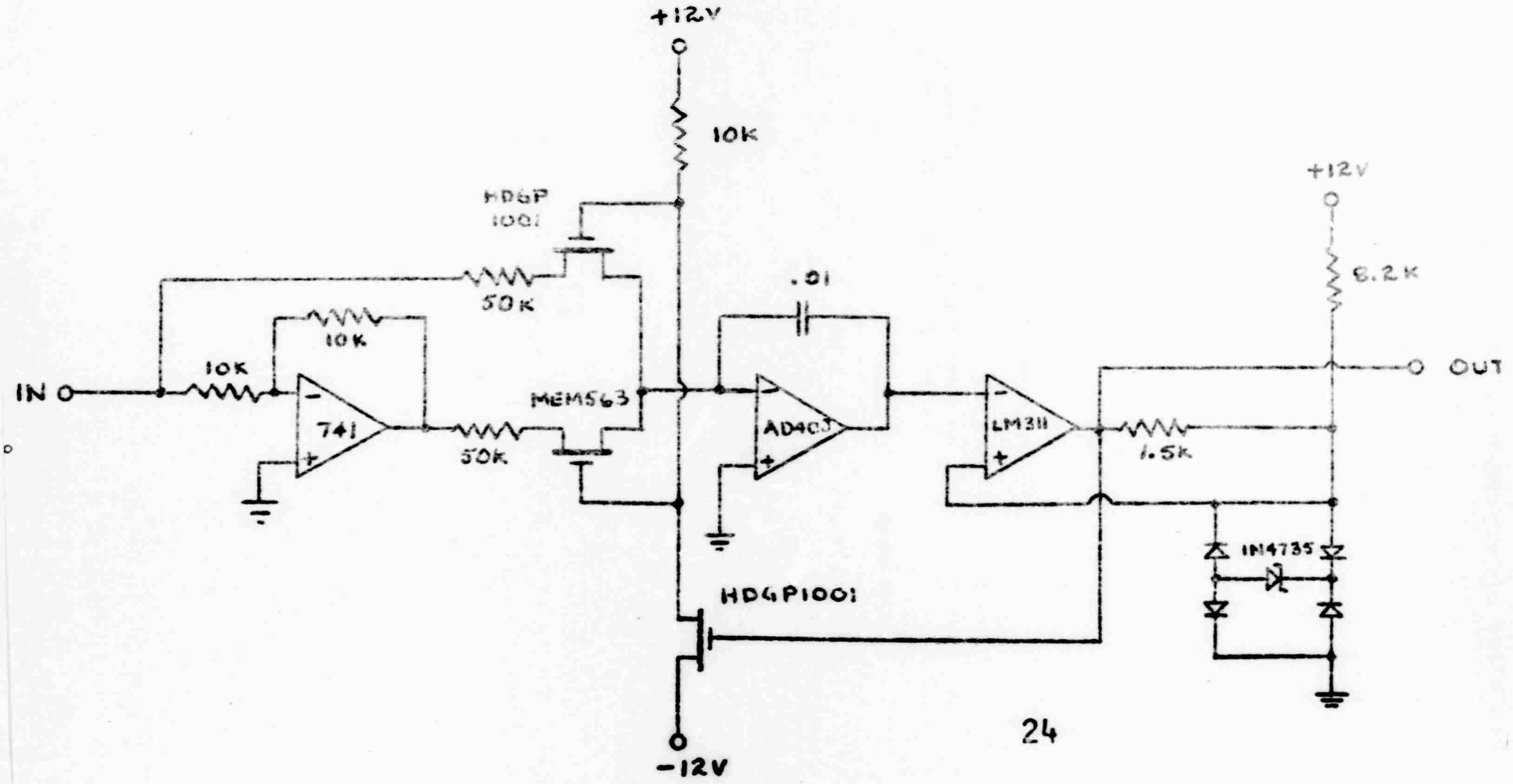

Figure 2. Voltage to Frequency Converter

B. Accelerometer

The principle difficulty with the accelerometer has been the temperature control system. This problem has been solved in the land based instrument by putting a great deal of thermal insulation between it and the external environment. Space limitations in the capsule discussed here preclude the use of such extensive insulation[1]. Fortunately, the ocean bottom temperature varies on the order of millidegrees, rather than several degrees for land based environments, making the control problem solvable. The temperature coefficient of the accelerometer is about 4×10^{-4} g/°C (g = acceleration of gravity, 980 cm/sec^2), so temperature regulation to 10^{-6}°C will reduce the maximum temperature effect to 4×10^{-10} g, which is allowable.

Figure 3 is a diagram showing the components of the accelerometer relevant to this problem. One would ideally like to control the quartz torsion fiber which supports the mass, as its temperature coefficient is the principle source of the instrumental temperature coefficient. However, this is not practical. The next best procedure is to control all sources of heat transfer to the quartz fiber. It is in a high vacuum, so the principal thermal transfer will occur by conduction through the metal parts connected to the fiber. These parts are connected to the stainless steel lid of the accelerometer can (Figure 3) by means of sturdy support legs. Thermal radiation and other sources are negligible. Thus, good temperature control of the lid should result in good temperature control of the quartz fiber. Efforts to date have been centered around accomplishing this.

A principal difficulty in temperature control systems arises from the finite thermal conductivity of the material to be controlled.

FIGURE 3. Diagram of accelerometer parts which are important to its temperature control. The support legs, vacuum can lid, and vacuum can are constructed from 304 stainless steel. The aluminum plate is 6061 aluminum. Its purpose is to minimize thermal gradients on the vacuum can lid. The volume between the outer can and vacuum can is at atmospheric pressure. The outer can is at capsule temperature.

The accelerometer itself is contained within the vacuum can and is connected to the lid with sturdy support legs.

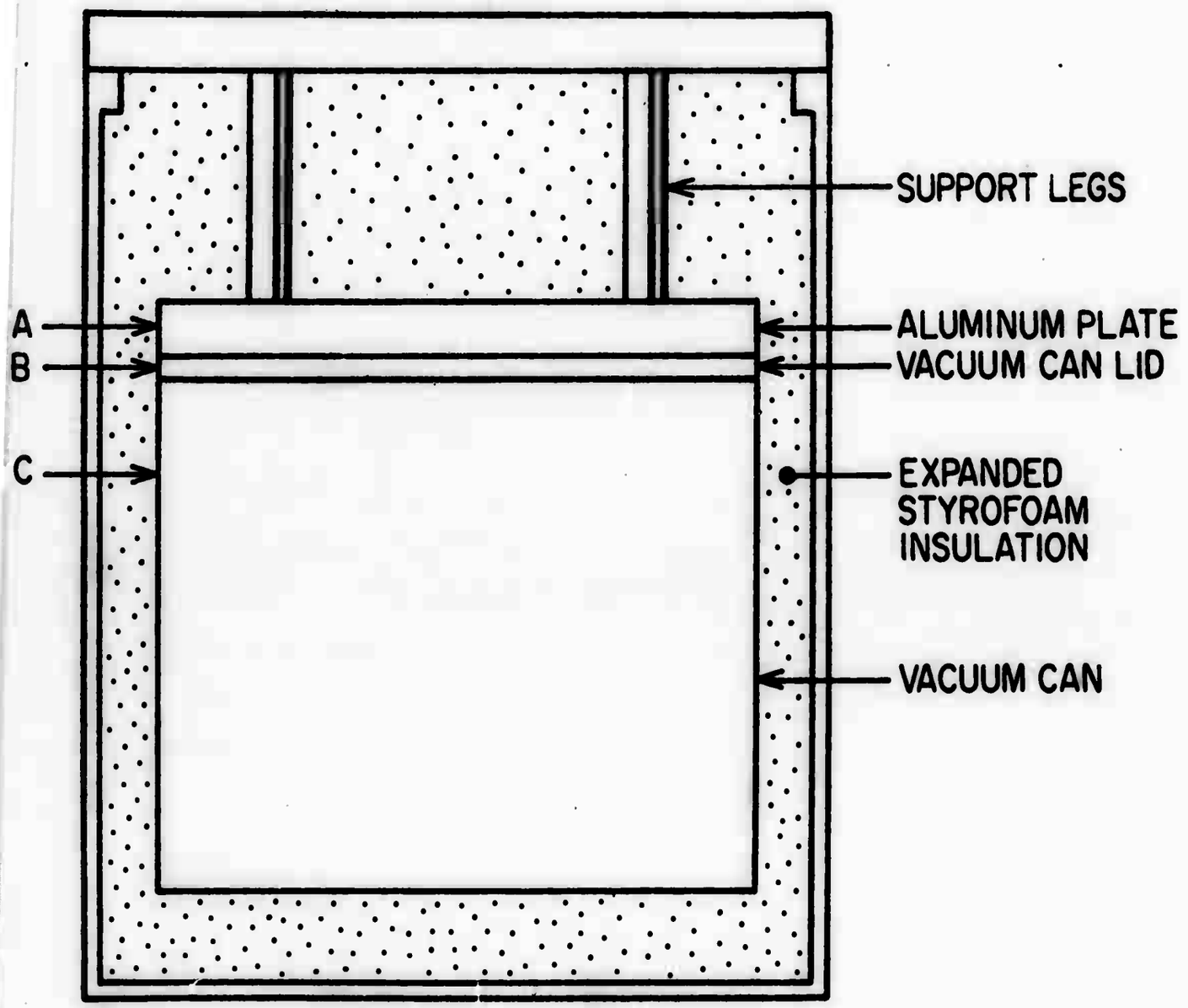
SUPPORT LEGS
A
B
C
ALUMINUM PLATE
VACUUM CAN LID
EXPANDED
STYROFOAM
INSULATION
VACUUM CAN

27

Figure 3

Thermal transfer to the environment occurs over a fairly extensive area, and may vary with time as well as location. The heater which applies power to hold the instrument above ambient temperature is fixed in its spatial distribution. Also the temperature is generally measured at a single point. Thus, different points on the regulated surface will be at different temperatures, depending on the external temperature and temperature distribution. This problem may be minimized by extensive insulation, using material of high thermal conductivity, or by surrounding the material of low thermal conductivity with a regulated surface of high thermal conductivity. Because we are constrained to use stainless steel (low thermal conductivity) for the vacuum can (the system must be baked to insure a good vacuum) we must shield the regulated surface with a high conductivity material.

Figure 3 shows an aluminum plate one inch thick bolted to the top of the vacuum can lid. Its thermal conductivity is about ten times that of stainless steel and should hold the lid temperature quite uniform. The support legs are bolted to the aluminum plate so that heat cannot pass through directly to the lid. The first test was made with the heater wound uniformly around the vacuum can and the control thermistor at position C. This configuration resulted in an attenuation of room temperature variations of about 30. We need about 10^3 attenuation for our purposes. Next we wound the heater on the outside of the aluminum plate with the control thermistor at position A. This also resulted in a factor of about 30 attenuation. A monitor thermistor on the plate indicated attenuation of better than 500, so it appeared that thermal transfer was occurring through the edge of the lid by means of conduction up the sides of the can.

In another experiment we separately and simultaneously controlled the temperature at position C, increasing the attenuation to 100. So the system behaves qualitatively as we expect. A test is now in progress with the heater wound around the aluminum plate and extending down the can about a third of the way. The control thermistor is at B on the vacuum can lid. If this does not improve the regulation sufficiently, the next step is to construct a shield of high thermal conductivity which is in contact with the vacuum can and aluminum plate and extends part way down its length. This should be very effective in reducing uncontrolled conduction up the side of the can. The temperature control which we achieve at a point near to the control thermistor is nearly adequate, so the elimination of the thermal gradient problem should complete this aspect of the project.

29

C. Data Logging System

The data logging system was manufactured by Honeywell and arrived early in June. It has been installed in the capsule and is now taking data for the temperature control tests. For actual ocean bottom operation, we are planning to sample six data channels. These are two axes of tilt, capsule temperature, accelerometer temperature, accelerometer output, and and accelerometer output filtered to amplify seismic frequencies relative to tides. Appendix II describes the properties and operation of the system. The 1970 annual report[1] describes the low power tape recorder and analog to digital converter.

30

D. SQUIB Explosive Cable Cutter

The instrument package release unit and outer pressure housing are doubtlessly the most critical parts of the entire package; for, if either fails the entire unit is lost to the sea. The pressure housings employed have been proven by several other projects, but no known release which is reliable enough yet suitable for a rigidly bound battery to instrument package could be found.

Investigation indicated that the Aerospace industry had found explosive type releases to be far more reliable than other types for stage to stage separation; thus, since this problem is essentially the same, a search for a suitable explosive release was initiated. Unfortunately, the more extreme pressure and conditions encountered in the oceans made all available releases unsuitable; therefore a completely new design was required. This was undertaken by us in conjunction with Holex Incorporated, manufacturers of similar aerospace explosive release devices. The requirements for a suitable unit included:

1. A 20,000 foot operating capability (the ability to work at approximately 10,000 psi).
2. Corrosion resistance in the open ocean from surface depths to the maximum operating depth for a minimum of 45 days.
3. Relatively easy to manufacture with a simple, small and safe to handle construction.
4. Reuseable main frames to hold down expense of replacement.

31

The main problem turned out to be finding a suitable alloy that was corrosion resistant, yet strong enough and inexpensive enough to meet all the above criteria. For a period up to 45 days a final compromise resulted in the choice of 316 stainless with a 440 stainless cutter. This appears completely suitable for 45 days, yet marginal for any longer period applications. A titanium alloy would be the best overall choice to use for construction of a non-time limited unit, but expense and difficulty in manufacturing prohibits its use unless the total package is eventually redesigned for a longer run time (greater than 30 days). The final design is shown in Figure 4.

The project is in good shape according to the schedule of Figure 8 of the last report, although the importance and order of some tasks prior to September 1, 1971 has been altered. As scheduled, however, we expect to be testing the complete package in September or early October in the IGPP vault. The major unknowns involved in the concept of the project have been solved and major task remaining is to finish putting the various components together. One unknown which we disposed of was whether pendulous leveling of the accelerometer would be sufficiently accurate. We found that orientations achieved in this manner were consistent to .1 degree, which is well within the .5 degree range we require. A remaining unknown concerns the quartz accelerometer. The present unit is sufficient for our work if it is taken apart and cleaned carefully. We also have assumed it would be necessary to modify it so the moving mass could be clamped during transport, drop, and recovery. Experience with the land based instrument leads us to believe that the quartz torsion fiber may be strong enough so that this is not necessary. The cleaning will probably not cost us much time,

as other personnel will be available to perform it. However, a certain number of headaches will be eliminated if mass clamping is unnecessary, as this does involve a change in the cor guration of the instrument.

Future testing plans for 1972 include drops off San Clemente Island and hopefully a deep ocean drop off the California coast.

33

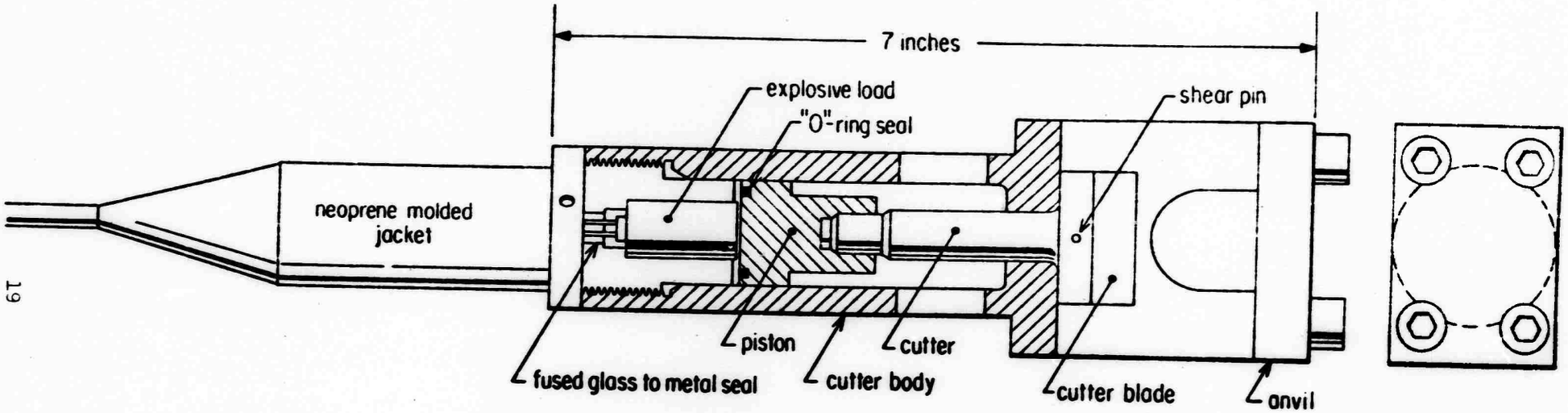

Figure 4. Explosive Cable Cutter

References

1. Moore, R. D., and W. H. Munk, "Benthic Array", Annual Report, Advanced Ocean Engineering Laboratory, Scripps Institute of Oceanography, December 31, 1970, O.N.R. Contract N00014-69-A-0200-6012, AOEL Report #16, S.I.O. Reference 71-4.

2. Block, B., and R. D. Moore, Tidal to seismic frequency investigations with a quartz accelerometer of new geometry, *J. Geophys. Res.*, *75*, (8), 1493-1505, 1970.

35

BLANK PAGE

APPENDIX I

SPECIFICATIONS FOR ACOUSTIC COMMAND SYSTEM

W. A. Prothero
Institute of Geophysics and Planetary Physics
University of California, San Diego
8 June 1971

System Purpose

To provide a command and diagnostic sonar link between a surface ship and an experimental capsule on the ocean bottom to depths as great as 20,000 feet.

General Description

The system will include a shipboard transmitter which, upon command, will transmit a coded acoustic signal to the subsurface capsule. The signal will be received and, depending on the code, will initiate an appropiate action within the capsule.

In order for the capsule to indicate its response to a surface command and to transmit diagnostic information to the surface, a pinger must be provided which will be activated by capsule control logic. Special ping sequences or ping rate will contain the basic information.

Acoustic Command Transmitter and Command Receiver

The acoustic command system must consist of a shipboard transmitter and subsurface receiver. The transmission should consist of at least four different independently selectable frequencies which make up the transmitted code. The receiver must have at least eight channels, so that a good code

will consist of four ON channels and four OFF channels. Thus, the system will be nearly immune to high amplitude, broadband acoustic noise from passing ships and other sources. The command function is altered by choosing a different frequency combination. Alternative systems of equal or better immunity to spurious commands will be considered. At least twenty different command codes must be available.

Range

The receiver sensitivity must be limited by background acoustic noise rather than electronics noise in a sea state 1 or 2. The command transmitter must have a great enough output to command the capsule from a distance of 3 to 5 miles at a depth of 10,000 to 20,000 feet.

Capsule Pinger

The subsurface capsule must be capable of pinging on command from internal capsule logic. All electronics necessary to drive the pinger with a logic level change or pulse input, as well as the transducer are required. The transducer and high voltage electronics will be mounted in a separate pressure housing. The ping function must not interfere with the command receiver, so that commands may be initiated while pinging is occurring. Ping power output must be comparable to that from the command transmitter.

Surface Receiver

The surface receiver is intended to receive the ping signal from the subsurface capsule. It must provide an audio output and a logic level output.

Power

Power consumption is not critical for the surface equipment, but the subsurface components must use the minimum possible power. The command receiver and pinger electronics must operate from a 12v. power supply and require less than 1 ma. current continously. The pinger power supply may be 24v. and will draw energy from the batteries proportional to the number of pings transmitted.

The surface equipment will normally be operated from shipboard power. Optional battery operation is desirable.

Manuals

Two manuals including all schematics, circuit board layouts, parts lists, operating instructions, interface recommendations, checkout test data, and a block diagram of the operation must be supplied with the system.

System Equipment

1. Multichannel acoustic command transmitter and transducer.

1a. Optional battery power.

2. Surface acoustic receiver for subsurface pings. (may use command transducer).

3. Acoustic command receiver with logic level outputs from each channel. We will provide decoding circuitry.

4. Capsule Pinger including pressure case. The high voltage transducer electronics will be mounted in the pressure case.

4a. Deduct cost of pressure case and mounting.

Bids must be accompanied by full equipment specifications, block diagrams, theory of operation, etc. If special beam patterns are used on transducers, indicate beam patterns and design philosophy.

BLANK PAGE

APPENDIX II

UCSD DATA LOGGER

PHYSICAL DESCRIPTION

The Data Logger is housed in a card cage that contains three rows of circuit boards, each row capable of holding up to 11 boards. The Data Logger electronics occupy only eight boards, all in the center row, leaving the outer two rows available for other applications. A hinged front panel covers the center row and parts of the outer two rows. Control switches, indicator lights, and output jacks for the Data Logger are all located on this panel. These switches, lights, and jacks are hardwired to the card cage connectors via a flexible cable bundle. A single schematic (Honeywell Drawing No. 37270496) shows all the electronics and wiring included in the Data Logger. This includes the internal wiring of the individual boards, the card cage wiring, and the card cage to front panel wiring. On this schematic, the cards are referred to by their location in the card cage. These positions are identified as locations A1 through A11 corresponding to the 11 card locations in the center row. Card A1 is at the hinged end of the front panel, A11 at the latch end. All switches, lights, and jacks are shown on the schematic. The locations of these switches, lights, and jacks are identified in the marked up drawing (Figure 1) of the front panel artwork.

Outputs to the tape recorder are as identified on the schematic.

Power inputs to the Data Logger are to Card A11 Pins 18, 19, and 20. Pin 18 is +12 VDC, Pin 19 is ground, and Pin 20 is -12 VDC.

Electrical control signals may be input to Pins 7, 9 and 11 of either cards A10 or A11. These signals are:

Pin 7: A +12 volt signal starts the data logger

Pin 9: A +12 volt signal stops the data logger

Pin 11: A +12 volt signal resets the data logger

Each of these inputs have a 100 K input impedance to ground.

Front panel components are:

Indicator Lights: Shelly Model BEP-066-C-B-P
Type T-1, 12 Volt Lamp

Switches-Toggle : Alcoswitch MST 105D

Push-button : Alcoswitch MSP 105F

Banana Jacks : E. F. Johnson #108-0901-001

All other components are identified on the schematic.

UCSD DATA LOGGER

FUNCTIONAL DESCRIPTION

The Data Logger samples eight analog input signals, converts these signals to a digital format, and records the digital information on a 7 track incremental tape recorder. One analog signal is sampled and recorded each second. The sequence of analog channel selection is controlled by the eight select switches on the front panel and the internal system clock.

The basic sequence or block is 64 seconds or 64 samples long. A 131.072 crystal clock is divided down to produce a 1 hertz square wave that, in turn, drives the 64-second counter. The 1/64 hertz square wave out of the 64-second counter, in turn, drives a 12-bit time code counter. The contents of the time code counter are stored on the tape during the first second of each 64-second block (when the 64-second clock is at zero). Converted analog data is stored during each of the next 63 seconds. The different sequences for sampling and storing the eight analog signals (channels 0 through 7) are briefly described below:

- Channels 6 & 7 are both selected--
  Record channels 0→5 once (if selected), then repeatedly sample and record channels 6 & 7 until the 64-second clock reaches 63 and resets to 0. Repeat sequence every 64 seconds. If select switches 2 and 4 are in the "OUT" position, the sequence will look like:

```
64-second clock - 0 1 2 3 4 5 6 7 8 9 . . .
                  | | | | | | | | | |
Selected channel- T 0 1 3 5 6 7 6 7 6 . . .
```

T=Time

- Channel 6 or 7 selected (not both)--

  The sequence is the same as above except that after the selected 0 → 5 channels have been recorded once each, the duration of the 64-second block is spent sampling and recording the selected 6 or 7 channel. If 3, 4 and 7 are all "OUT", the sequence looks like:

  64-second clock- 0 1 2 3 4 5 6 7 8 • • •
  Selected channel-T 0 1 2 5 6 6 6 6 • • •

- Channels 6 & 7 both "OUT" (not selected)--

  Repeatedly sample and record the first four selected channels. If fewer than four channels are selected, sample the selected channels once each every four seconds. If channels 1, 2, 3, 4, and 5 are selected, the sequence looks like:

  64-second clock- 0 1 2 3 4 5 6 7 8 9 • • •
  Selected channel-T 1 2 3 4 1 2 3 4 1 • • •

Once the Data Logger is started, it will record data in 64-second blocks continuously until the STOP button is depressed. Every 128 blocks, a 3/4-inch record gap is written on the magnetic tape. During the 64 seconds that make up the 128th block, no data is recorded. The record gap is generated, then the Data Logger waits the duration of the 64 seconds for the start of the next 64-second period when data recording resumes. A record gap is also generated whenever the Data Logger stops.

The timing signals that control the sampling, converting and recording operations performed once each second are shown in Figure II. These signals are generated by a decade counter with decoded decimal outputs (I. C. 39). During the first half of each

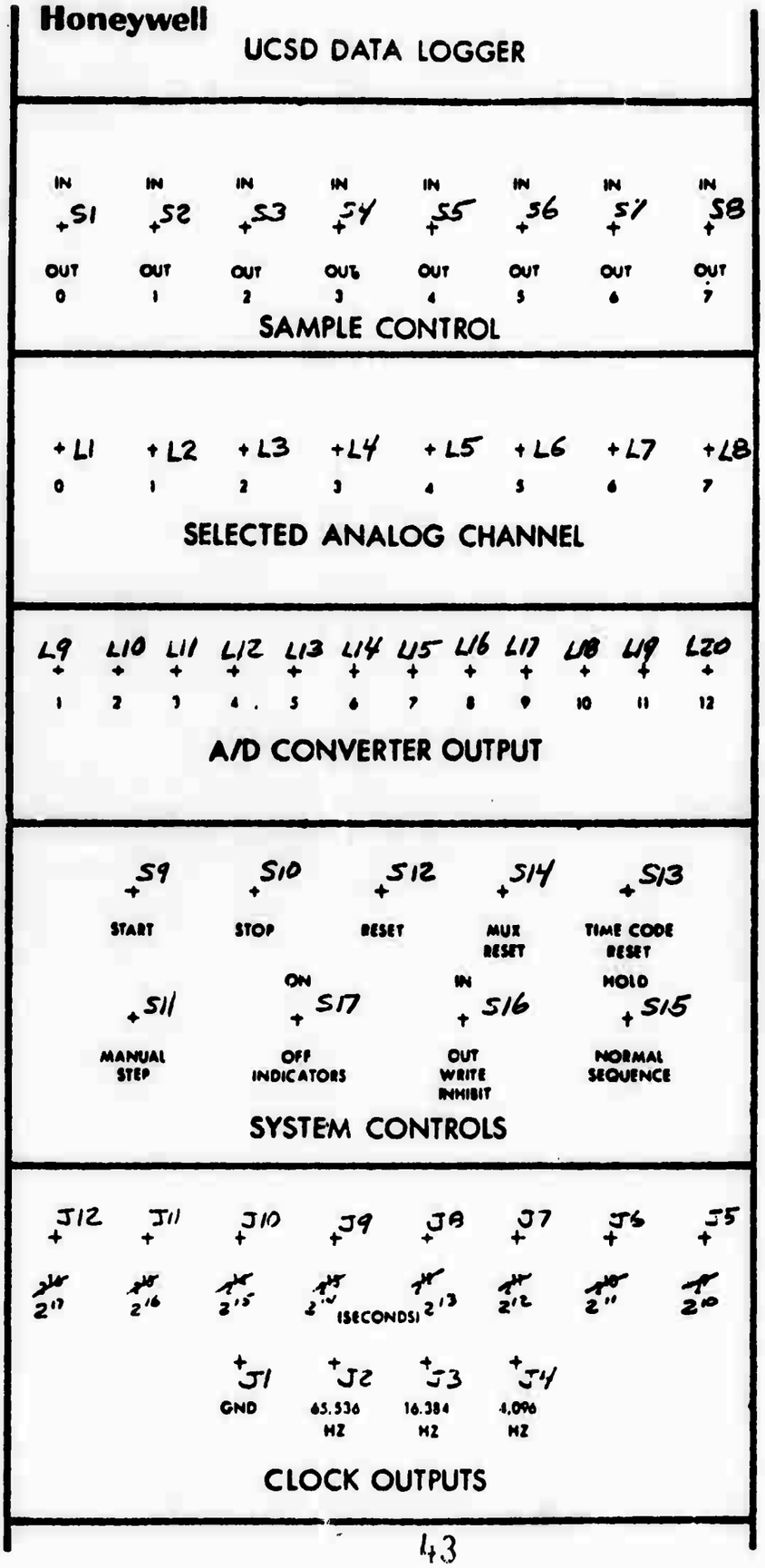

FIGURE I: FRONT PANEL SWITCH, LIGHT, AND JACK LOCATIONS

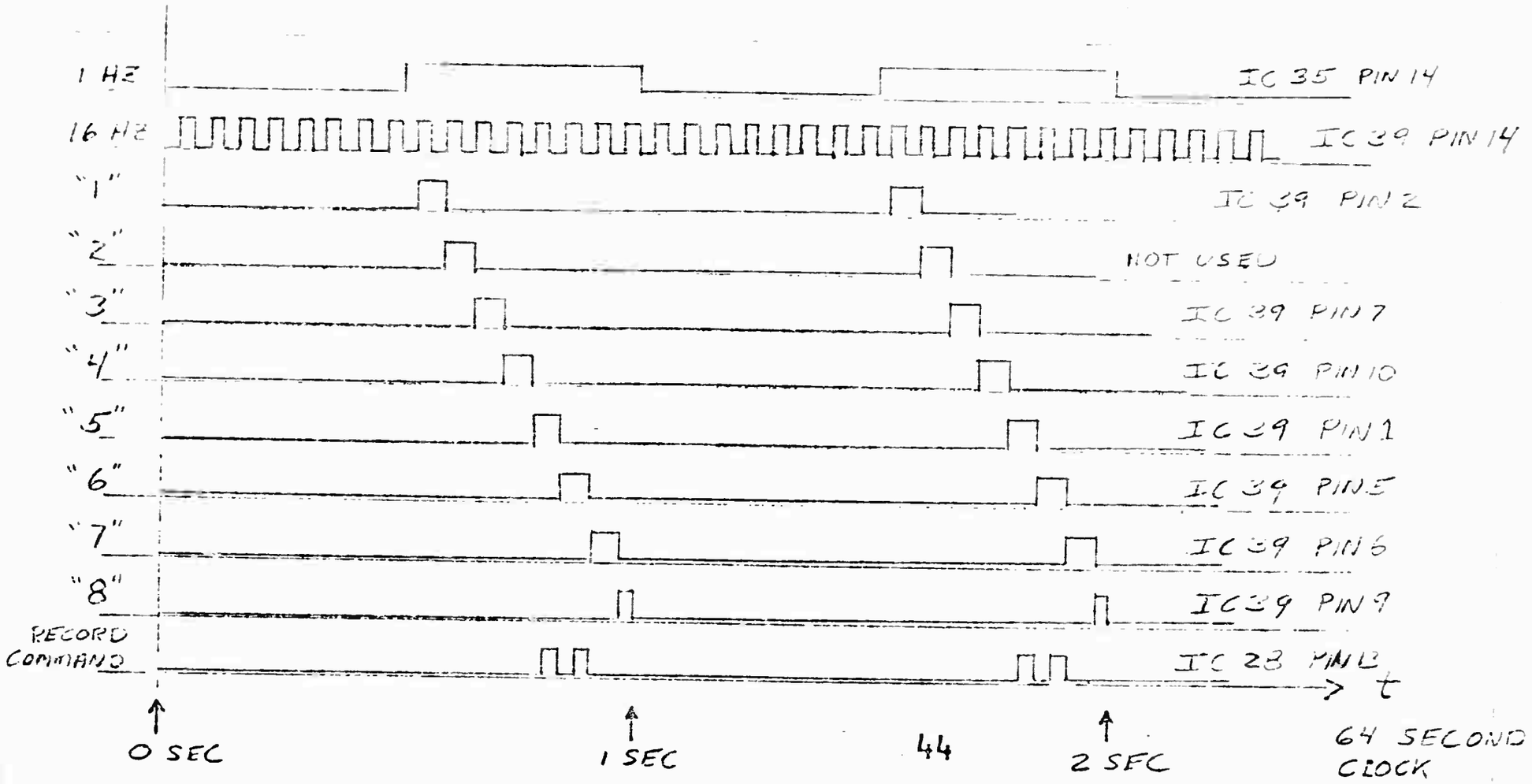

FIGURE II : UCSD DATA LOGGER TIMING DIAGRAM

second, this decade is held reset by the inverted 1 hertz signal. During the second half of the second, the reset is released and the decade counter starts counting from the 16-hertz input signal. The counter reaches eight before being reset at the start of the next second. The functions of each decoded output are described below:

"1" - ● If the 64-second clock is at zero, reset the multiplex sequence control.

● If the 64-second clock is at zero and the stop flip flop is set, send a record gap command to the data recorder.

● No function when the 64-second clock is not at zero.

"2" - ● Not used.

"3" - ● If the 64-second clock is at zero and the stop flip flop is set, the Data Logger halts.

● No function if the 64-second clock is not at zero.

"4" - ● This signal is differentiated and input to the Analog to Digital Converter to command a conversion.

"5" - ● If the 64-second clock is zero, this signal causes the six least significant bits (L.S.Bs) of the time code counter to be output to the recorder. The "RECORD" command subsequently strobes this information onto the tape.

● If the 64-second clock is not zero, the six L.S.Bs from the A/D converter are output to the recorder.

"6" - ● If the 64-second clock is zero, the six M.S.Bs from the time code counter are output to the recorder.

● If the 64-second clock is not zero, the six M.S.Bs from the A/D converter are output to the recorder.

"7" - ● Whenever the manual step flip flop is set, the Data Logger will halt on the trailing edge of this pulse with the manual stop flip flop reset. When the manual stop flip flop is again set (by depressing the corresponding pushbutton switch) the Data Logger resumes operation, stopping again at the trailing edge of the next "7" pulse.

● If the channels 6 and 7 select switches are both in the "OUT" position and the 64-second clock is at 0, 4, 8, . . . 60, this pulse resets the multiplex sequence control.

"8" - ● This pulse advances the multiplex sequence to the next channel. A channel is selected and input to the A/D converter 3/4 of a second before a conversion is commanded by pulse "4" of the next second. When the multiplex sequence control is reset by pulse "7", it is reset to a condition where none of the eight channels are selected. The subsequent "8" pulse advances the sequence to select the first channel specified by the front panel select switches.

Record Command

- This signal commands the tape recorder to strobe the data on its six input data lines (plus one parity line) onto the tape. The record command pulses are blocked by the WRITE INHIBIT switch or when the 7 L.S.Bs of the time code counter are all at "1". (This occurs for a 64-second period once every 64 x 128 = 8112 seconds = 2 hours 15 minutes and 12 seconds).

The multiplex sequence control is contained on logic board No. 2 (location A7). The cirucit is basically a 9-bit shift register. At any given time, one of the nine flip flops will be in the set condition, the remainder reset. The last eight flip flops correspond to the eight analog channels. The flip flop that is set gates the corresponding analog channel through the multiplexer to the A/D converter. When the shift register is clocked (by timing pulse "8"), the set condition moves to the right to the next flip flop that corresponds to a selected channel. When the set condition reaches the last two flip flops, it will either cycle back and forth between the two (if both channels 6 and 7 are selected) or hold at the selected flip flop (if only one of the two is selected). When the multiplex sequence controller is reset, the first flip flop is set and the last eight flip flops are reset so that none of the eight analog channels are selected. The next clock pulse will move the set condition from flip flop 1,to the first flip flop corresponding to a selected channel.

The functions of the front panel controls and indicators are described below.

SAMPLE CONTROL SWITCHES - Each switch controls whether or not the corresponding analog channel is IN or OUT of the sampling sequence.

SELECTED ANALOG CHANNEL INDICATOR LIGHTS - These lights (8) indicate which analog channel is currently being sampled. These lights are disabled, as are the A/D CONVERTER OUTPUT lights when the INDICATORS ON-OFF switch is to the OFF position.

A/D CONVERTER OUTPUT LIGHTS - These lights indicate the output of the A/D converter. Bit 1 is the MSB and bit 12 is the LSB.

SYSTEM CONTROLS - START - This switch, when pushed, resets all counters and the multiplex sequence controller and starts the Data Logger.

STOP - This switch sets the stop flip flop (when it is pushed). The stop flip flop will cause the Data Logger to generate a record gap and halt when the present 64-second block is completed.

RESET - Depressing this switch causes all counters to be reset. The Data Logger continues to run (unless the STOP switch was previously pushed).

MUX RESET - This switch resets the multiplex controller and the 64-second clock.

TIME CODE RESET - Pushing this switch resets only the time code counter. Data Logger operation proceeds uninterrupted.

MANUAL STEP - Pushing this switch causes the Data Logger to operate for one second (sampling, converting and recording one analog channel) then halt. Each subsequent time the switch is pushed the recorder will resume operation for one additional second processing one more channel, then halt again.

INDICATORS ON/OFF SWITCH - In the OFF position, the SAMPLE CONTROL and A/D CONVERTER OUTPUT lights are disabled.

WRITE INHIBIT IN/OUT SWITCH - In the IN position, the data record and record gap commands to the tape recorder are blocked.

SEQUENCE NORMAL/HOLD - When this switch is placed in the HOLD position, the multiplex controller, the 64-second clock, and the time code counter are held in the condition they were in when the switch was thrown. The timing pulses are not blocked so the same analog channel is continuously sampled, converted and stored on the tape. When the switch is returned to NORMAL, the Data Logger continues on as it was before the switch was put to HOLD.

CLOCK OUTPUTS - The top row of jacks contain the outputs of the eight most significant bits of the time code counter. The most significant bit represents 2^{17} seconds. The total time code counter capacity is 2^{18} seconds which represents approximately 3.25 days.

The bottom row of jacks contains three frequencies derived from the 131.072 kHz countdown chain plus a signal ground jack.

BLANK PAGE

Part III

OVERPRESSURES DUE TO EARTHQUAKES

Co-Principal Investigators

Dr. Hugh Bradner
Phone (714) 453-2000, Extension 1752

Prof. John D. Isaacs
Phone (714) 453-2000, Extension 1141

ADVANCED OCEAN ENGINEERING LABORATORY
Spcnsored by
ADVANCED RESEARCH PROJECTS AGENCY
ADVANCED ENGINEERING DIVISION

ONR Contract N00014-69-A-0200-6012

Part III

Overpressures Due to Earthquakes

Table of Contents

List of Figures

OVERPRESSURES DUE TO EARTHQUAKES

I. PROJECT SUMMARY

A. Purpose and History

The Overpressures Due to Earthquakes project work is directed toward the understanding of the various effects, at the sea surface, at the ocean floor, and between, of nearby undersea earthquakes. The present goal is the study of pressure variations in the water column which result from seismic events. At the beginning of the program various experimental approaches were considered. One such consideration was the development of inexpensive long time instruments that could be scattered over know seismic areas and left for extended lengths of time(i.e. several years). The idea of attempting to measure the overpressures using such instruments was subsequently abandoned, mainly because of the gross uncertainties involved with trying to make such measurements in the near field of adequate seismic activity. It was decided, instead, to attempt measurements during the aftershock sequence of large earthquakes located beneath the sea. There is almost invariably a sequence of aftershocks following a large earthquake. By definition, the size of the aftershocks are all smaller than the main event (the greatest aftershock is usually about 1.2 in magnitude less than the main event) and continue for from a few days to a number of weeks after the main shock. They are usually located in the general region of the main shock and most probably along the edges of the displacement area of the main shock.

B. Hardware Development

A major effort, especially during this reporting period, has been made to develop instrumentation for immediate delivery to the seaquake area for aftershock measurements.

The main instrument package contains a pressure transducer which allows the measurement of a maximum overpressure equivalent to 1 g acceleration. A level detector which senses the size of the signal, activates a tape recorder. The amplified signal is also modulated, recorded, and sent up to the surface buoy where it is transmitted to a boat containing monitoring equipment. This system has been tested in local waters and is now packaged and ready for transmittal to an area of aftershocks following a major seaquake.

Also under development has been modifications of Navy sonobuoys which will have the frequency and dynamic range required while still having the capability of being airdropped. In this case the sonobuoy hydrophone and preamp are replaced with a set which has suitable response. This is followed by a logrithmic amplifier and a pulse width modulator. The modulated signal is sent through a standard sonobuoy audio amplifier and transmitter, and transmitted to the drop plane flying nearby. Complete testing and evaluation of this system has been postponed pending a re-evaluation of program direction.

C. Experimental Procedure

The experimental procedure to be followed is essentially the same for both the air dropped and ship-deployed instruments. The instruments are deployed initially around the position given by the preliminary

epicenter of the main shock (this determination may be off by as much as 50 miles). Once the area of greatest aftershock activity has been determined, the instruments are redeployed and left for a number of days (In the case of air dropped instruments, new ones would have to be dropped every eight hours). The experiments would continue until seismic activity dropped below some set level of interest. The collected data will give information on transient pressure changes during earthquakes as a function of distance from the epicenter magnitude and, hopefully, dip of the fault.

II. TECHNICAL REPORT

A. Instrumentation

The major project effort has been to develop instruments which would measure pressure at some point in the water column and which could be rapidly transported to the area of a large quake and be easily deployed from a relatively small boat. A general description of these instruments is presented here. The main instrument package contains a pressure transducer which has a range equal to twice the ambient pressure at the measuring point (presently 120 feet below the sea surface). This allows the measurement of a maximum overpressure equivalent to 1 g acceleration. The signal from the transducer is amplified by a factor which depends on the magnitude of quakes expected. A level detector senses the size of the signal and switches on a small tape recorder contained inside the package when the signal reaches a certain level. The detector keeps the recorder on until the signal falls below and remains below the preset level for approximately 40 seconds. The amplified signal is modulated and recorded. The modulated signal is sent

up to the surface buoy where it is transmitted using a VHF-FM transmitter obtained from Navy ASW SSQ/41A sonobuoys. The signals from two or three like instruments are recorded on a nearby ship. Internal recorders are used in case of the need to leave a buoy and deploy other instruments out of transmitting range. Intentions are to record some events from spatially separated instruments on one tape to get an idea of the spatial distribution of overpressures. The surface buoy contains a flashing light and Citizen Band Beeper transmitter to aid finding the buoy when the experiment is completed.

The cable connecting the surface buoy with the subsurface package has a weight attached at the desired measurement depth. Between this weight and the instrument package there is a series of weights and floats which, together with the package itself, forms a neutrally buoyant system. This provides a sort of spring effect which allows the cable weight to rise and fall with the surface wave action without transmitting this motion to the instrument package. Figure 1 is a drawing of this instrument when deployed.

Figure 2 shows a block diagram of the package. The signal-level sensor (SLS) and pulse-width modulator (PDM) schematic is shown in Figure 3 The signal from the pressure transducer is amplified and sent through an absolute value circuit (ABS). This is then compared with some preset voltage. When the signal rises above this voltage, IC2 fires Q2. Q2 trips the relay, turning on the tape recorder. The RC decay holds Q2 on for about 40 seconds after the op amp shuts off and remain so.

The modulator (PDM) generates a 40 cps square wave; the length of the positive half pulse is proportional to the signal level. This is

accomplished by generating a 1/40 second ramp which is compared to the signal at IC3. IC3 saturates as long as the signal is greater than the ramp level, and gives zero output otherwise. The positive half pulse from IC3 then triggers a COS-MOS chip set to oscillate at 4 kc. The series of 4 kc bursts (the width, or duration, of each being proportional to the signal at that time) is then recorded on the internal tape recorder, and is sent up to the surface buoy transmitter. (There is also a provision to transmit the unmodulated signal).

This instrument was tested off shore and found to work quite satisfactorily. Some of the shipboard puripheral equipment did not perform so well, however, so that quantative analysis of sensitivity and noise levels was postponed and will be presented in a later report.

Dr. Hugh Bradner, while on sabbatical at the NATO ASW Research Centre in La Spezia, Italy, has developed modifications of the Navy sonobuoy SSQ/38A which give it the frequency range and dynamic range we required, still leaving it in a condition suitable for airdropping. The SSQ/38A sonobuoys were selected because of their long (72 hour) operating time and their deep (300 feet) hydrophone.

The sensitivities of all ordinary sonobuoys and of PB 3 receivers (ARR 52 or ARR 72) diminish very rapidly below 10 Hz. Therefore the sonobuoys must be modified to have sensitivity at lower frequency than 10 Hz and the telemetered signal must be maintained at a frequency above 10 Hz if PB 3 gear is to be used. The low frequency sensitivity was obtained by replacing the hydrophone, preamplifier and amplifier. The telemetered

signal was obtained by using pulse duration modulation. The piezoelectric bimorph hydrophone of the ordinary SSQ/38A is encapsulated with its pre-amplifier, and cannot be separated from it. Therefore an available cylindrical PZT/5A hydrophone was substituted. It is 1 1/2" outside diameter, 1 1/2" long, with 1/8" wall and has a capacitance of 0.012 μf. Its sensitivity is - 94 db resp/volt/microbar.

Two types of preamplifier were designed and built by Engineer K. Rasmussen of the Centre. Both types can be encapsulated inside the hydrophone cylinder. The first type has ultra high input impedence, ($2x10^3$ Megohm) but requires internal mercury batteries with sea-water contact closure. (Figure 4). The second type does not require internal batteries it has 20 megohm impedence, which is sufficient to give flat response down to approximately 1/20 Hz. This frequency response is possible because the expected signals from seismic events are so large that the hydrophone can be shunted with a 0.15 μf capacitor. Figure 5 shows the FET/20 megohm preamplifier. A higher roll off frequency than 1/20 Hz may be necessary in the Pacific Ocean, where long period swells are common.

The hydrophone cylinder and preamplifier are designed to replace the normal assembly in the SSQ/38A sonobuoys. The signal is carried to the sonobuoy amplifier by the normal 300 ft. two-wire cable. A prototype production preamplifier has been built, but assembly and installation of units in SSQ/38A sonobuoys has not been undertaken pending word of airborne program approval from COMASWFORSIXTHFLT.

The SSQ/38A amplifier has been replaced by a logarithmic amplifier to give large dynamic range, and a pulse duration modulation circuit to

convert the low frequency signal to a form suitable for reception by the PB 3 aircraft or commercial f m receivers. The output of the PDM feeds directly to the input of the radio frequency transmitter in the SSQ/38A.

The log amp./PDM circuit was designed to use inexpensive general purpose operational amplifiers, and a minimum of components. The circuit is shown in Figure 6. The 13K potentiometer is used to adjust the repetition rate of the PDM square wave, (eg, R=26K gives a 20 hz square wave; R=13K, a 40 hz square wave). The calibration is shown in Figure 7 and Figure 8. The vertical flags on the curves show the range of calibrations of nine production units that have been built. Auxilary scales in Figure 7 show equivalent telemetry - PDM output (in counts) vs. input acceleration, $\Delta g/g$ (or equivalent pressure change, $\Delta p/p$) for the modified SSQ/38A, with the hydrophones at 300 ft.

An assembly has been checked for proper functioning in a sonobuoy, and the telemetered signal has been checked for proper reception with a commercial f m receiver; but final installation in SSQ/38A sonobuoys was withheld for the reason mentioned above.

B. Experimental Procedure

The experimental procedure to be followed is essentially the same for both the air-dropped and ship-deployed instruments. The instruments are deployed initially around the position given by the preliminary epicenter of the main shock (this determination may be off by as much as 50 miles). Once the area of greatest aftershock activity has been determined the instruments are redeployed and left for a number of days. (In the case of the airdropped instruments, new ones will have to be dropped every eight hours). The experiments will continue until seismic activity has dropped below some set level of interest. The collected data will give information on transient pressure changes during earthquakes as a function of distance from the epicenter, magnitude and, hopefully, dip of the fault.

C. Hazards Estimate

Dr. Bradner has begun work on a preliminary hazards estimate based on the seismicity of the various tectonic regions of the ocean. The purpose of the estimate is to give the probability of an earthquake of some magnitude occurring near a vessel as it passes through a seismic zone. The overpressures associated with such events will be determined theoretically (Richards[1]) and experimentally.

The preliminary hazards estimate is based on the idea that the probability of an event occurring in some area within some time span is proportional to the historical time density of earthquakes in that area. Tapes and/or lists used in compiling seismicity charts for the world have been requested. When received, the earthquake density of the various tectonic regions will be calculated and a probability number, which is a function of magnitude, will be assigned to the different areas. The experimental work should allow association of the probability number and the usual type of faulting in that area with the hazard that some size overpressure would occur.

D. Progress

The San Fernando Quake of 9 February 1971 has given an added impetus to the study of overpressures in the oceans. The record taken at the Pacoima Dam, 5 miles from the epicenter contained several acceleration peaks greater than 1 g, even though the magnitude was only 6.5[2]. The fact that such large accelerations occur near a relatively small earthquake was heretofore unknown. This makes the overpressure problem perhaps more serious than originally thought.

59

On 2 May 1971 there occurred an event off Adak, Alaska given a magnitude 7.1. A project representative flew to the Navy Base there to arrange a ship for our use in monitoring aftershocks while final preparations to take the instruments were made. By the evening of 4 May, it was clear that the quake did not have the expected aftershock sequence. What few aftershocks occurred were widely separated and quite small. Though the experiment was aborted, contact with the Navy was made to arrange use of an ATF on short notice when it is not otherwise used. The Coast Guard has also been contacted and agrees to provide ship time pending availability of a ship in the incident area.

Some of the difficulties in aftershock chasing are evident. The aftershock sequence itself is not entirely predictable. It is not certain that once a port near the epicenter has been reached we will have transportation to the region of interest. In addition, foreign travel complications have limited the plans to a small geographic area. The faults off Oregon and Washington usually have small quakes occurring in swarms with predominately horizontal motion. This leaves the Aleutian Trench area which, though highly active, contains only a fraction of the large earthquakes occurring around the world.

E. European Activities

The Eastern Mediterranean is normally a region of high seismic activity, spread broadly over Italy, Greece, the Adriatic and Aegean Seas. Discussions with Directors of seismology observatories at Rome, Trieste and Athens revealed that two areas near Greece are especially favorable from the standpoints of high activity, frequent large aftershocks, shallow sources, and aftershock locations that center close to

the main shock. To date, however, there have been no seaquake of even moderate size anywhere in the Eastern Mediterranean this year. The Directors all offered to send immediate notification of seaquakes and the Trieste Observatory volunteered to make preliminary epicenter determinations.

Exploratory discussions were held with COMASWFORSIXTHFLT personnel at Naples, who indicated that measurements might be made conveniently with PB 3 aircraft, though not with surface craft. Dr. Bradner designed a modification for the SSQ/38A sonobuoy for low frequency operation. Exploratory discussions at Sigonella Air Base confirmed that conventional sonobuoys internally modified for low frequency can be used in a conventional way with the PB 3 aircraft. The aircraft are already equipped with gear for navigation, buoy location, and multichannel signal recording. The only necessary addition to their standard equipment would be a small low speed strip chart recorder. Simple interface equipment has been built (Figure 9) Preflight test gear has also been constructed. The airborne operation would be very similar to a normal ASW flight. A detailed Operations Plan has been drafted, and is available if desired for future studies. As a result of a Scripps decision to drop the Mediterranean part of this project COMASWFORSIXTHFLT personnel and the above mentioned Directors of seismological observatories now have been informed that preparations for the operation have been terminated.

61

---

1. Richards, *BSSA*, In print

2. Cloud & Maley, Preliminary comments on strong-motion data from the San Fernando California Earthquake of February 9, 1971. *BSSA, 61,* (2) 497-498 (April 1971)

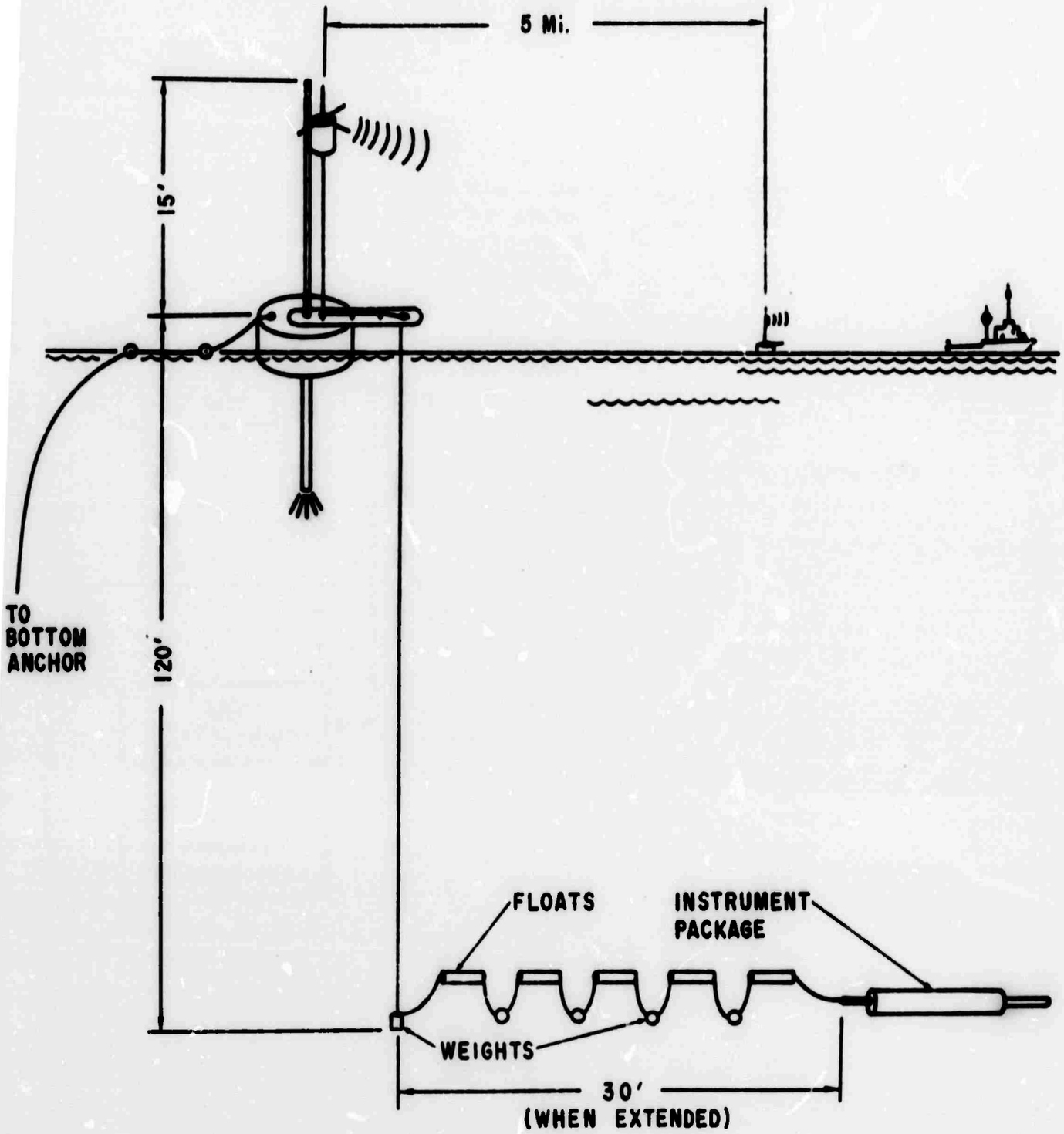

Figure 1

Ship-deployed Instrument in operation

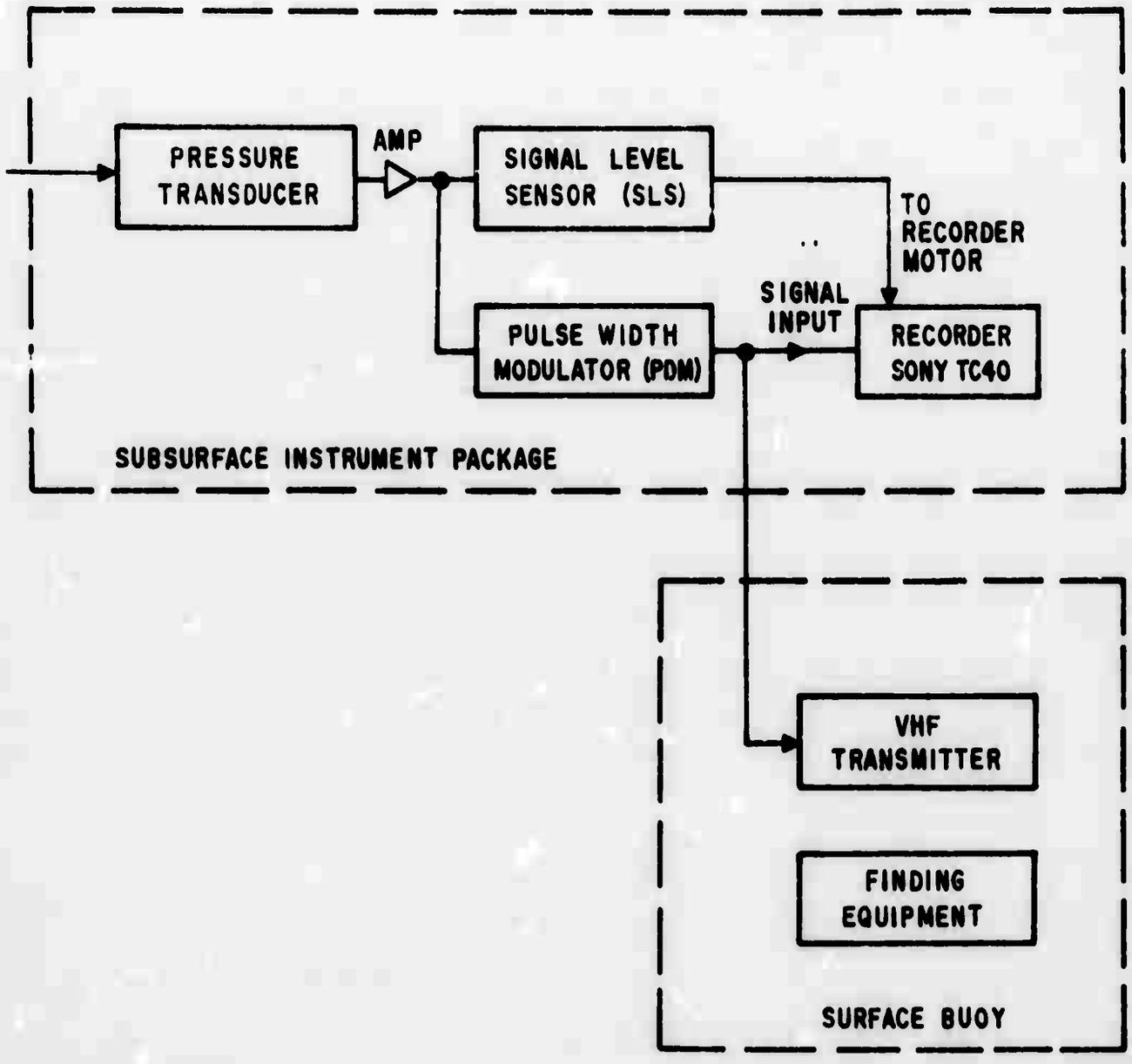

Figure 2

Block diagram, Ship-deployed Instrument

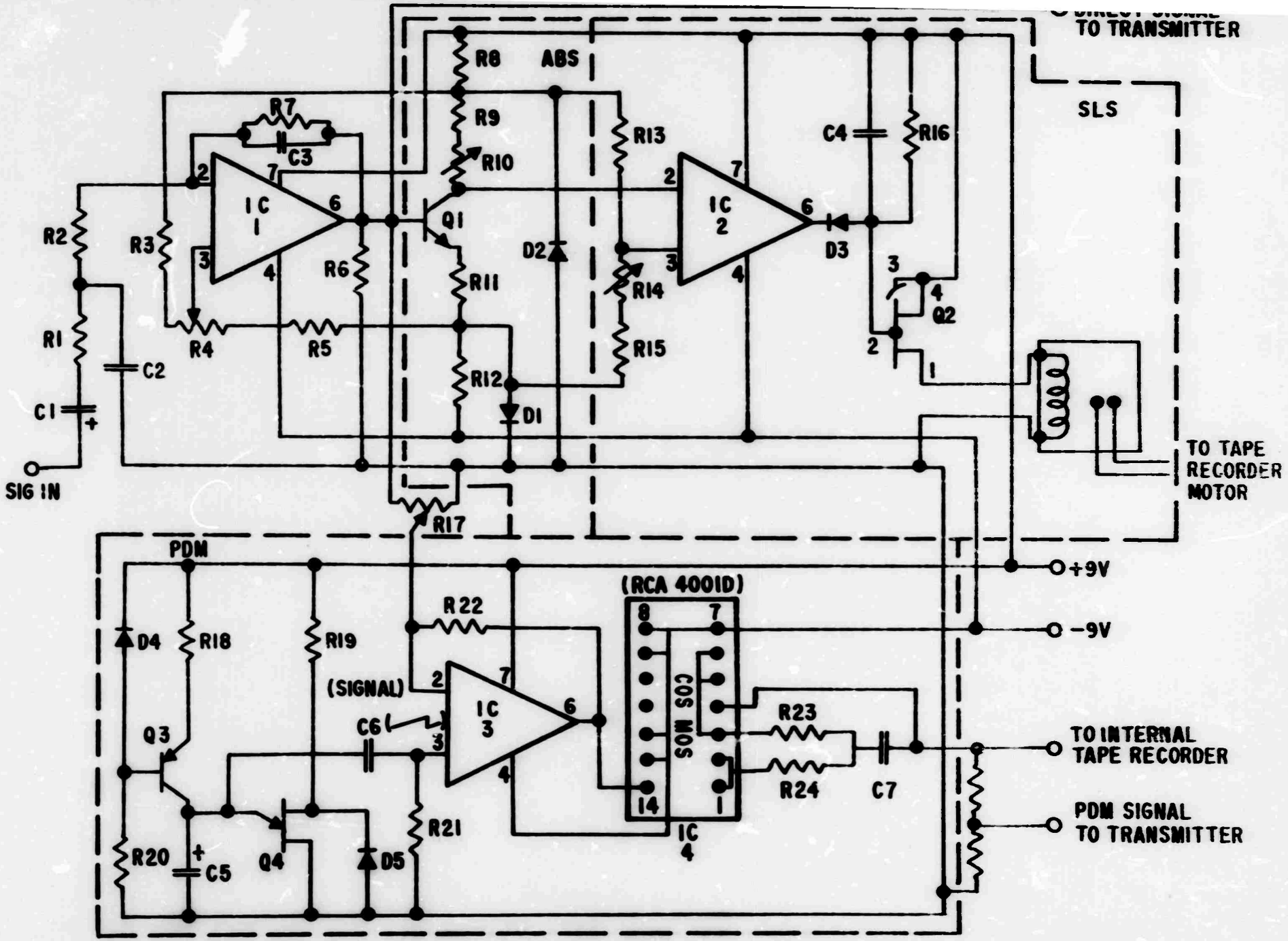

Figure 3. Instrument Package Schematic

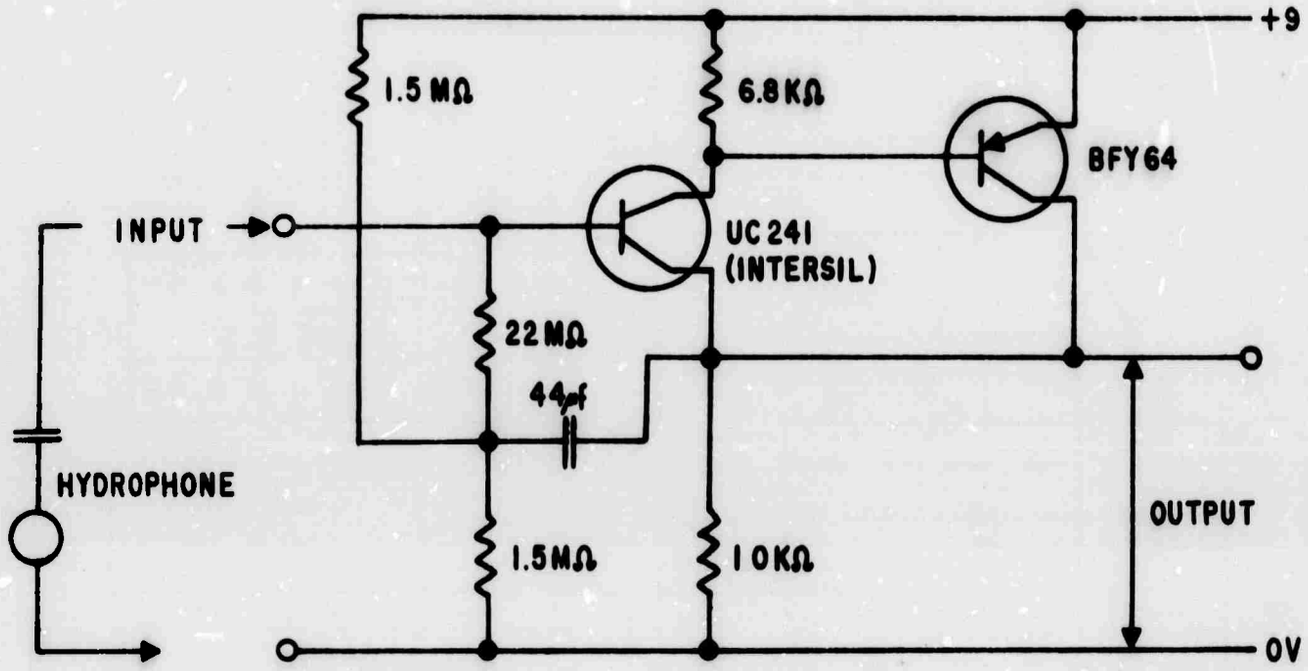

Figure 4

2000 Megohm input impedence preamplifier

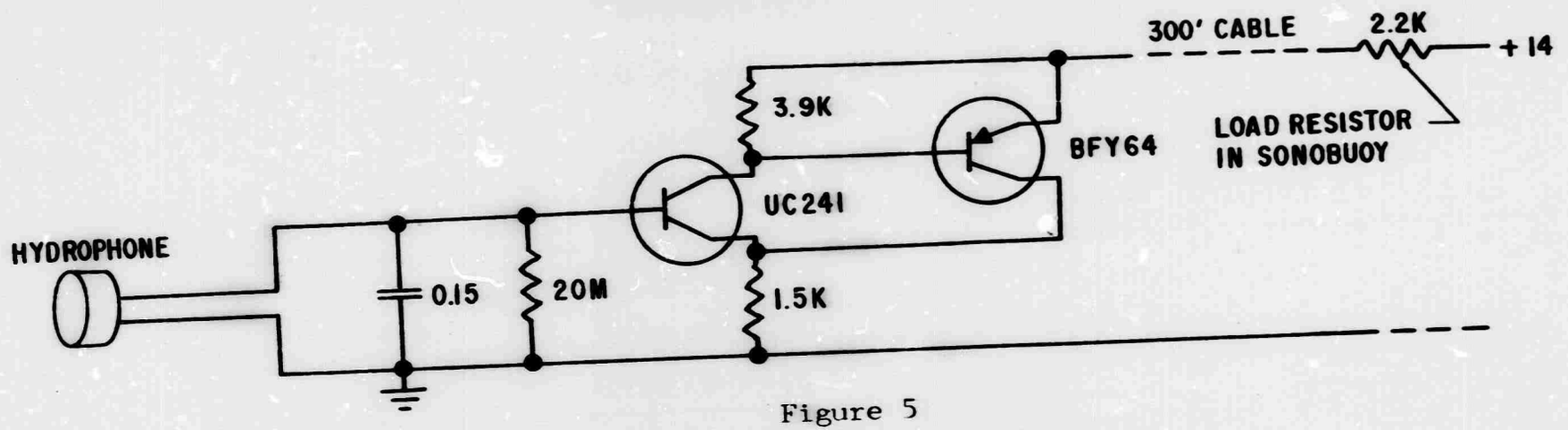

Figure 5

20 Megohm input impedence preamplifier

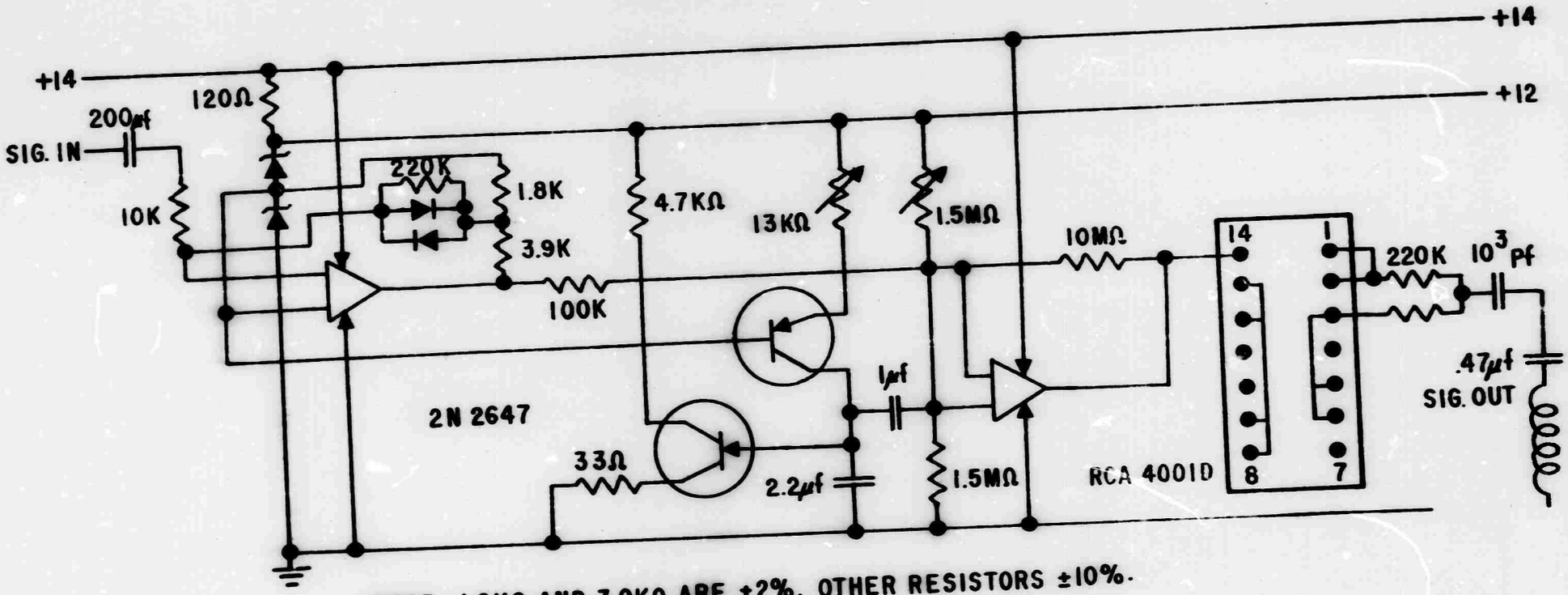

NOTE: 1.8KΩ AND 3.9KΩ ARE ±2%. OTHER RESISTORS ±10%.

Figure 6

Logamp - PDM circuit

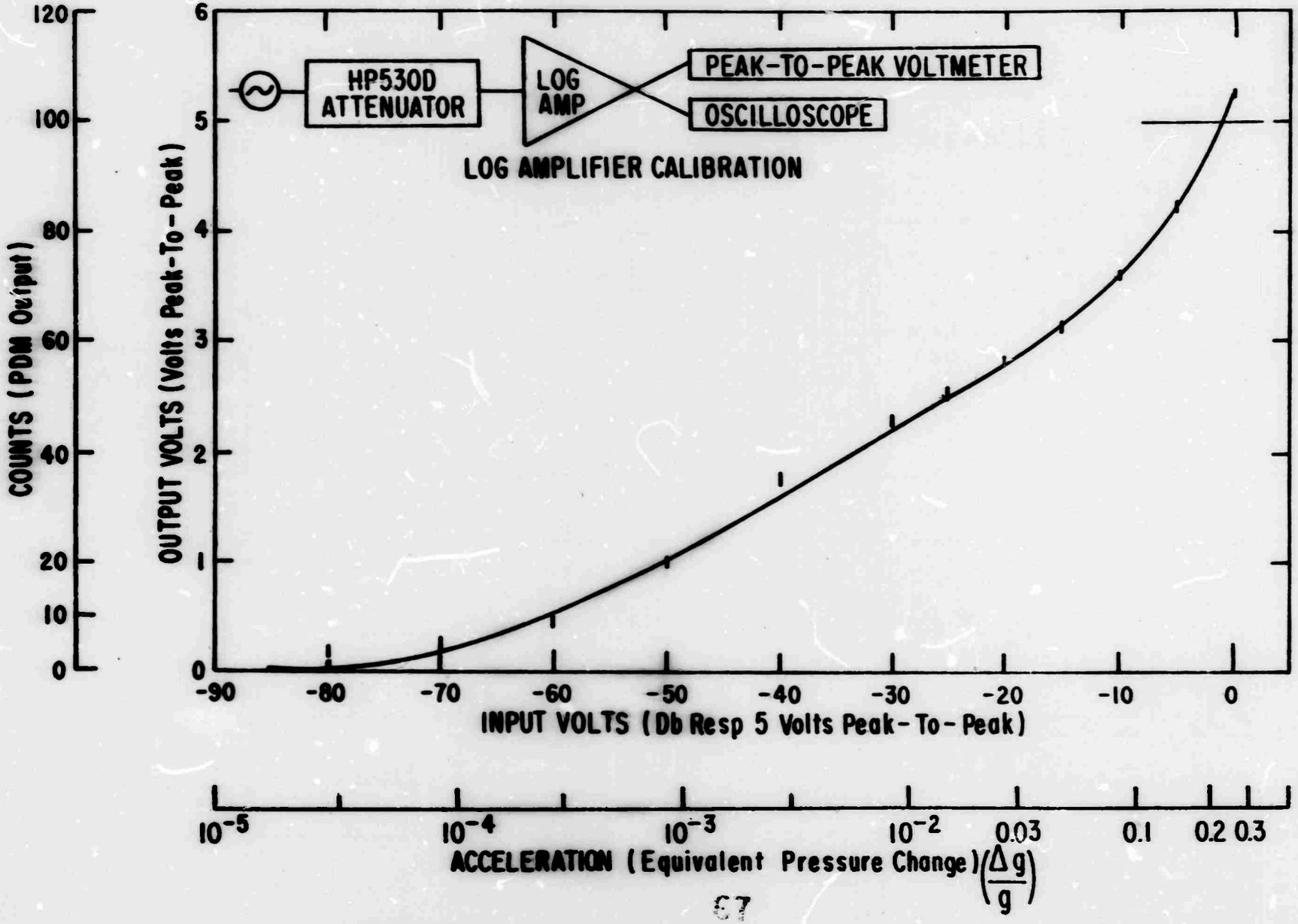

Figure 7. Log Amplifier Calibration (AC input)

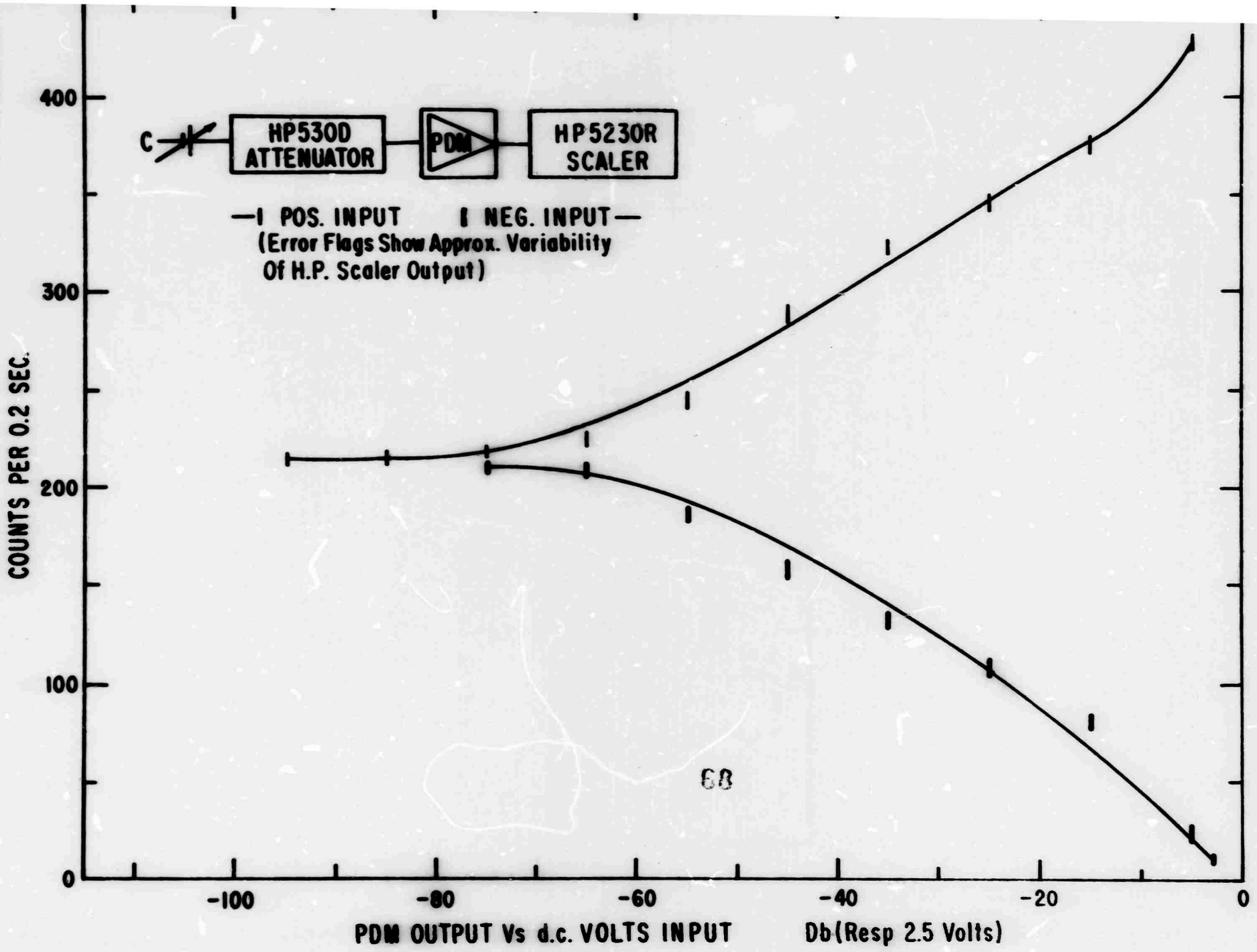

Figure 8. Log Amplifier Calibration (Plus and minus DC inputs)

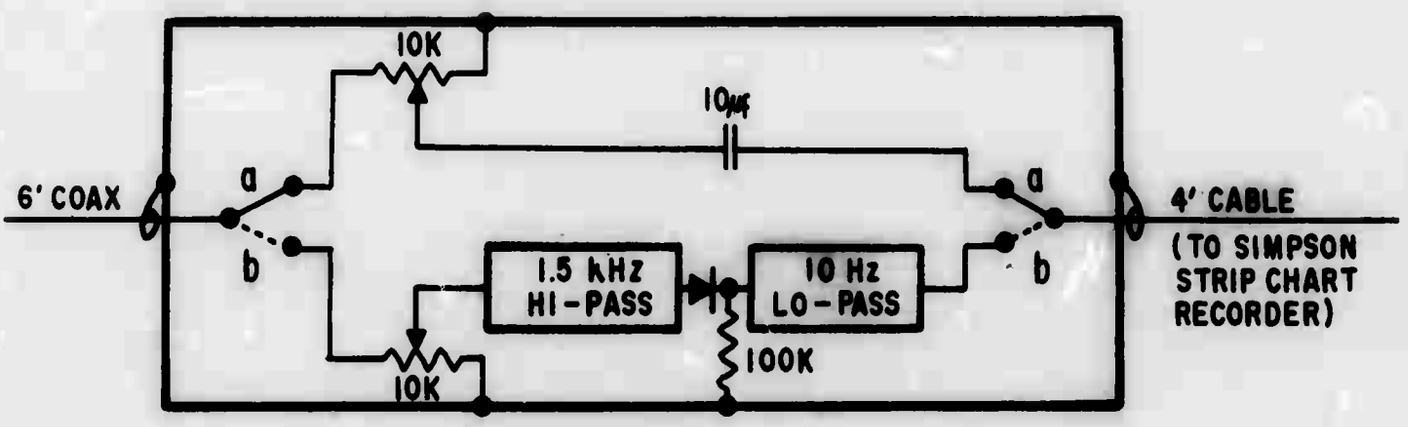

Figure 9

Interface equipment for PB-3 aircraft

Part IV

ADVANCED STUDIES IN NEARSHORE ENGINEERING

Co-Principal Investigators

Dr. Douglas L. Inman
Phone (714) 453-2000, Extension 1175

Dr. William G. Van Dorn
Phone (714) 453-2000, Extension 1179

ADVANCED OCEAN ENGINEERING LABORATORY
Sponsored by
ADVANCED RESEARCH PROJECTS AGENCY
ADVANCED ENGINEERING DIVISION

ONR Contract N00014-69-A-0200-6012

Part IV
Advanced Studies in Nearshore Engineering

Table of Contents

List of Tables

List of Figures

BLANK PAGE

I. PROJECT SUMMARY

Studies of the transport and circulation mechanisms which are cooperative in the nearshore zone (as they apply to military and civil pre-engineering) increasingly emphasize the importance of the interactions between waves, currents and sediment at the water-sediment interface. These studies have concentrated on understanding of the wave-current interactions in terms of: (1) the velocity field of the water in near-breaking and breaking waves; and, (2) the complex interactions in the boundary layer at the water-sediment interface. They have general application to the design of vehicles or structures intended to perform useful tasks within the surf zone, and particularly to the problems of sand and sediment transport and control.

A summary of the work done in the above two categories follows:

1. A laboratory study of the velocity and momentum fields in breaking waves, with the object of defining not only the particle displacements, velocities, and accelerations within individual waves, but the net circulation induced by their combined interactions over representative beach slopes. Present progress includes: (a) completion of revised instrumentation for measurements as a function of time and position, of flow velocity, particle displacements and trajectories, surface elevation, and sub-surface pressure; (b) eighty percent completion of a series of flow measurements, comprising over 1000 test runs and 7000 data points, taken within wave trains at four different periods, and incident upon each of three beach slope angles. All data are programmed on punch cards for computer processing. Analysis of the data thus obtained is well under way, and some preliminary results are included in the text, and; (c) design and partial construction of a

portable instrumentation platform for field observations.

2. A field and laboratory study of the water-sediment interface under wave action, that includes: (a) analysis and comparison of wave-induced boundary layer theories with previous laboratory investigations over both smooth and rough bottoms; (b) measurement of the interface geometry and interpretation of motion films of particle movement at, and above, a naturally rippled water-sediment interface in the Pacific Ocean, and on an intermediate scale near the surf zone in the Gulf of California, Mexico; and, (c) construction and testing of phase-dependent roughness elements in the hydraulic laboratory wave tank.

The foregoing summary reflects only a portion of our overall program. During the next half-year, work will include:

1. A detailed, joint field study of nearshore circulation in three dimensions, to be conducted in the surf zone adjacent to the Scripps institution. This study will include simultaneous observations of orbital and mean velocities at a number of different stations, with the object of defining the energy balance, modal shelf interactions, and the general circulation scheme in a natural environment, and on a time scale of enough duration to observe trends important to the determination of sediment transport.

2. Continuing adaptation of specialized instrumentation and techniques for measuring important flow, circulation, and transport parameters. This will include hot film probes, two types of new current meters, and a high resolution sonar for in situ measurement of ripple geometry.

3. The continuing study of full scale mechanisms and devices for controlling sediment transport, erosion, and deposition. These include:

phase-dependent roughness elements, modular structures for flow control, and the construction of artificial undersea barriers.

These findings promise to lead to new technology that will permit the control of erosion and deposition by phase-dependent roughness elements placed on the ocean floor. A "crater sink" sand transfer system proposed earlier in this study (Inman and Harris, 1970) provides a revolutionary and inexpensive mechanism for transport and control of the budget of sand along coastlines. Together, as a system, these technologies should permit the rapid development and deployment of portable harbors along sandy coasts that will be free from the severe problems of erosion and deposition. The perfection of this system will be the subject of next year's proposal for continuation of this project.

II. VELOCITY FIELD IN BREAKING WAVES

A. OBJECTIVES

This is a comprehensive laboratory and field investigation of the velocity and momentum fields within the breaker zone which is formed by a succession of waves approaching a sloping shoreline. We are concerned not only with the motions within individual waves, but also with the mean surging motions that result from their interactions. This study is basic to the mechanics of sediment transport, as well as to the engineering design of any structures intended to function within, or to withstand the effects of breaking waves in shallow water.

To our knowledge, there is no adequate theory that describes motions in this regime, nor any previous study that provides a basis for such a theory. Therefore, a second objective is to describe these fields in useful parametric form, and to attempt to advance the theory of wave behavior by an explanation of them. The study is divided into two phases: a laboratory study of trains of periodic waves breaking on uniformly sloping beaches, and a field phase where similar measurements will be conducted in the ocean.

B. METHODOLOGY

Our techniques (more fully described below) comprise five independent sets of measurements:

a) quartz hot-film fluid velocity probes (0.5 ms response)

b) fluid pressure at bottom, beneath probes

c) digital surface elevation and wave run-up staffs

d) strobe photography of wave profiles and neutral-density particles for orbital velocity and displacements

e) single-exposure streak photography for fluid direction

Observations have been conducted at 6 to 12 probe elevations, eight stations, and four wave periods, for each of three uniform slopes, covering the full range of natural (prototype) wave conditions on a scale of 1:16.

As previously noted, Inman and Van Dorn (1970), our study is being conducted in two phases:

a) laboratory phase. A comprehensive investigation of water particle motions in trains of breaking periodic waves incident upon uniformly-sloping beaches has been conducted in the 100 foot, glass-walled wave channel at the SIO Hydraulic Facility. The measurement program is 80% completed, and data are being processed and analyzed on the IBM 1130 computer. Some preliminary results are included below.

b) Field phase: A somewhat-similar, but less extensive, series of observations in the oceanic surf zone will be carried out this summer and fall in conjunction with other field measurements. Work is in process on a portable platform capable of supporting the necessary instrumentation in the breaker zone.

Because of the difficulties previously reported in obtaining stable and reproducible operation of the hot-film velocity probe anemometers, and also because it was found impossible to monitor flow continuity and phase velocity of multiple wave systems with flash photography, instrumentation for the laboratory phase was completely revised during the period Jan-Mar 1971. The system finally employed for our experiments is shown in Figure 1, and contains the following components:

a) A 50 cm digital wave staff, permanently located 2 m before the toe of the beach slope, records incoming wave elevations before shoaling transformation.

b) A permanent 5 m digital staff just over the beach slope records water motion at the shoreline.

The remaining sensing devices were mounted on a traverse car, capable of being rolled to any position along the wave channel. Among the devices mounted on the car are:

c) Two 20 cm digital staffs for monitoring local elevation and phase velocity of individual waves. These staffs can be raised and lowered by a rack and pinion.

d) Two hot-film water velocity probes mounted on similar racks can also be vertically adjusted, and raised clear of the water for calibration before each data run.

e) A vertical 2 m cylinder, supply pump, and flow nozzle provide a means of dynamic flow calibration between runs. The cylinder is filled with water, the nozzle slipped over a (raised) velocity probe, and the water is discharged under decaying hydrostatic head, its level being indicated at known intervals

by electrical contacts in the cylinder wall. From simultaneous records of probe output voltage and discharge, as a function of time, each probe can be calibrated over its entire range (10-250 cm/sec) in about 2 minutes.

f) A pressure transducer on the car is connected to a tube strut, which can be vertically adjusted to just clear the bottom.

g) Stroboscopic flash or flood lights at the car ends provide illumination for telescopic polaroid photography through the glass side walls.

Equipment changes also include:

a) Purchase of two DISA Model 55D01 hot-film anemometers to replace the unstable model 55D05 units previously purchased, which were returned for credit. The new units cost three times as much, but have performed perfectly and retain their calibration without continuous readjustment.

b) The purchase of a Varian Statos III eight-channel strip chart recorder to replace a Brush six-channel recorder on loan from the SIO Ocean Research Division. The response of this recorder is fifty times faster (1-KHz) than the Brush unit, and the two additional channels were needed for the traversing elevation sensors.

All laboratory experiments were conducted in the 0.5 m x 1.2 m x 30 m, glass-walled wave channel at the SIO Hydraulic Facility with a uniform still-water depth of 36 cm. On a prototype-model scale of 16:1, the wave and beach slope parameters shown in Table 1 covered the full range of prototype conditions normally encountered on local beaches proposed for field experiments. The eight observation stations were experimentally

altered for each beach slope and wave period, so as to best observe all phases of wave development. As depicted schematically in this figure, each test run comprised a sequence of five waves, whose total duration was limited by the time required (about 18 seconds) for the first wave to be successively reflected from the slope and wave generator, and to return to the first sensor. All wave trains were produced at the maximum generator stroke setting. Thus, wave breaking heights were highest (20 cm) for the shortest period, and lowest (10 cm) for the longest.

At each observation station, test runs were repeated from four to eight times with the velocity probes at different elevations, and facing both into and away from the incident wave direction, so as to obtain relatively complete velocity profiles within each wave. Sensor calibrations were checked, and repeated, if necessary, at each station position.

Following completion of the velocity measurements, all runs were repeated, taking stroboscopic flash photographs of neutral-density, nitrile-rubber spheres at 1/10 sec intervals to obtain particle orbit displacements and velocities, as well as sequential wave profiles. Secondly, streak photographs of smaller particles were taken with flood lighting and 1/5 second exposures to obtain particle trajectories at all points within the flow field.

All told, over 1000 test runs were made, comprising more than 7000 data points, exclusive of photography. Thus, we believe that the flow fields are fairly completely determined for all input conditions. Any experiment is readily reproducible, should additional data be needed.

C. TECHNICAL RESULTS

Owing to instrumental problems, instrument reconversion, and periodic interruptions, the laboratory experiments required about two months longer to complete than estimated at last reporting. As a result, data processing and analysis have been similarly delayed, and are being carried out in conjunction with preparations for the field experiments described below. However, some early results are forthcoming, which can be summarized as follows:

Our experiments were generally patterned after, and included the same range of wave parameters as those reported by Divoky, et al (1970), with the exception that their breakers were produced in uniform water depth by horizontal channel convergence, so adjusted as to maintain virtually constant breaking height. Because our gear-driven wave generator could not be adjusted to exactly reproduce their experimental wave periods, and also because our waves were substantially higher for similar wave periods, only qualitative comparisons between our results can be made here.

Based on an assumed equivalence between horizontal energy convergence and that inferred from conservation of energy flux over uniform slopes, Le Mehaute (1960) and Divoky present curves showing relative breaker height H/H_b versus relative breaker depth h/h_b for a wide range of beach slopes $1/S$, where H is the incident wave height in water of depth h ahead of the slope (Figure 3). Our data for four wave periods at four stations (D-G, Figure 2), breaking on a 1/25 slope, do not appear to support this theoretical model, except in the immediate vicinity of breaking. Our relative breaker (bore) heights were consistently higher than those reported by Divoky, et al (1970) although this may, in part, be due to

the transient surge over the slope produced by an impulsive train of five waves, which would be expected to give higher relative heights than in the steady-state experiments of Divoky, et al (1970). This effect will be examined in detail before final reporting.

Preliminary comparison of our velocity profiles with those predicted by the Stokes third-order wave theory (Skjelbrea, 1959), and the cnoidal theory of Keulegan and Patterson (Mash, 1961), are shown for incident waves of 1.6 second period in the uniform depth section of the channel (Figure 4), and at the breaking point (Figure 5). The latter figure also shows experimental data for the same wave period from Divoky, et al(1970). These profiles are typical of some 22 cases so far reviewed, from which we tentatively conclude that:

a) Both cited wave theories converge to common velocity profiles that are reasonably close to the observed values for small, but finite, amplitude, periodic waves in uniform depth; both predict profiles and gradients that are much too large, when applied to waves near the breaking point.

b) Experimental data in a convergent channel are in close agreement with those measured over a slope, thus justifying the above-cited energy-flux equivalence. This result is of great importance, since it says, in effect, that waves of similar steepness have the same velocity profile and will break in water of the same relative depth. This implies that the velocity profile is a critical breaking parameter, and is a much more sensitive index than the wave profile.

For all wave periods, the time histories of surface elevation at the shoreline (Station H, Figure 2) consisted of single smooth surges

Figure 6). Over the 1/25 and 1/50 slopes, individual crest arrivals from a five-wave sequence could not be distinguished, although they show up as small perturbations on a 1/12 slope. This result demonstrates the importance of wave-wave interactions over gentle slopes, and accounts for much of the ambiguity of run-up data previously reported for breaking waves (Battjes, 1971). This mass-surging action is clearly of dominant importance to nearshore circulation, and its elucidation will be one of the key objectives of our analysis.

In summary, our preliminary data reveal a wealth of heretofore unstudied phenomena, too numerous to report at this date, but which give promise of the first significant breakthrough in the study of nearshore breaking dynamics. Despite our initial difficulties with hot-film probes, they have ultimately proved invaluable in determining not only the flow characteristics, but also the magnitude and range of turbulent fluctuations after breaking.

D. CONTINUING WORK

In accordance with our original proposal, a series of field experiments under natural ocean wave conditions is projected for late summer and early fall, 1971. Our experiments, again confined to determining the velocity field within and near the breaker zone, will form a portion of a larger field program aimed at measuring various other aspects of nearshore circulation. For our purposes, the incoming wave field will be monitored by bottom-mounted pressure sensors outside the breaker zone, and surface elevation, as a function of time, will be recorded at several points within the surf zone, using digital wave staffs.

Because the incident wave field comprises a spectrum of wave heights, directions, and periods, and also because natural waves often combine and

reform within the surf zone, the velocity field at a single point cannot be determined on a wave-by-wave basis, but instead must be regarded as a continuum resulting from the interactions of numerous wave ensembles. However, by simultaneously recording wave elevations and the inshore-offshore and longshore components of velocity at one or more subsurface points, and by altering the vertical locations of the velocity sensors, at intervals of, say, 10 minutes throughout a tide cycle, statistics can be accumulated, which we hope to correlate with other data to interpret as:

a) The maximum horizontal velocity components as a function of wave height, period, and elevation, and;

b) The mean velocity and momentum as a function of elevation in the low-frequency surf-beat modes of the nearshore circulation system.

The former we hope will confirm our 1/16 scale laboratory experiments, and the latter will provide input to the more general problem of the dynamics of nearshore circulation.

Our present DISA hot-film sensors appear to function satisfactorily in sea water, and are not significantly affected by temperature fluctuations over the range normally encountered on an hour-by-hour basis. Their range (20-500 cm/sec) is adequate for the largest anticipated velocities. The principal problems now being investigated is their sensitivity to natural debris and dissolved gases, and methods whereby frequent calibrations can be conducted in situ. Our present laboratory calibration scheme will be resorted to, if necessary, but we hope to find a more convenient means, such as mechanically oscillating the probes at known amplitudes and frequencies.

84

b) Elevation measurements: We are constructing a special digital wave staff 4 m long, which will accomodate the anticipated range of wave heights.

c) Sensor platform: We plan to mount both velocity sensors and wave staff on faired, rigid struts, dependent from a portable platform that can be easily assembled and disassembled at any desired point within the surf zone, as shown schematically in Figure 7. The top of the platform will be always above water, and includes provisions for the necessary support electronics and an operators seat. Amplified signals will be cable-transmitted to a shore-based recording van. By installing the platform near shore at low tide, intermittent recording throughout a tide cycle will, in effect, move the surf zone relative to the platform, such that the entire surf zone can be sampled in one or two steps.

E. FUTURE STUDY

During our present investigations, we have become aware that there exists a large "grey" area in wave dynamics that is almost completely unstudied: the breaking of storm waves in the open sea. While there have been significant recent advances in the statistical theory of sea state under storm conditions, there is no mention of, let alone a prescription for, the number of waves that are breaking at any instant. Yet, aerial photographs indicate that most of the waves are breaking at elevated sea states. At the same time, it is evident that many practical applications of sea state information would benefit from an understanding of breaking dynamics, and breaking statistics.

Our present instrumental capability, and the availability of the new 8' x 8' x 150' ARPA wind-wave channel with a programmed wave generator and auxiliary IBM 1130 computer, provide the necessary and compatible facilities for a detailed study of:

a) Velocities and accelerations in mixed-frequency, reproducible "deep-water" wave systems.

b) Evaluation of breaking instability criteria in two-dimensional, random seas.

These studies could be later supplemented with similar measurements at sea, using the SIO Vessel R/V-Flip.

We have solicited advice on, and received strong recommendations for support of such a study from several authorities in this field, and feel that it represents a natural continuation of our present investigations.

Because this program does not fall under the category of nearshore engineering, it will be the subject of a separate proposal to ARPA for consideration for calendar 1972.

III FIELD AND LABORATORY STUDY OF THE WATER-SEDIMENT INTERFACE UNDER WAVE ACTION

The flow conditions in the boundary layer that forms at the water-sediment interface under wave action are poorly understood. Theoretical and experimental studies of the boundary layer over a smooth flat bed have been carried out with some success. Since smooth bed boundary theory provides the only mathematical models for this interface, a summary of this work and its application to the present problem is given in the following section A-1. Definitive studies over a movable sand bed and over artificially roughened beds have not yet been made and are now under study.

Inman and Bowen (1963) showed that the boundary layer over sand beds is dependent upon the nature of the waves above the bed, and upon the bed roughness (ripples) produced by the interaction of the waves and the bed. Generally, the thickness of this boundary layer, referred to as the "vortex-sublayer" is of the order of the size of the ripples. They also showed the intensity and direction of particle motion in the vortex-sublayer is a phase dependent phenomena associated with the bottom roughness. Their experiments, which showed that the difference between net onshore and offshore motion of sand is related to this subtle phase-dependent mechanism, led to the concept that the direction and amount of sand transport could be controlled by properly designed roughness elements.

The field investigations to date have been directed towards understanding the motion in the vortex-sublayer. They are not yet completed because the study has required modification of existing instruments such as the hydrogen bubble tracer and the high resolution sonar (Section III-C).

The laboratory phases of the boundary layer study and the water-sediment interface study will be conducted in the two wave channels in the hydraulic laboratory. The laboratory phase has been delayed because of the use of these facilities for the study of the velocity field in breaking waves (Section II) and for other ARPA supported projects. However, initial work on feasibility of phase-dependent roughness elements to modify and control sediment movement has started. The results to date from this work are described in section B2.

A. BACKGROUND THEORY AND EXPERIMENT AT THE WATER-SEDIMENT INTERFACE

1. smooth bottom theory

Present theories for an oscillating flow over a smooth, stationary boundary may be traced to Lamb (1932) in which the equations of motion are solved to yield the equation for the velocity profile in the boundary layer (u).

$$u = u_\infty + A \exp(-a/\delta) \cos(kx - \sigma t - z/\delta) \qquad (1)$$

where $$u_\infty = \frac{\pi H}{T} \frac{\cos(kx - \sigma t)}{\sinh kh} = A \cos(kx - \sigma t)$$

is the orbital velocity near the boundary associated with the potential flow of the progressive wave. The boundary layer thickness δ is

$$\left(\frac{2\nu}{\sigma}\right)^{\frac{1}{2}}$$

where H is the wave height, T is the wave period, h is the water depth, L is the wavelength, $\sigma = 2\pi/T$ is the radian frequency, $k = 2\pi/L$ is the wave number, z is the vertical cartesian coordinate which is zero at the bottom, and ν is the kinematic viscosity of the fluid. The thickness of the boundary layer δ over a smooth surface is about 2 mm for a 10 second wave in 10°C sea water. Longuet-Higgins (1961) shows that this solution might apply to both laminar and turbulent boundary layers. Note that equation 1 shows a phase lead for the velocity u in the boundary layer over the velocity u_∞ in the potential layer just above the boundary. Sleath (1970) found he could predict the velocity profile in a wave induced boundary layer over a flat bed

of coarse sand (median diameter 1030 μ) by modifying equation 1:

$$u = u_\infty + A \exp(-z/c\delta) \cos(kx - \sigma t - z/c\delta) \qquad (2)$$

where $c = 1.8$ is a dimensionless empirical correction factor.

2. boundary layer over a rough bottom

Kajiura (1968) proposed a three layer model to describe the boundary layer under water waves. The turbulent eddy viscosity is different in each layer. The governing equation in Kajiura's theory is:

$$\frac{\partial^2 u^*}{dz^2} - \frac{i\sigma u^*}{\epsilon} = 0 \qquad (3)$$

where $u^* = \left(\frac{\tau}{\rho}\right)^{\frac{1}{2}}$ is the friction velocity; τ is the bottom stress; ρ is the fluid density; i is $\sqrt{-1}$; and, ϵ is the kinematic eddy viscosity. This equation was solved in each of the three proposed layers.

Horikawa and Watanabe (1968) conducted experiments in a flume to attempt to verify Kajiura's solutions. They used a hydrogen bubble technique to obtain the velocity as a function of height above the bottom. These tests were conducted over both smooth and artificially rough bottoms. Differences between theory and experiment were about 1 to 5%.

Sensing that this model may be too artificial in that it contains many arbitrary constants, a model is being studied with an eddy viscosity which increases exponentially away from the bottom. The proposed model equations have been transformed to a zero order Bessel equation of the form

$$z^2 \frac{d^2u}{dz^2} + z \frac{du}{dz} - i\delta^2 z^2 u = 0 \qquad (4)$$

The solutions of this equation are currently being investigated as well as other types of eddy viscosity models.

In addition Johns (1970) proposed that the velocity in the boundary layer could be given by

$$u = u_\infty(x)\left(1 - F(z')\right)e^{i\sigma t} \qquad (5)$$

where $F(z')$ satisfies

$$\frac{d}{dz'}\left(\epsilon \frac{dF}{dz'}\right) - 2iF = 0 \qquad (6)$$

and $z' = z/\delta$ is the non-dimensional distance from the boundary, and the other terms are as described before.

Johns solves equation (6) numerically and gives plots of real and imaginary parts of $F(z')$. Values from this plot have been used to compute the velocity as described by equation (5). Figure 8 compares the velocity profile obtained by this method with a profile obtained by Jonsson (1963). The data of Jonsson (1963) was obtained in an oscillating water tunnel with artificial bottom roughness elements. If the modified theory of Johns can be fitted to the Jonsson data, a possibility exists to predict the flow field over natural and artificially controlled rough bottoms.

Future work along these lines will consist of programming Johns' equation (5) and varying ϵ to try and obtain a better fit between theory and experiment.

3. Vortex sublayer

All of the preceeding theories were based on smooth boundary theory and extended by artificial coefficients to rough boundaries. Some of the experiments, notably those of Horikawa and Watanabe and Jonsson were conducted over artificially rippled bottoms.

Over a rippled sand bottom, Inman and Bowen (1963) estimated the thickness of the boundary layer to be about one-half of the ripple wavelength. Further, they described the mechanism by which sand is lifted off the bottom and injected into the water column so it can be transported (Figure 9). During passage of the wave crest and trough, when there is the maximum horizontal velocity, eddies form in the lee of the ripple crests. These eddies are quite intense and entrain sediment from the lee slope of the ripple. During periods of velocity reversal, deceleration permits the eddies to rise above the ripple crests (to heights greater than the boundary layer thickness δ), carrying sediment with them. As the flow accelerates again this suspended sediment is carried by the flow until it settles out because of gravity.

B. TECHNICAL RESULTS

The field work has concentrated on developing a better understanding of the processes occurring at the water-sediment interface over rippled natural sand bottoms in order to be able to properly design phase dependent roughness elements. These preliminary experiments had to be carried out because of the dearth of information on the wave induced fluid dynamics over rippled bottoms. Once this work is completed, more rigorous criteria will be available for the design, construction and laboratory testing of phase dependent roughness elements.

1. Field studies

The field studies were carried out in the ocean to the south of the end of the Scripps Pier and outside the surf at El Moreno Beach on the Gulf of California. The work at Scripps consisted of the photographing of confetti particles injected in the water-sediment interface and in the potential layer above. Confetti particles were used because they are more-or-less neutrally buoyant and they follow the water motion fairly well. The photographs were taken with a scuba diver operated 16 mm movie camera and were shot against a wire grid for scale. The grid was located in approximately 6 meters of water and was oriented normal to the ripple crests.

Typical particle motion in both the boundary and potential layers for one of the data runs is shown in Figure 10. This figure shows confetti particle motion for 17 seconds during a portion of the observation of time series DAS 250 (spectrum for DAS 250 is shown in Figure 11). From this plot wave period T and instentaneous velocities in the potential layer can be directly measured. The ripple wavelength λ is about 10-12 cm, suggesting δ by the Inman-Bowen criterion would be about 5-6 cm. The trace of a confetti particle being lifted by the expanding lee-vortex is shown in Figure 10. As the particle moves over the crest just before the velocity reversal, it is caught-up as the eddy rises and is swept offshore by the now accelerating offshore flow, whence it is transported over several ripple crests while it is settling.

Phase lead in the boundary layer can also be observed with this technique. This is done by recording the time confetti particles at different levels change direction at velocity reversals. For example, during the frames shown in Figure 10, confetti less than 2 cm above the

the bottom reversed at frames 55-56 while particles 5 cm and above reversed at frame 58. This indicates a 1/2 to 3/4 second (14 to 21 degree) phase lead for this wave, which has a period of 13 seconds.

Although the confetti particles follow the fluid fairly well and are quite easy to photograph, their actual physical size and random placement on the bottom and in the water column limit the boundary layer resolution. The necessity of locating the camera housing above the bottom causes parallax problems at the interface. New techniques are being developed and tested to improve the resolution at the interface (see instrumentation).

During the most recent field trip to El Moreno, Baja California, Mexico (7-11 May 1971), measurements were made of wave formed ripples, in conjunction with a series of other nearshore environmental measurements were recorded on a magnetic tape data acquisition system (DAS). Sections of the bottom, seaward of the breaker zone, were sampled with one meter long, greased metal sheets, 6 inches high. The samples were brought to shore and ripple wavelength λ, height η, and assymetry measured directly. The data from four samples taken at approximately the same place and time during DAS 323 is given in Table 2. Here $\bar{\lambda} = 1.93 \pm 7.1$ cm (95% confidence limits), and $\bar{\eta} = 1.3 \pm 0.5$ cm.

2. Laboratory studies of phase dependent roughness elements

Laboratory work to determine the ability of phase dependent roughness elements to control sediment movement has commenced. Design of the elements is based on the observation by Inman and Bowen (1963) that assymetrical ripples can modify sediment transport by enhancing the formation of vortices during one part of the wave phase relative to the other part. Since the sand suspension mechanism (and therefore the

sand transport) depend on the strength of the vortex, transport over asymmetrical ripples is enhanced during one phase relative to the other.

The initial tests use an asymmetric ripple form which was constructed from aluminum sheet and situated in the hydraulic facility wave channel. The ripple form dimensions are shown in Figure 12. This shape results in a ripple asymmetry factor β/λ of 0.6, where β is the horizontal distance in a down wave direction between the ripple crest and trough. The dimensions used are commensurate with the naturally formed ripples of Inman and Bowen (1963); with the ripple form reversed such that the steeper slope faced up-wave.

The wave channel is 27.5 m long, 84 cm high and 50 cm wide (Figure 13). The water depth for the study was 36 cm. There is a sloping, smooth glass beach down-channel of the work area with a slope of 1:50. This beach effectively attenuated the wave energy through breaking and run-up, thus minimizing reflected waves in the channel. In order to reproduce the horizontal bottom displacement of Inman and Bowen (1963)(d_o = 9.6 cm), waves of 1.66 second period (T) and 8.5 cm height (H) were used. Wave heights of 9.2 cm were also used (d_o = 10.4 cm). The particulate materials used were:

(a) acrylic chips - density - ρ = 1.20 gm/cm^3

(b) polyvinylchloride (pvc) chips - ρ = 1.45 gm/cm^3

(c) Scripps beach sand - ρ = 2.65 gm/cm^3

The acrylic, with its small relative density ($\rho - \rho_{water}$ = 0.20 gm/cm^3), was used to emphasize the nature of the vortex action over the ripples. When the wave phase is such that the horizontal orbital motion is down-channel (corresponding to the passage of the crest), the gentler slope of the ripple, which is now in the lee of the crest, inhibits the

formation of a vortex. When the orbital motion reverses direction and the vortex rises above the crest, it is relatively weak (Figure 9a). Conversely, when the wave phase is such that the horizontal orbital motion is up-channel (corresponding to the passage of the trough), the steep slope, which is now in the lee of the crest, allows a strong vortex to form. On trough-to-crest reversals this strong vortex carries more sediment and carries it higher above the ripple crest than does the weaker vortex (Figure 9b). The net result is that sediment transport is enhanced down-channel relative to up-channel.* Figure 15 is an eight frame sequence photograph over one wave period showing the reaction of the acrylic particles to the wave phase. The phase is indicated by the water surface trace in the upper part of each frame. It is seen that the plumes over the crests are higher just after the trough-to-crest reversal (frame 2) than after the crest-to-trough reversal (frame 5).

To study the effect of an artificial asymmetrical array of ripples in controlling sediment transport, PVC chips were placed in the first trough (up-wave) and subjected to the motion of a train of waves of height H = 8.5 cm and T = 1.66 seconds. After passage of the first wave crest about a third of the chips had moved into the trough of the second ripple. After passage of the first wave trough (i.e., up-channel orbital velocity) only one or two chips moved up-channel. During succeeding waves, the chips continued to move exclusively down-wave so that after the fourth wave crest some chips had traversed the whole ripple array (21.0 cm). After the passage of the fifth wave crest, only a few chips were left in the up-wave half of the array; the majority were either in the down-wave half of the array or had traveled beyond the artificial array of ripples.

95

* (cf Figure 14 A & B symmetrical ripples)

C. INSTRUMENTATION

1. High resolution sonar

In order to be able to characterize the wave induced boundary layer over a rippled bottom, the size of the ripples (wavelength and height) must be accurately measured. The old method which employed scuba divers laying plastic T-squares over the ripples worked well for measuring ripple wavelength λ. No comparable method for accurately measuring ripple height η was developed. Other investigators at Scripps have developed a high resolution sonar for analysing the depth of penetration of the track of an underwater vehicle. We are modifying this instrument for accurate measurement of ripple geometry.

The sonar unit will be mounted on a one-to-two meter long track and will be powered by a small motor. The track will be placed across the ripples by scuba divers. When actuated the sonar unit will traverse the track and the difference in phase of the signals will be recorded. Using a 3.5 mega Hz signal, a resolution of 1 mm or better is expected.

2. Hydrogen bubble generator

The hydrogen bubble technique has been successfully used in flume studies to determine the velocity profile in the boundary layer. This technique employs a fine platinum wire (2.5 to 10 μ) attached to the anode of a battery to create a line of hydrogen bubbles. When the wire is placed in moving water and activated for a short length of time (approximately a millisecond) the monolayer of bubbles which formed on the wire is swept off by the current and the position of the bubbles as a function of time describes the fluid motion. The small size of the wire and holder permit insertion directly into the boundary layer with minimal distrubance of the flow. Usually in the laboratory the bubble trace is recorded on motion picture film which can then be analyzed frame-by-frame.

This photographic technique will be used in the field with appropriate modifications to compensate for suspended material in the water.

A pulsing circuit has been developed to drive the hydrogen bubble generating wire (Figure 16). The circuit has a variable pulse width which is changed by changing resistors. Output voltages and pulse width will be first determined in flume experiments. When final design is completed, the circuit plus platinum wire will be mounted on a frame for in situ boundary layer velocity profile studies.

3. Electromagnetic flowmeter

A great deal of time has been invested in the search for a suitable flowmeter for the use of the Shore Processes Research Group. Existing instruments, of the inferential type were reviewed and discarded and the following guidelines became a policy. Any suitable meter must be: (a) passive; (b) minimally-inferential; (c) rapid (response time 1/10 second or less); (d) hydrodynamically streamlined in form, and of sufficiently small dimensions to enable the sensing of orbital motion; (e) capable of sensing at least two orthogonal directions; (f) drift free; and (g) reliable as flow decreases and approaches zero.

Two meters were seriously considered*/, and of the two the Colnbrook meter, modified from the Tucker two-component ships log (Tucker, 1970) was selected. The Tucker meter was developed to measure ships speed, and also by means of the cross component of flow to measure lee way or sideways drift of the ship when it is extended below the ships keel.

*/ Bowen, A. J. and D. L. Inman, 1971, Personal communications

With a shorter response time it is now available to measure any two of three components of flow. The sensor is mounted on a spar in the water and a coil with an oblate spheroidal shape carries two sets of two electrodes on its outer encapsulated surface. The shape, in section, is 11.4 cm on the major axis and 3.8 cm on the minor axis. It is a bifilar wound coil, center tapped, and each coil half, referenced to a capacitor, senses one of two components of flow (Figures 17 and 18).

The meter, with three interchangeable sensor heads arrived at Scripps in July and every effort is being made to place the instrument under penduium tests in the hydraulic laboratory wave tank at the earliest date.

IV. REFERENCES

Battjes, J. A., 1971, "Run-up distributions of waves breaking on slopes", Jour. Waterways, Harbors and Coastal Engineering Division, Proc. Amer. Soc. Civil Eng., vol 97, no WW1.

Divoky, D., B. Le Mehaute and A. Lin, 1970, "Breaking waves on gentle slopes", Jour. Geophys. Res., vol 75, no 9, p 1681-92.

Horikawa, K. and A. Watanabe, 1968, "Laboratory study of oscillatory boundary layer flow", Coast Eng in Japan, vol 11, p 13-28.

Inman, D. L. and A. J. Bowen, 1963, "Flume experiments on sand transport by waves and currents", Eighth Conf on Coastal Eng., Proc. Amer. Soc. Civil Eng., p 137-50.

Inman, D. L. and W. G. Van Dorn, 1970, "Advanced studies in nearshore engineering", Annual Report Advanced Ocean Engineering Laboratory, Scripps Institution of Oceanography, Univ. of Calif., ONR contract N00014-69-A-0200-6012, AOEL Report No 16, SIO Ref 71-4.

Inman, D. L. and R. W. Harris, 1970, "Crater-sink sand transfer system", Twelfth Conf on Coastal Eng., Amer. Soc. Civil Eng., Abstract No 171, p 525-528.

Johns, B., 1970, "On the mass transport induced by oscillatory flow in a turbulent boundary layer", Jour Fluid Mech., vol 43, pt 1, p 177-85.

Jonsson, I. G., 1963, "Measurements in the turbulent boundary layer", Int. Assoc. Hyd. Res. Cong., London, p 85-92.

Kajiura, K., 1968, "A model of the bottom boundary layer in water waves", Bull Earthquake Res. Inst., vol 46, p 75-123.

Lamb, H., 1932, Hydrodynamics, 6th Edition, New York, Dover Publ., 738 pp.

Le Mehaute, B., 1962, "On the nonsaturated breaker theory and wave run-up", Proc. Eighth Conf Coastal Eng., Amer. Soc. Civil Eng., p 77-92.

Longuet-Higgins, M. S., 1961, "The mechanics of the boundary layer near the bottom in a progressive wave", Sixth Conf. Coastal Eng., Amer. Soc. Civil Eng., p 184-93.

Mash, F. D. and R. L. Wiegel, "Cnoidal waves, tables of functions", Council on Wave Res., Univ. of Calif., Berkeley, 1961.

Skjelbrea, L., 1959, "Gravity waves, Stokes' third order approximation: tables of functions", Council on Wave Res., Univ. of Calif., Berkeley.

Sleath, J. F. A., 1970, "Velocity measurements close to the bed in a wave tank", Jour. Fluid Mech, vol 42, p 111-123.

Tucker, M. J., N. D. Smith, F. E. Pierce and E. P. Collins, 1970, "A two-component electromagnetic ship's log", Jour. Inst. of Navigation, vol 23, no 3, p 302-316.

Table 1. Laboratory Wave and Slope Parameters

Wave Periods (sec)	1.6(6.4)	2.4(9.6)	3.4(13.6)	4.8(19.
Beach Slopes	0.02	0.04	0.08	
Stations: (see Figure 2)	A-uniform depth	B-1/3 toe to break point	C-2/3 toe to break point	D-break
	E-max horizontal velocity	F-early bore	G-late bore	H-run-up

Numbers in ( ) denote prototype values

Table 2. Four sets of measurements of ripple wavelength λ, and height η, taken simultaneously at one station during DAS 323.

Sample	λ cm	η cm
1	21.7	3.1
	21.8	1.1
	18.3	1.5
2	22.8	1.8
	17.0	0.5
	23.9	0.5
	16.1	1.4
3	16.0	1.3
	18.8	2.9
	18.1	0.7
	24.3	0.6
4	16.0	0.7
	16.3	0.9

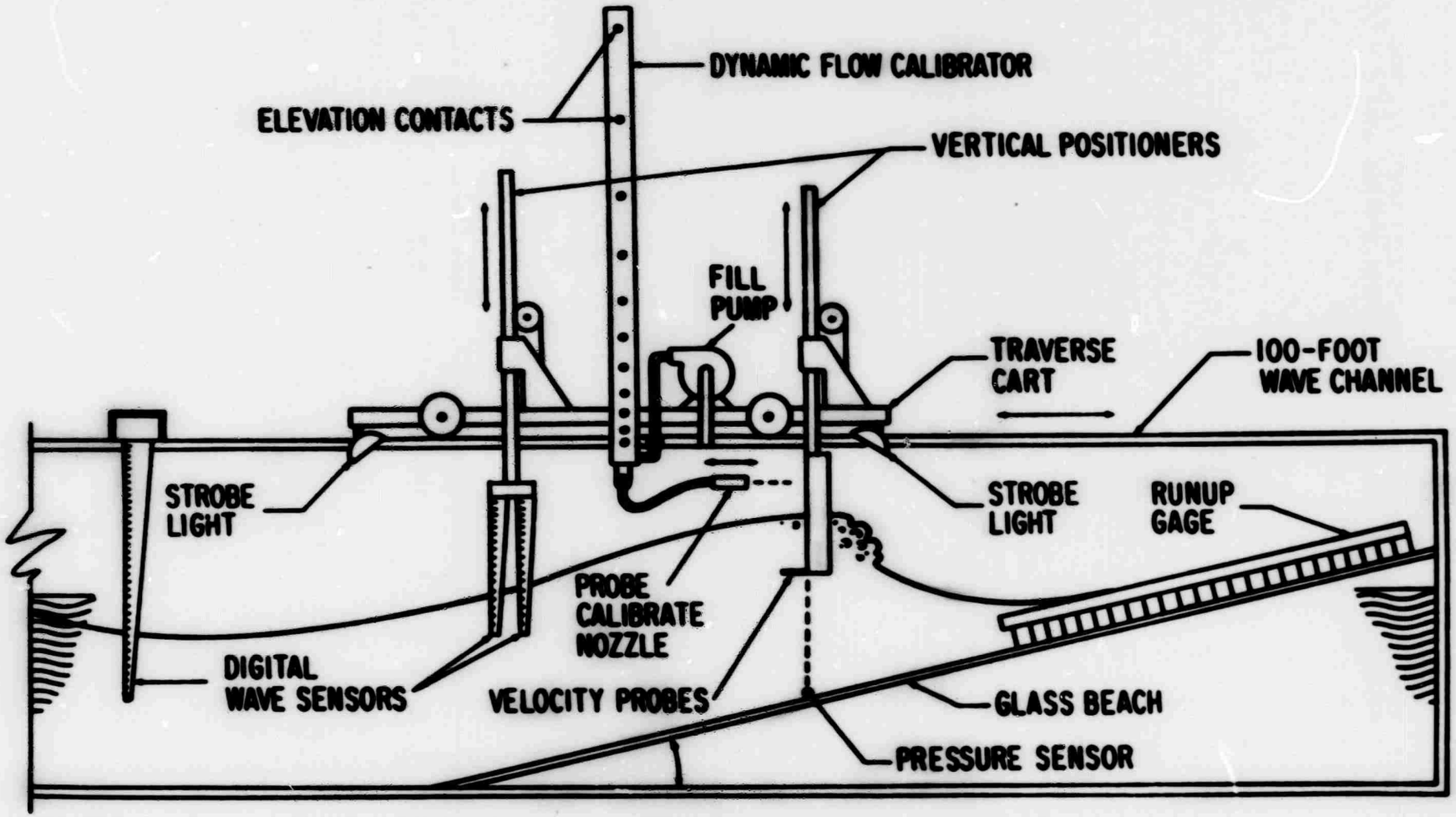

Figure 1. Revised instrumentation for velocity and surface elevation measurements.

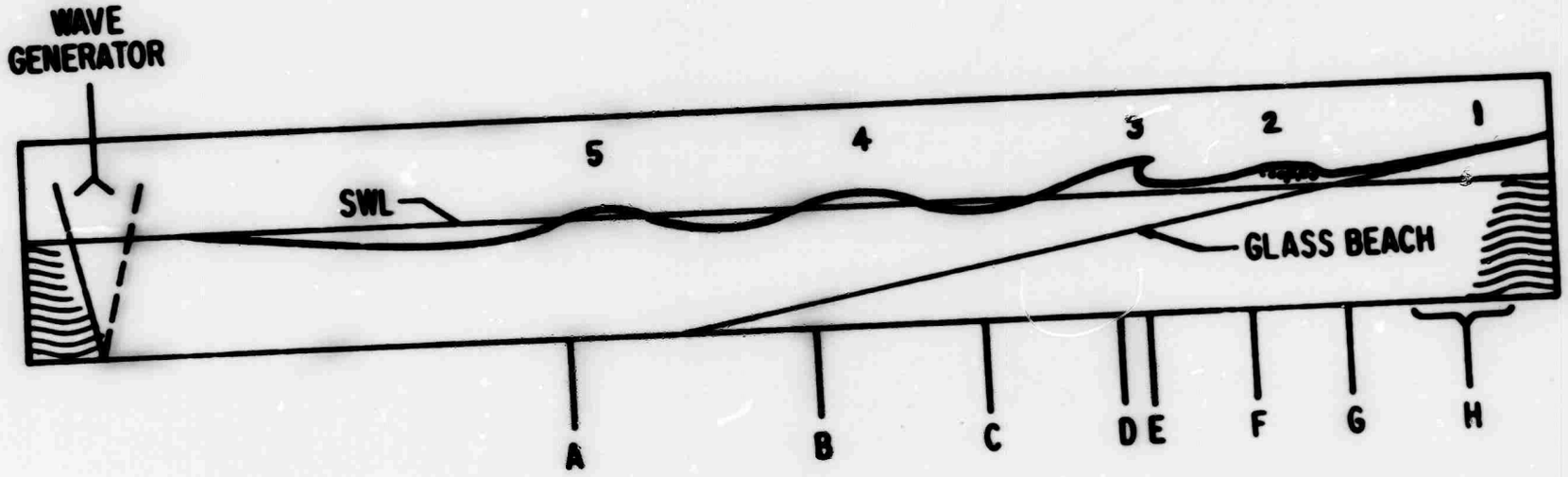

Figure 2. Station locations and typical five-wave sequence.

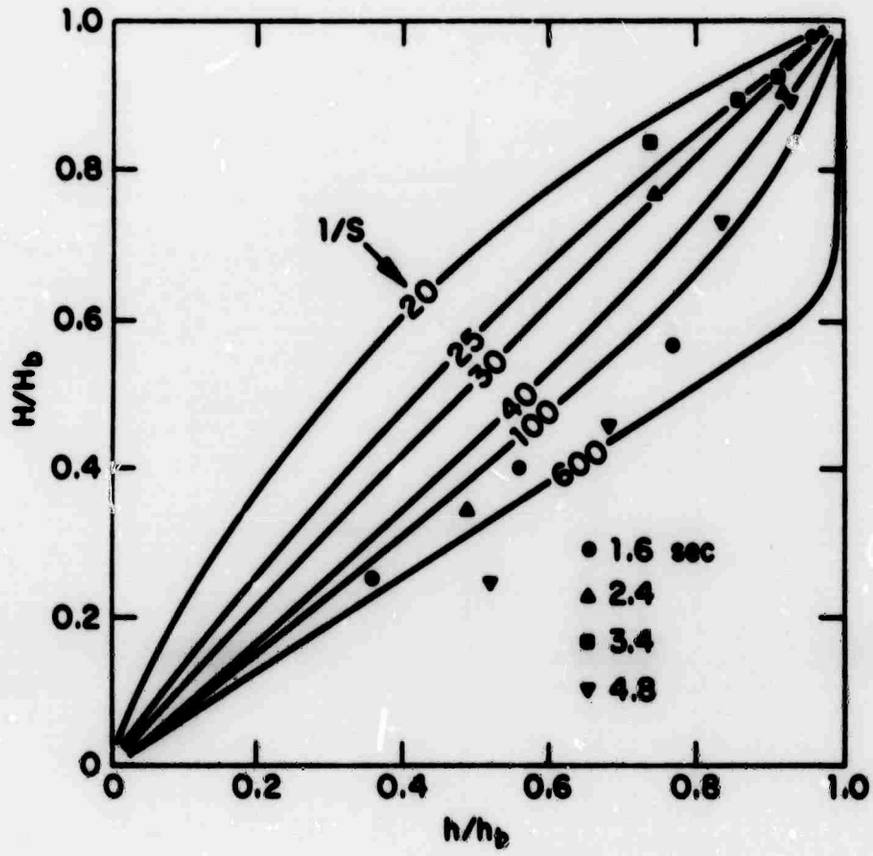

Figure 3. Relative breaker height versus relative breaker depth from unsaturated breaker theory. Our data points are for 1/S = 25.

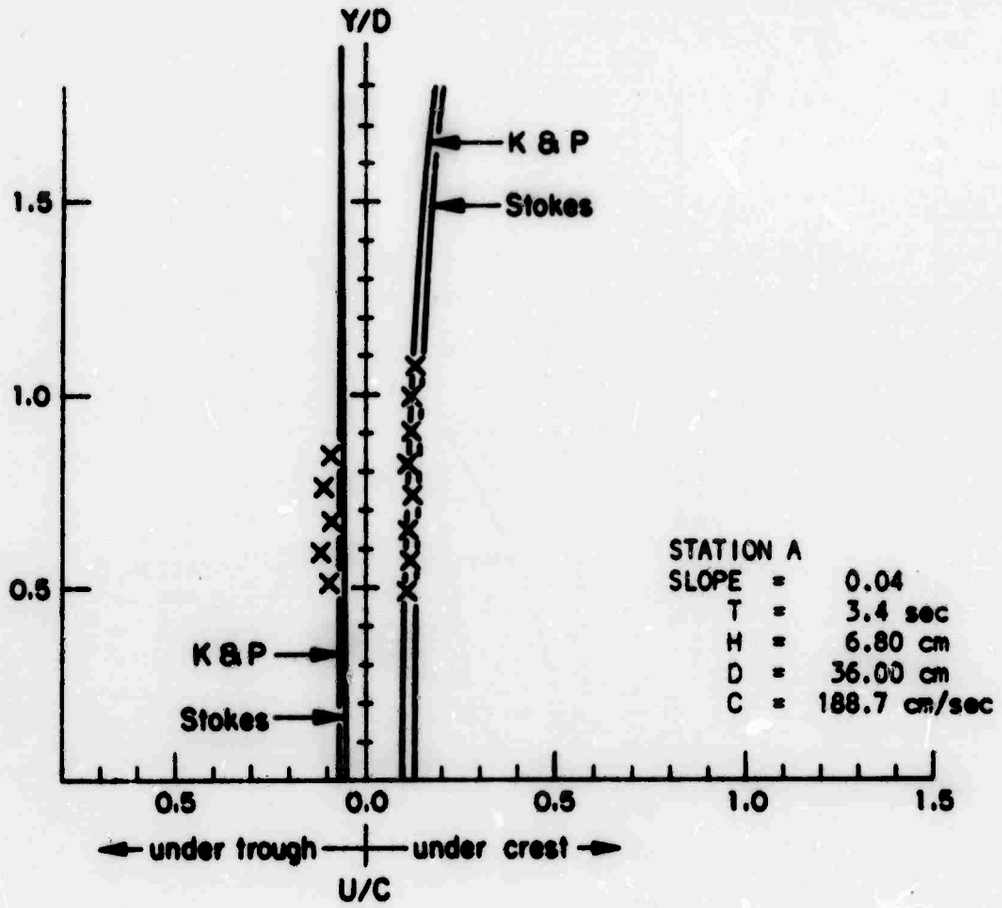

Figure 4. Comparison of theoretical and experimental horizontal flow velocities under crest and trough for third wave of five wave sequence in uniform depth.

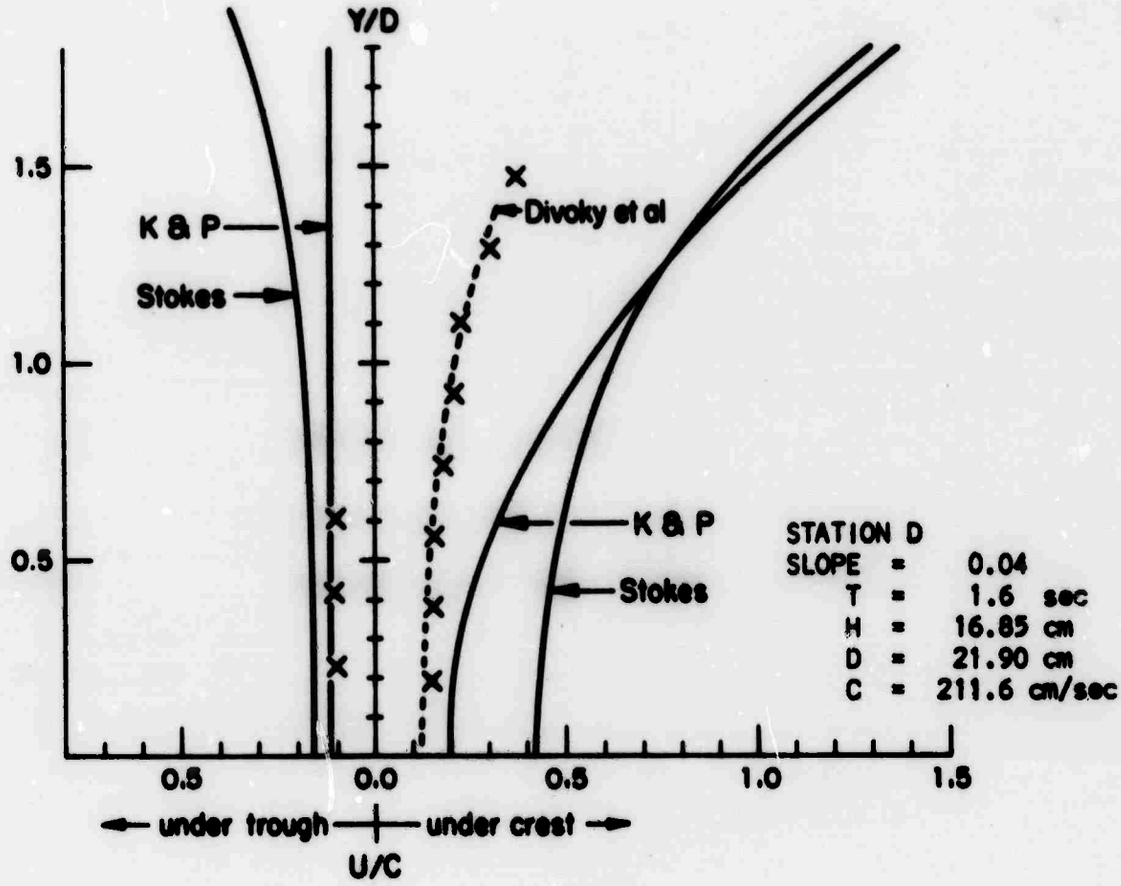

Figure 5. Comparison of theoretical and experimental horizontal flow velocities under crest and trough for third wave of five wave sequence at breaking point.

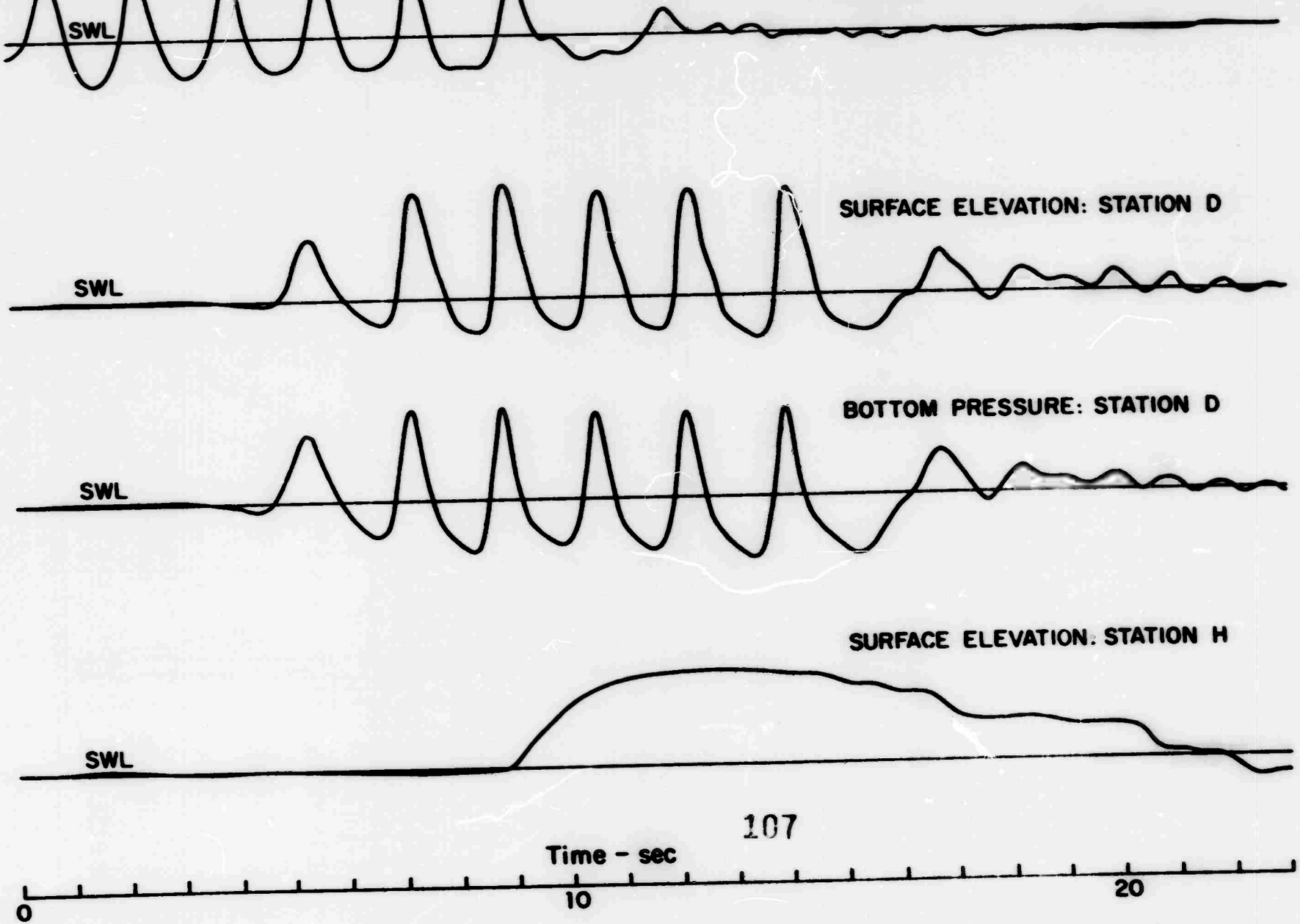

Figure 6. Typical time record of five wave sequence, showing smooth run-up surge at shoreline. Period T = 1.6 sec, slope S = 1/25.

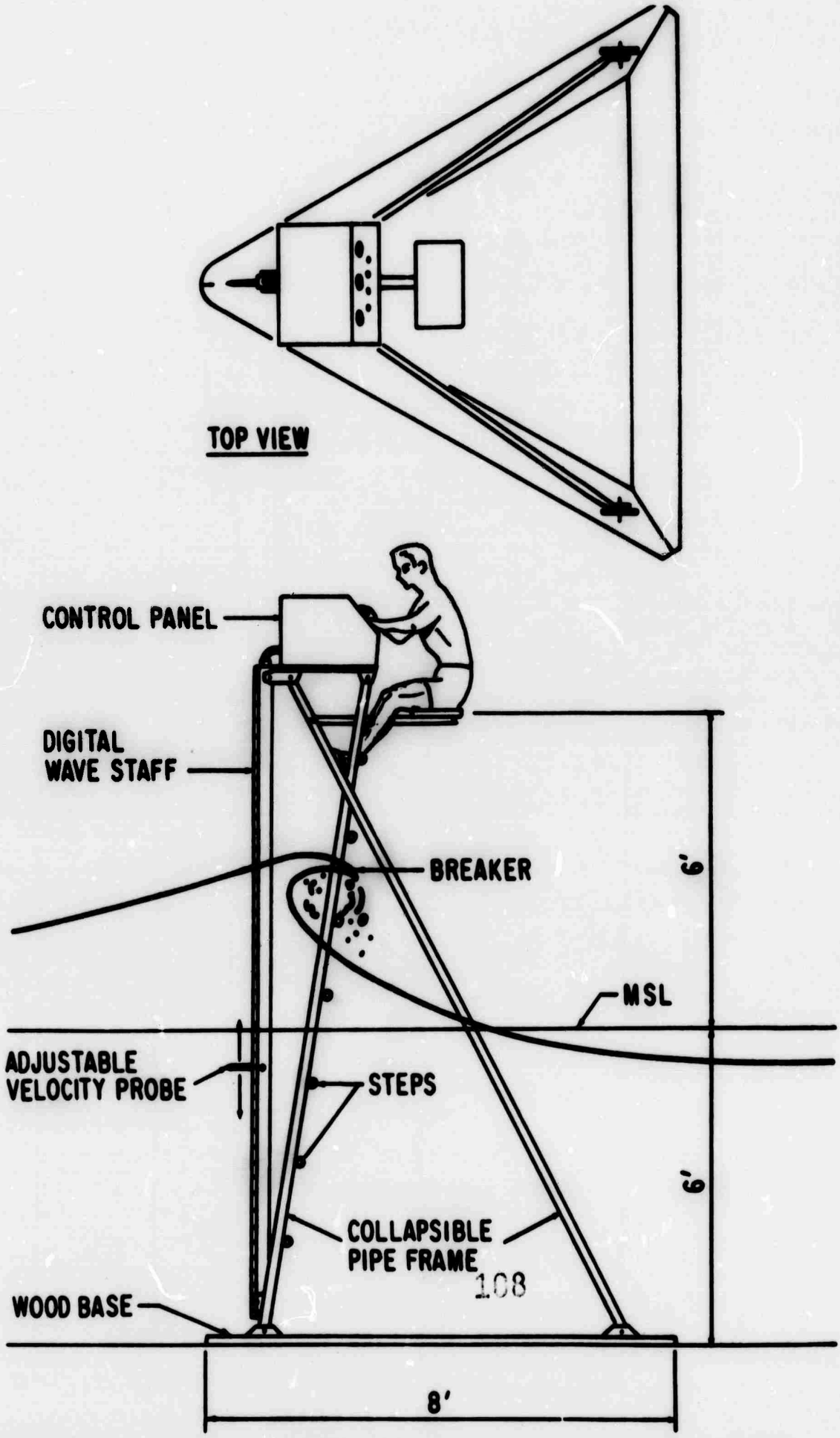

Figure 7. Portable instrument platform for field measurements within surf zone.

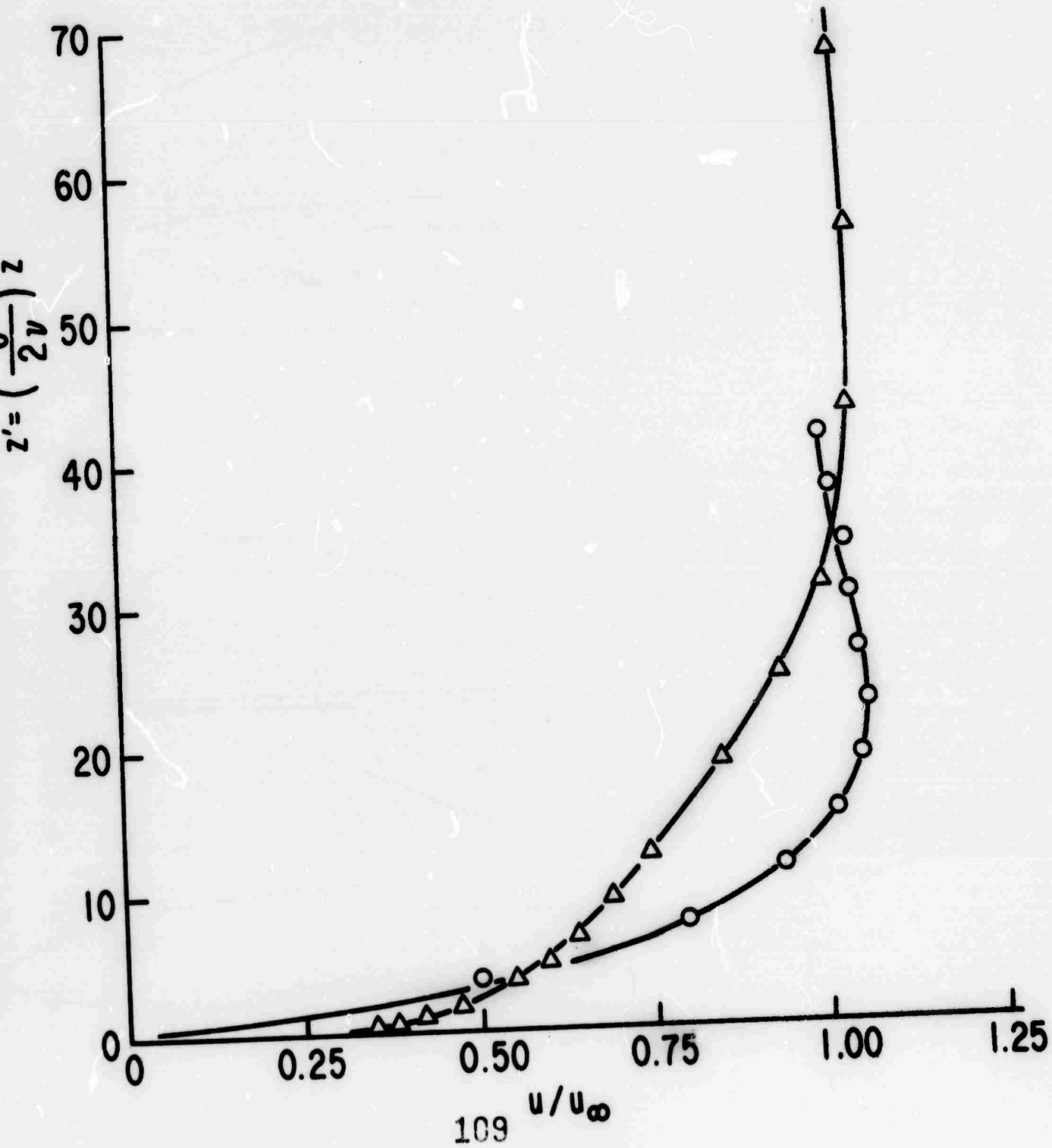

Figure 8. Comparison between Johns theory (o) and Jonssons data (Δ) for $z' = 6.18z$.

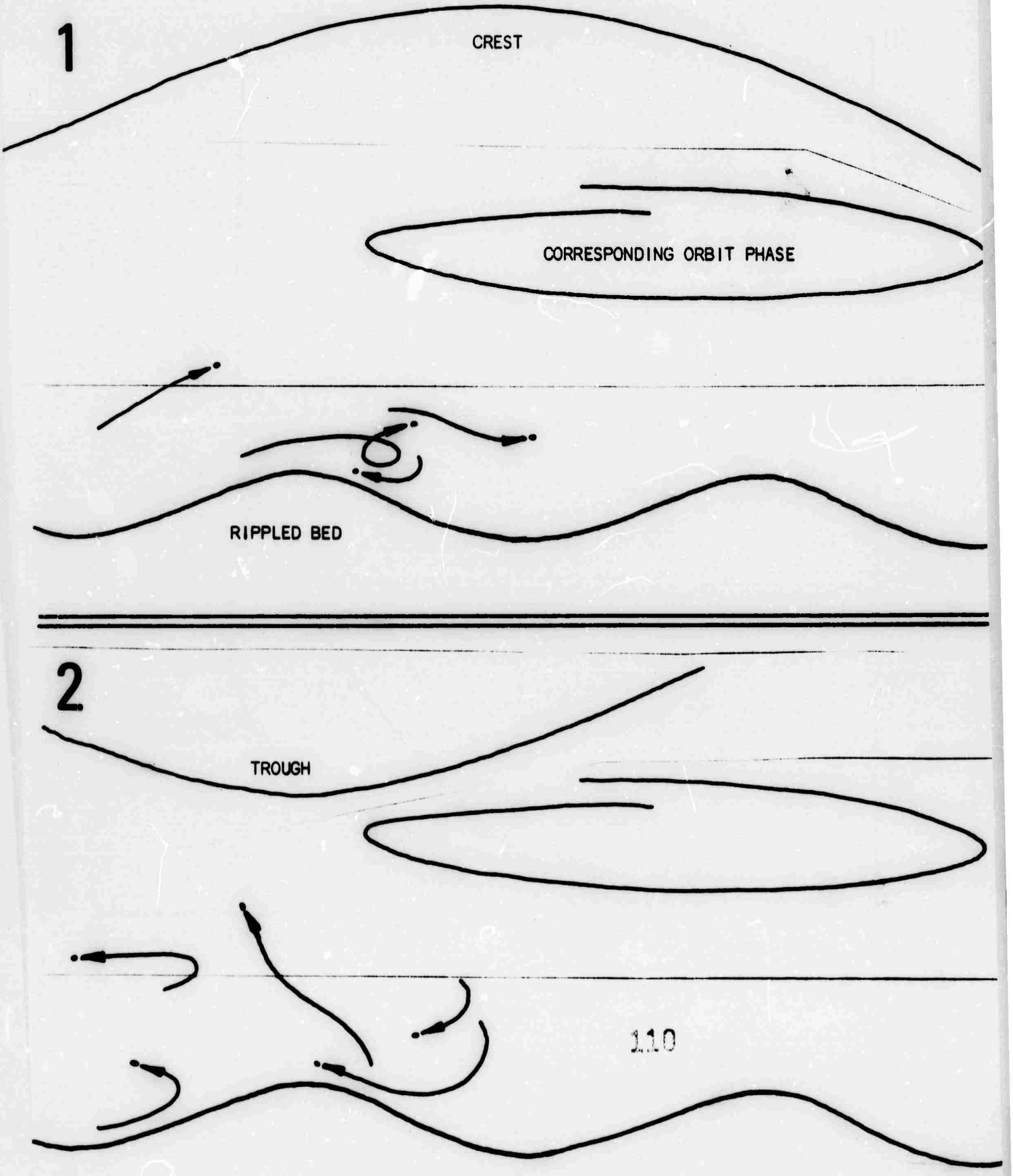

Figure 9 A. Selected representative particle trajectories over a rippled bed (after Inman and Bowen, 1963, vertical scale distorted for representation).

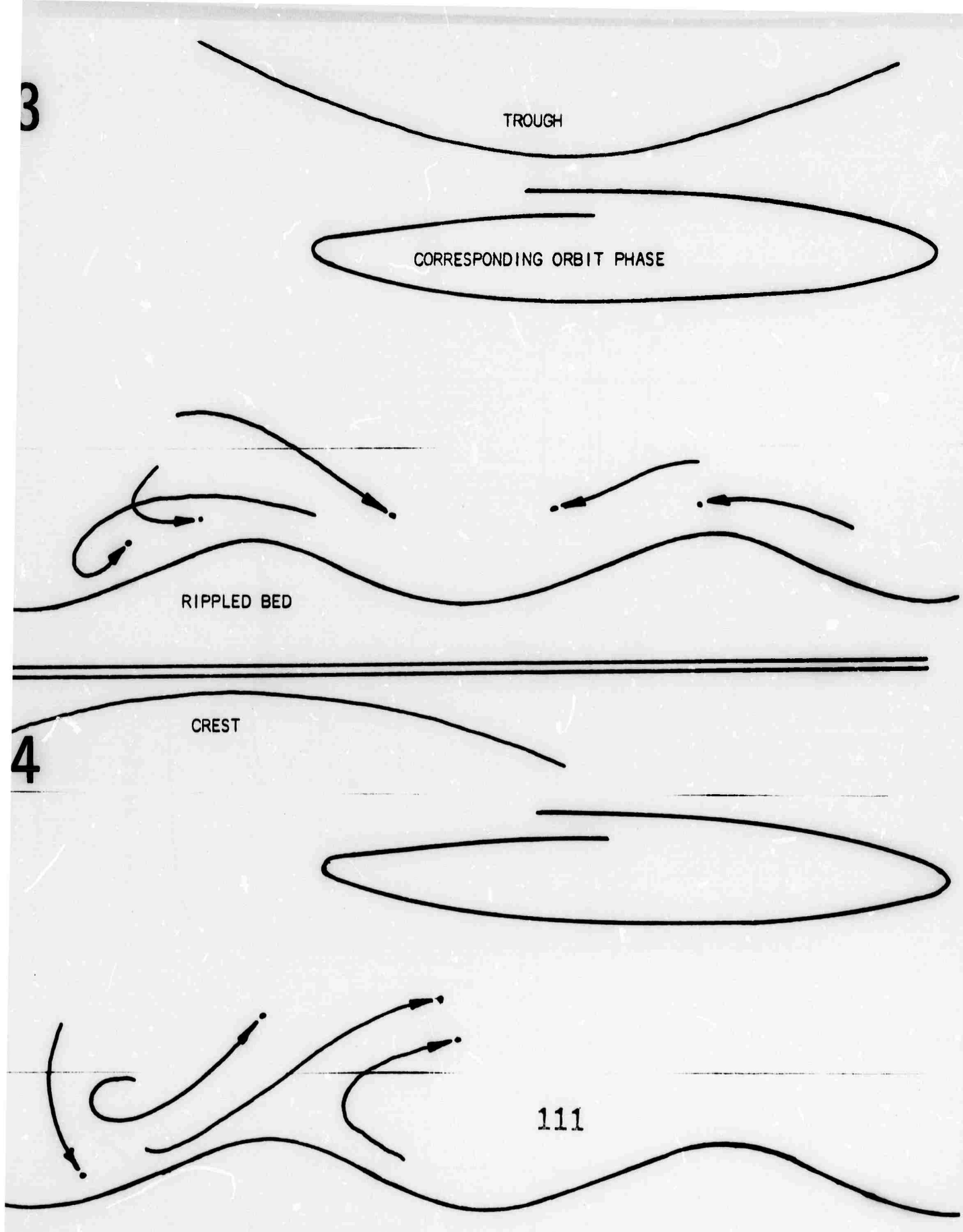

Figure 9B. Particle trajectories (concluded).

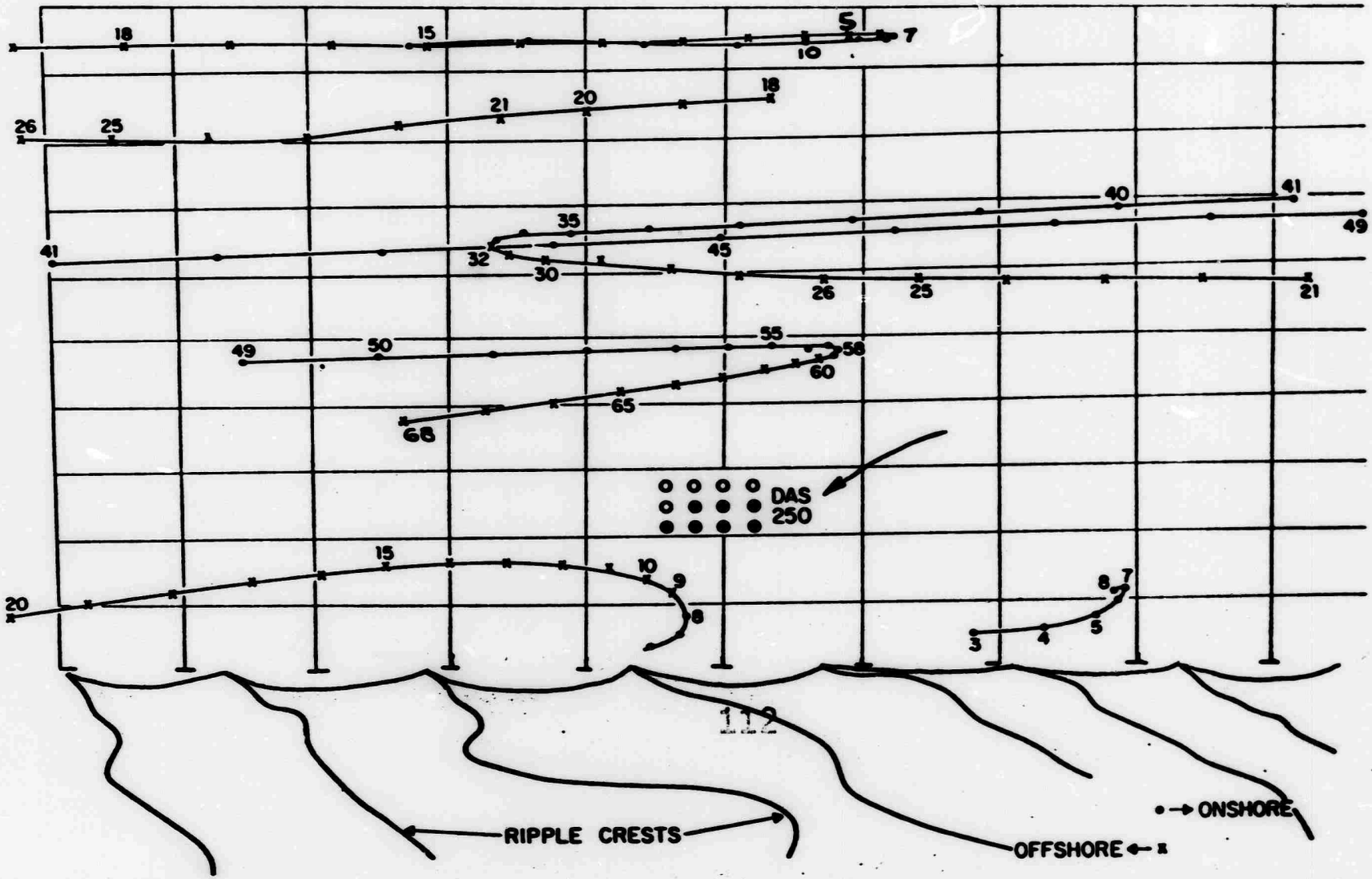

Figure 10. Particle motions measured during data run DAS 250 at a depth of 7 meters, grid dimensions are 5 x 10 cm. Points are 0.25 second intervals. Light array indicates starting (octal) time for plot (after Inman).

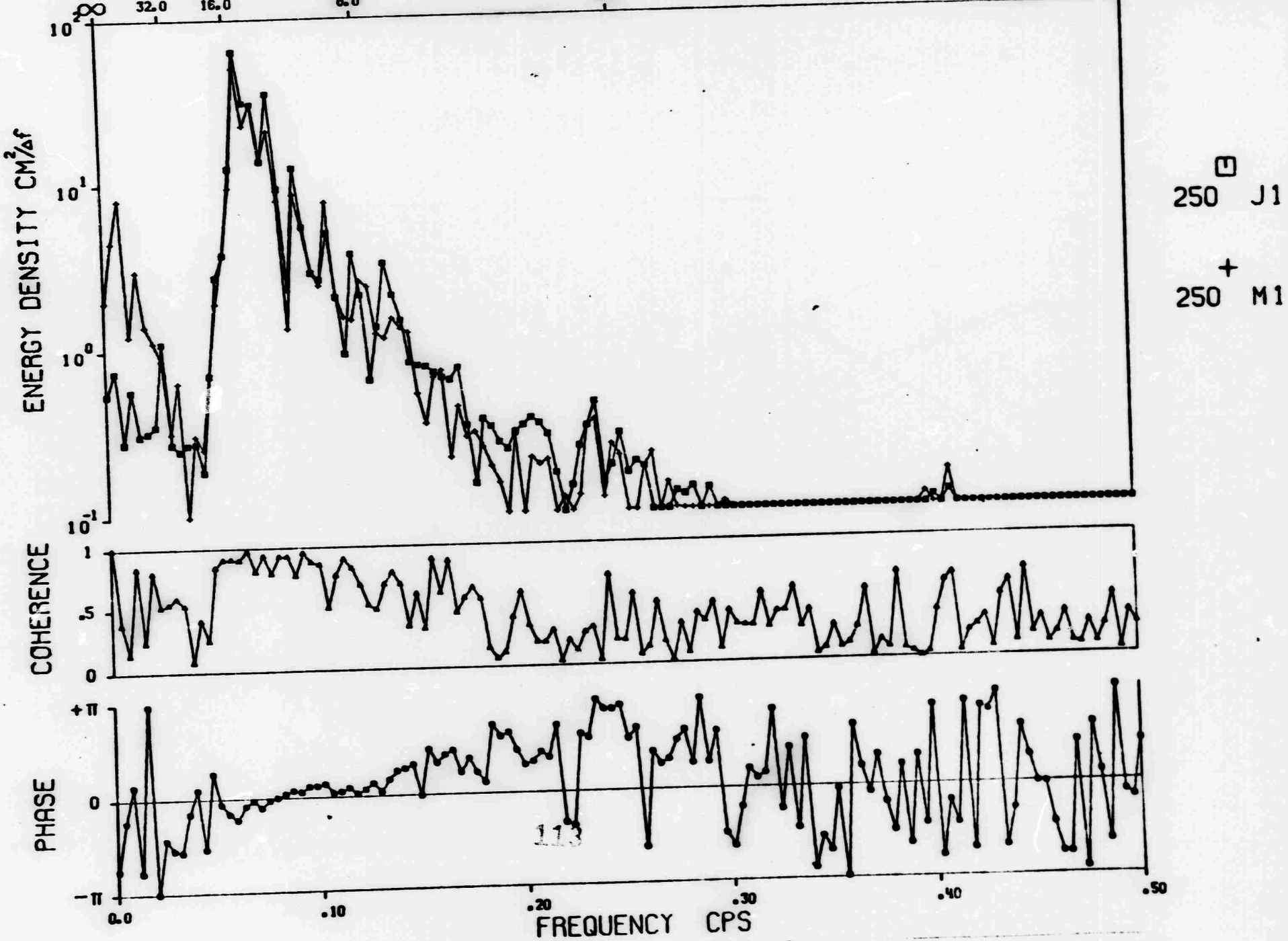

Figure 11. Spectrum for data run DAS 250.

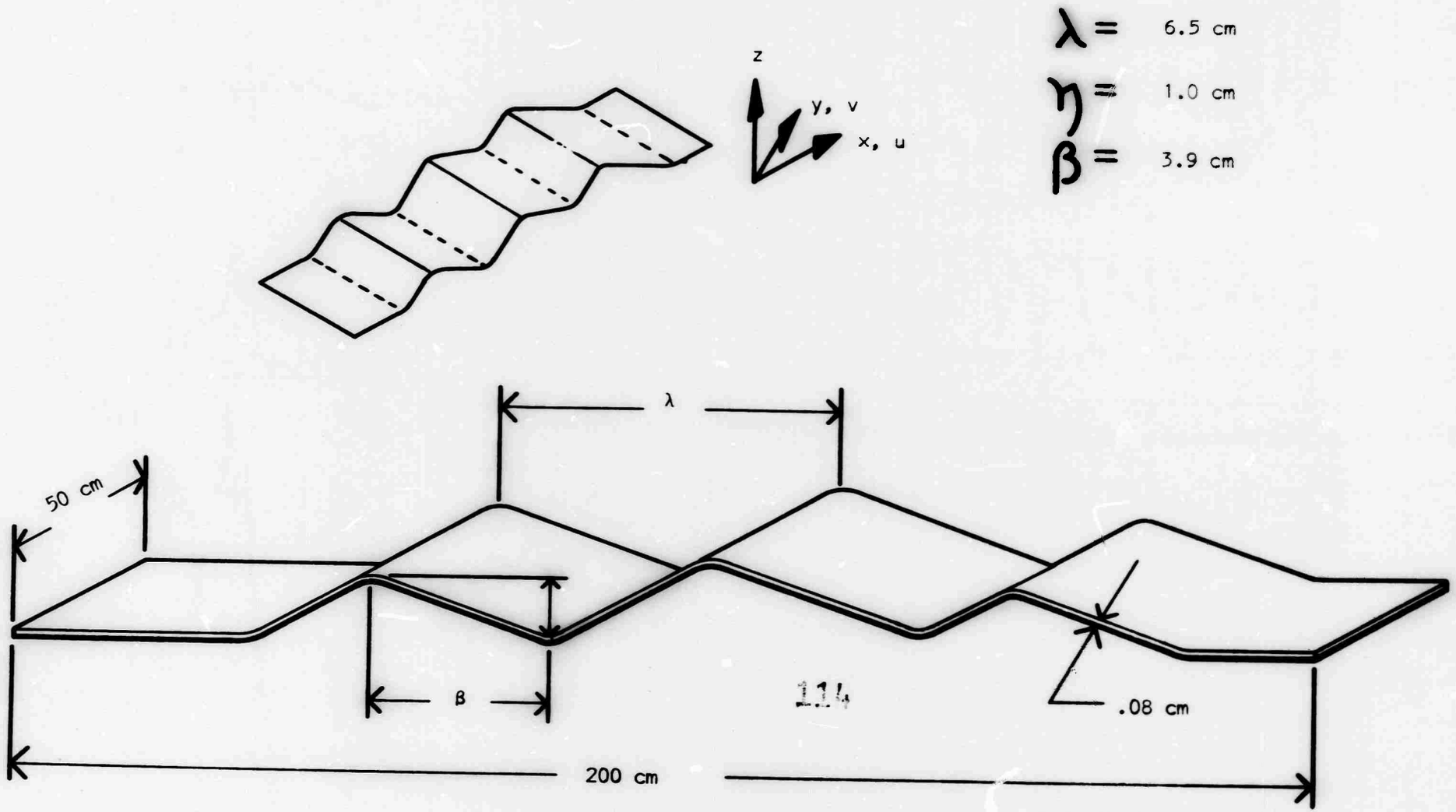

Figure 12. Typical modular roughness element for wave tank study.

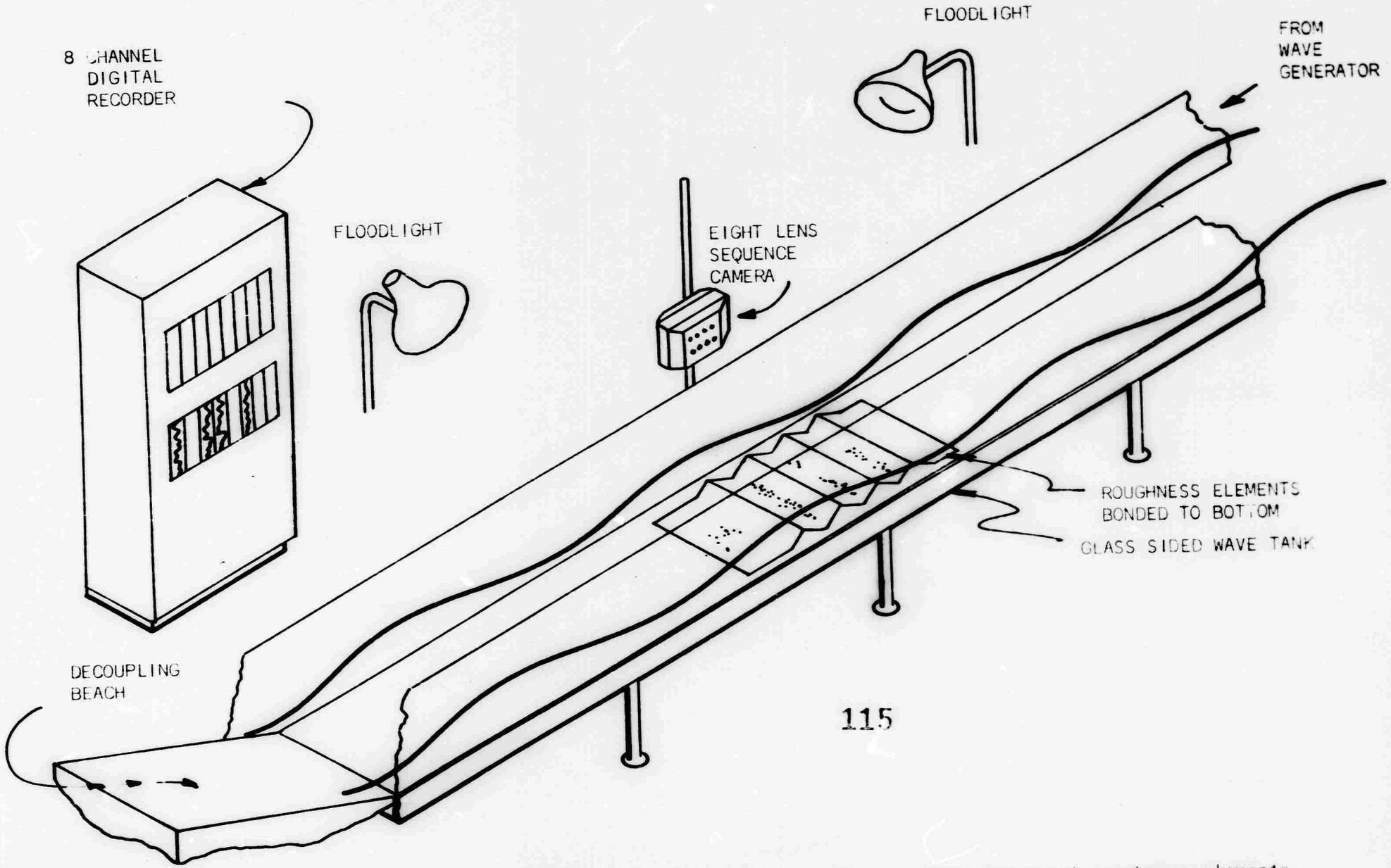

Figure 13. Test setup for particle studies on phase-dependent roughness elements.

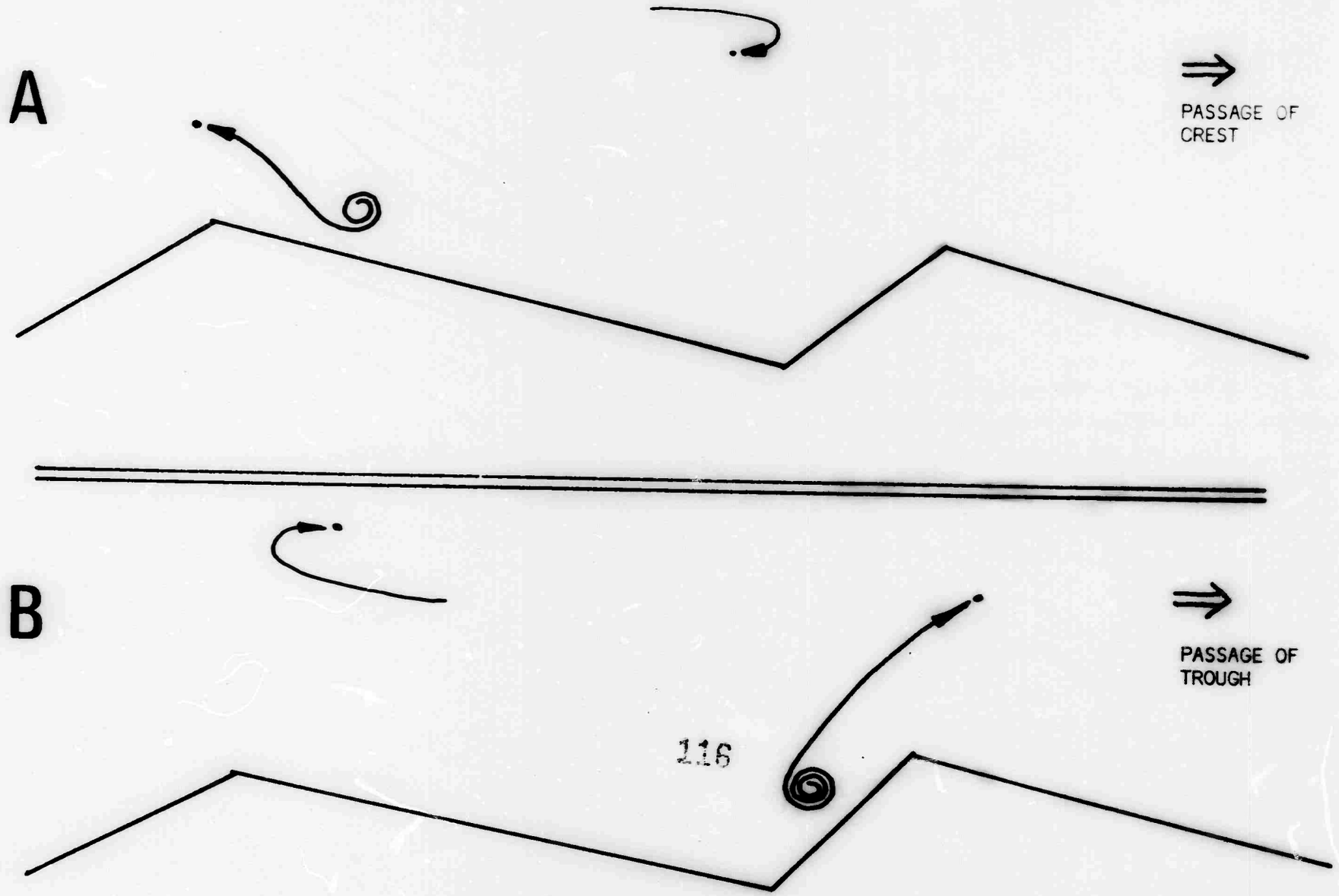

Figure 14. Vortex changes accompanying orbital motion

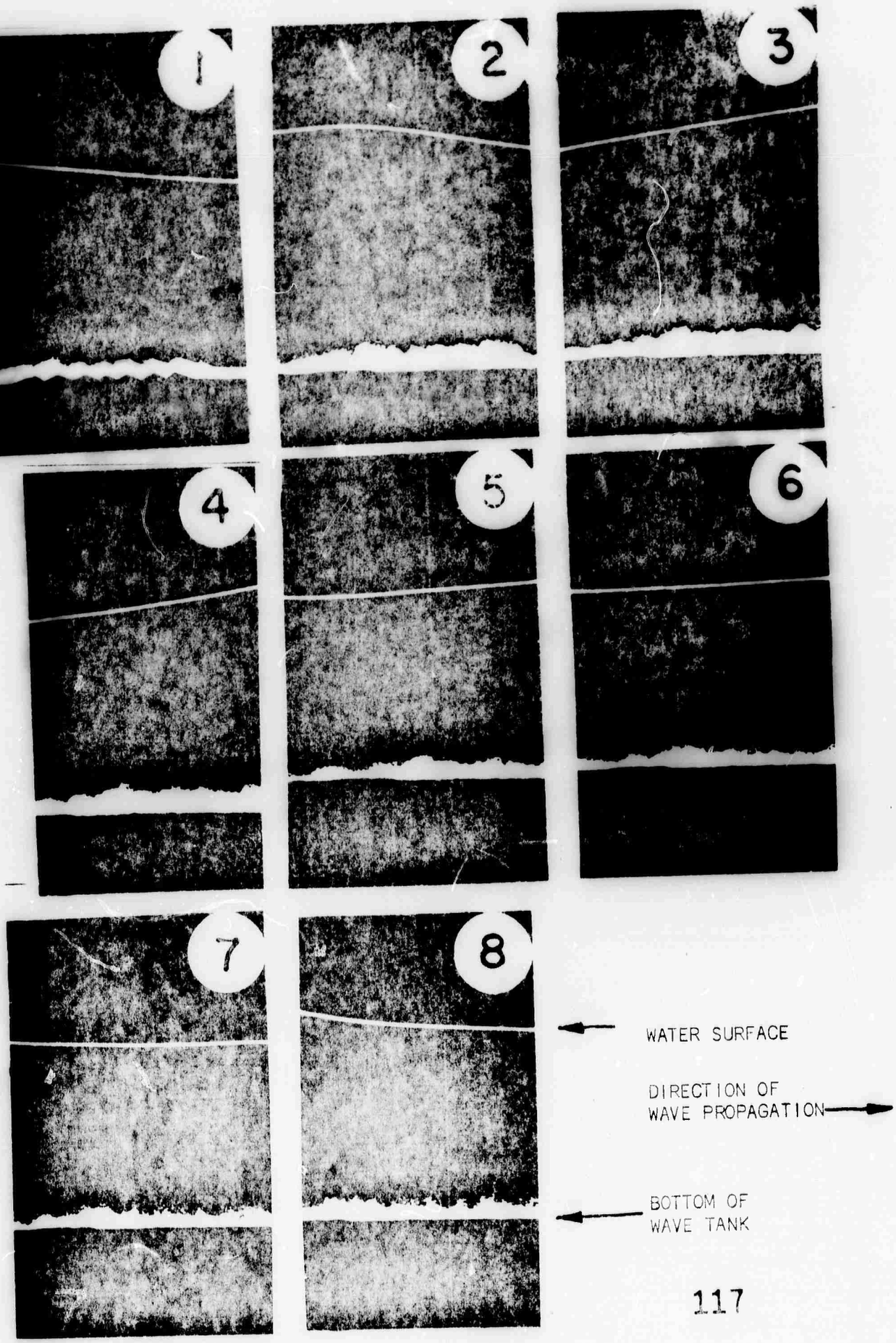

Figure 15. Photographs taken through glass walled 27½ m wave tank.

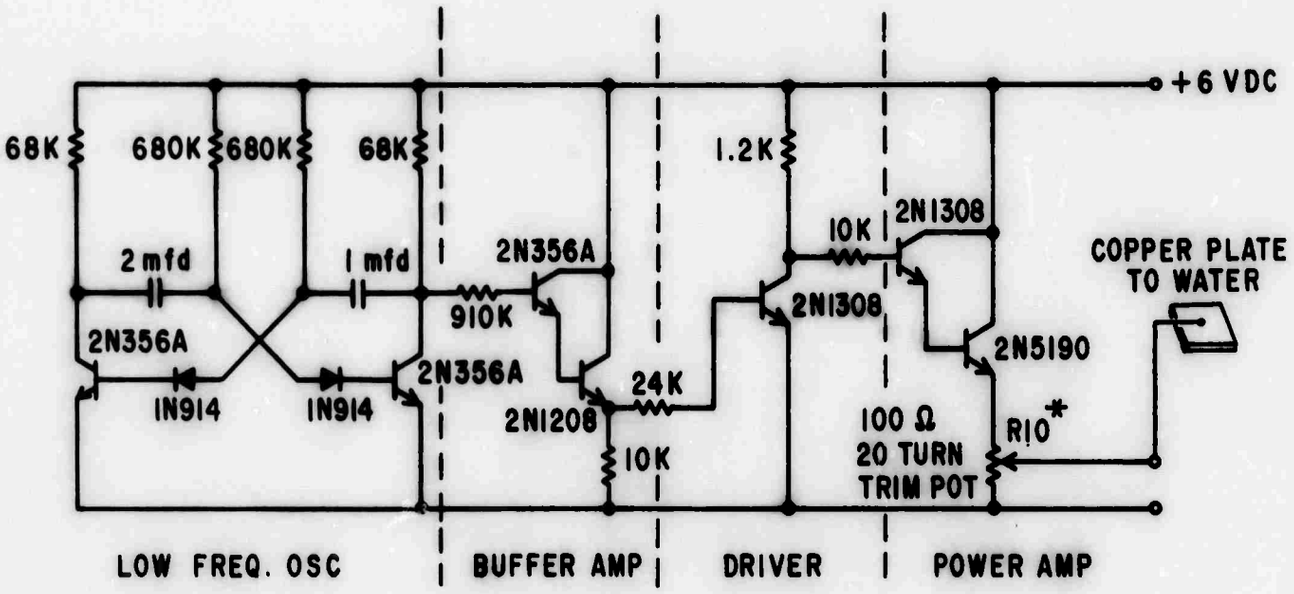

R10* VARIES CURRENT TO PLATINUM WIRE

ALL RESISTORS 1/2W

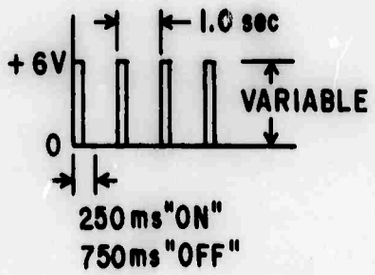

DRIVING CIRCUIT
HYDROGEN BUBBLE GENERATOR

FIGURE 16

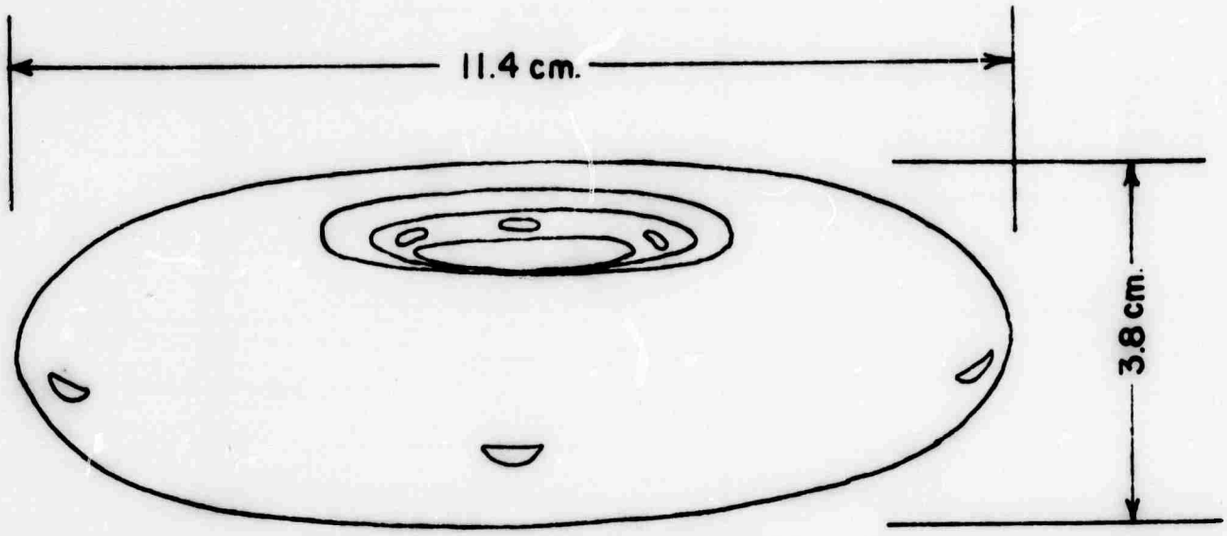

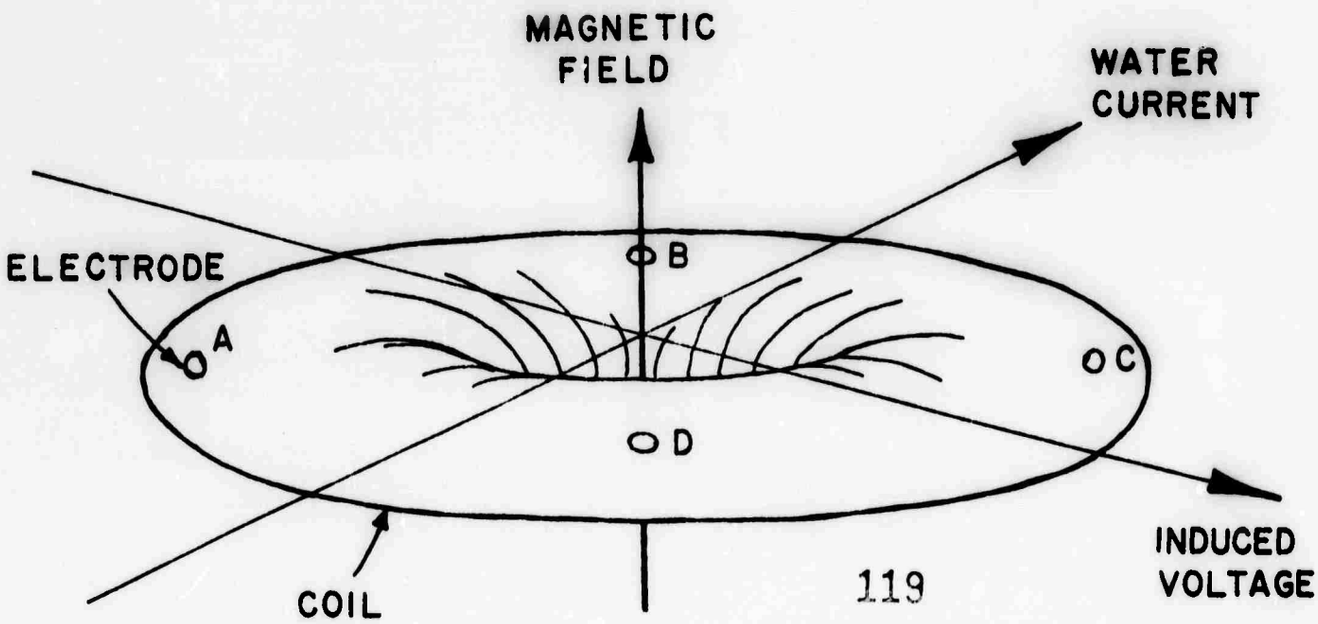

Figure 17. The electromagnetic flowmeter sensor. The head geometry was chosen for hydrodynamic utility, gives comparatively small emf's. Approximately ten watts of power gives a sensitivity of about 75μV/knot when in use.

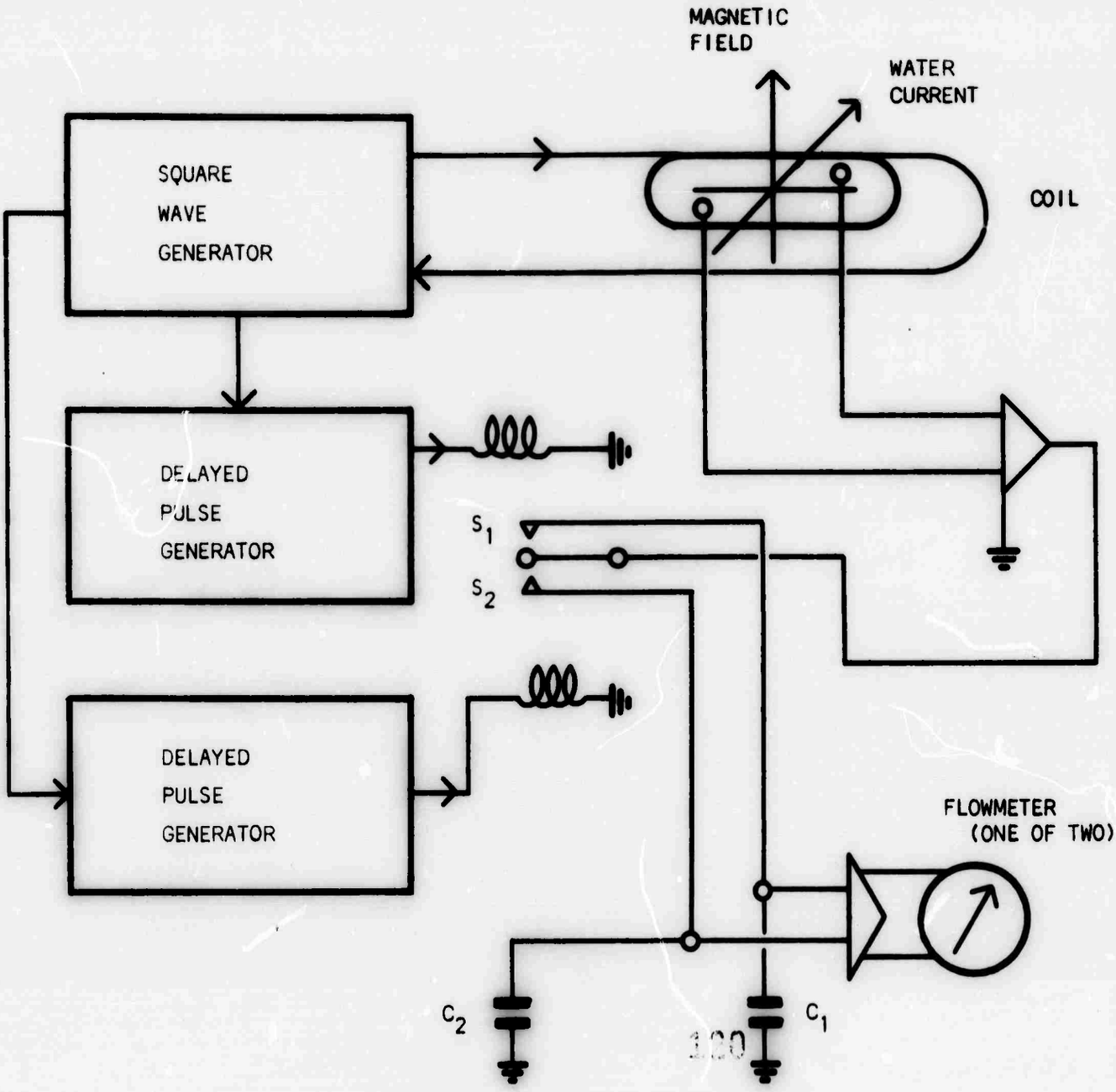

Figure 18. Switch 1 closes during the positive half cycle of the square wave energizing the coil in the measuring sensor, and switch 2 during the negative half cycle, so that the differential voltage between C_1 and C_2 is proportional to the component of the water velocity flowing at right angles to the line connecting the electrodes. The other pair of electrodes measure the other velocity component.

Part V

ELECTROMAGNETIC ROUGHNESS OF THE OCEAN SURFACE

Co-Principal Investigators

Dr. William A. Nierenberg
Phone (714) 453-2000, Extension 1101

Dr. Walter H. Munk
Phone (714) 453-2000, Extension 1741

ADVANCED OCEAN ENGINEERING LABORATORY
Sponsored by
ADVANCED RESEARCH PROJECTS AGENCY
ADVANCED ENGINEERING DIVISION

ONR Contract N00014-69-A-0200-6012

Part V

Electromagnetic Roughness of the Ocean Surface

Table of Contents

List of Figures

List of Appendices

I. SUMMARY

In our annual report for 1970 we stated that, together with a group at Stanford University, we were involved in a program to use radar to measure the statistical properties of ocean waves, particularly the ocean-wave directional spectrum; and that our immediate goal was the testing of various methods of measuring the ocean-wave directional spectrum using LORAN signals in preparation for future field experiments using multifrequency, pulsed Doppler radars. The methods to be investigated were 1) monostatic geometry with an antenna array, 2) bistatic geometry with simple antennas, and 3) monostatic geometry using a synthetic aperture (side-looking radar).

The major proportion of our work for the first six months of the contract has been directed towards the construction of equipment necessary to investigate these methods. Some of this equipment has been constructed, and the rest is in the final stages of construction, so no technical reports are presently available; however, a brief description of each item is included here. The remainder of our work has been concerned with 1) planning an experiment designed to both test the bistatic method and to obtain good directional spectra of ocean waves, 2) writing computer programs to analyse this data, and 3) examining the mechanisms producing second-order scattering of radio waves from ocean waves, and its importance in our experiments.

123

II. TECHNICAL REPORT

A. Second Order Theory

About six months ago, Hasselmann[1] proposed that the second-order

scattering of radio waves from the sea should produce sidebands to the first-order Doppler spectrum, that these sidebands carried important information about the ocean waves, and that they should be strongest when large, low-frequency, ocean waves are present during the measurement of higher-frequency ocean waves. We have examined the various mechanisms involved in this scattering and estimated the strength of the sidebands produced by the most important of them. Under some conditions these sidebands can be quite large, and could confuse the interpretation of the data obtained by the bistatic or synthetic-aperture experiments. A brief description of this work is given in the appendix, a summary of an invited lecture to be given at the 1971 IEEE International Antennas and Propagation Symposium and USNC/URSI Meeting in Los Angeles.

B. EQUIPMENT

1. 30 MHz Radar

Because of the potential importance of second-order scattering, and because of the lack of experimental verification of its existance, we wish to measure 30 MHz radio waves backscattered from the sea while large, low-frequency ocean waves are also present in the scattering area. To this end, the group at Stanford has constructed a simple, 30 MHz, pulsed-Doppler radar.

The radar transmitter consists of a frequency synthesizer which produces a constant, stable, 30 MHz signal; a balanced mixer to switch this signal on and off to produce a pulsed, 30 MHz, wave train; and a linear

amplifier. The width of the pulse is variable: 10, 50, 100, and 200 u sec; the pulse repetition rate is 2.5 KHz; and the transmitted power is approximately one watt.

The receiver consists of a radio-frequency amplifier, demodulator, and a low-pass amplifier. The received signal is recorded in analog form on magnetic tape. Some components of the radar (i.e. the frequency synthesizer and linear amplifier) already existed; other components were designed and fabricated at Stanford. The radar set is now complete and is being tested.

2. Portable LORAN Receiver

Both the side-looking radar and the bistatic-geometry experiments require a portable, LORAN receiver that is self contained, easily operated, and which uses relatively little power. The previous receiver (used in the first LORAN experiments) required a bulky frequency synthesizer and tape recorder. The signal from the receiver was degraded by the analog tape recorder; and, in addition, drifts of the stable oscillator's frequency caused drifts in the position of the digitized ranges. So a new receiver was necessary.

This new receiver 1) uses a stablized quartz crystal as a stable oscillator, 2) locks to the LORAN transmitter pulse rate, 3) digitizes the data, stores it in a temporary memory, and writes it in serial form on a cassette tape recorder, and 4) operates automatically (automatically locks to the desired LORAN signal and blanks out interfering signals). The entire

receiver is compact, uses about 100 watts of power, and its frequency stability exceeds that of the California LORAN stations.

3. Antennas

Bistatic-geometry experiments require an antenna to select the signal scattered from one of four symmetric points on the scattering ellipse. This could be done using several slightly selective antennas (ones having a beamwidth of say 100°), for example, by switching between two cardioid antennas set at right angles to each other, or by shifting the phases of the signals from two vertical antennas separated by some distance.

To test the usefulness of the cardioid antennas, the Stanford group has attempted to build small, ferrite-core, loop antennas; but failed to produce a good cardioid pattern because 1) the loop was sensitive to nearby conductors, and 2) it was difficult to match the loop to its vertical reference antenna. Furthermore, it was hard to adjust the impedence of the antenna to that of the receiver and still have both operate effectively.

4. Pitch-and-Roll Buoy

The design of this buoy and its data-recording system was completed in 1970, and the buoy was briefly described in the last annual report. Basically the buoy consists of a five-foot-diameter disc containing a vertically stablized accelerometer and a low-power, data recorder. It will be

used to measure the ocean-surface height and slope at a point, from which the first five Fourier coefficients of the angular distribution of ocean-wave energy can be computed. The buoy is being constructed by Honeywell Marine Systems of Seattle to our specifications. Delivery is expected some time in July 1971.

One low-power, data recorder, which will be installed in the pitch-and-roll buoy, was constructed by Monitor Labs, again to our specifications, and delivered on 2 July 1971. The data recorder samples up to eight channels of analog data, converts each sample to a 12-bit, digital word, and writes it onto seven-track, magnetic tape. The number of data channels, the rate they are scanned, the number of scans per tape record, and the number of records per file are variable. Provision is made for turning off external equipment after a set number of records or files, waiting a variable interval of time, and then restarting the equipment and data recording. In addition, the recorder includes an accurate, digital clock; and, once per tape record, a time word (consisting of minutes, hours, days, and year) is written. The entire system, excluding the tape recorder, uses about 80 mw of power (the tape recorder requires one watt) and fits easily into the wave buoy.

C. LORAN Data Analysis

The bistatic geometry LORAN experiment will produce large amounts of data which must be processed in a straightforward, but time consuming manner; so we have spent some time writing efficient programs to process this data.

The LORAN data consists of 8-bit digital samples of the received radio signals as a function of range for each LORAN pulse. This data must be translated into computer words, interchanged to obtain the time history of the scattered signal at a particular range, Fourier transformed to obtain the Doppler spectrum at this range, and then plotted in some suitable cordinate system (such as range-Doppler, ocean-wave number space, etc.) before the data can be interpreted and related to the statistics of the sea surface. Since adequate resolution in range-Doppler space may require 2048 samples at each of 64 ranges for a single range-Doppler plot, large amounts of data must be processed. Preliminary data reduction on an IBM 1800 computer indicated that seven hours of computer time would be required to process 15 minutes of LORAN data. (This would produce a single range-Doppler plot.) More efficient programs written for a Burroughs 6700 computer indicate that this work could be done in 30 minutes, and future improvements in the programs are expected to reduce this time to 15 minutes.

D. Bistatic Geometry Experiment

During the first week of September we plan to conduct a bistatic experiment with two, perpendicular baselines using LORAN signals. This experiment is designed to 1) test the feasibility of making precise Doppler measurements from a small ship in a trade-wind region, 2) test a shipboard antenna system suitable for bistatic measurements, and 3) obtain accurate, directional spectra of 7 to 10 second ocean waves in a homogeneous, trade-wind area.

Suitable perpendicular baselines in a trade-wind area can be obtained by placing a receiver on a ship situated anywhere

along a circular arc north of Hawaii depicted in Figure 1, during the summer months when the trade winds extend over this region. The expected ocean-wave-number coverage obtained with this geometry is shown in Figure 2, assuming waves at a distance of 1.67 baseline units can be observed. In this figure the wave numbers have been scaled by the maximum wave number observed, i.e., the wave number which backscatters the 1.85 MHz LORAN signals: 1/(81m). Furthermore, if the ship is positioned so that one of the baselines is perpendicular to the trades, the symmetry of the wave field with respect to the wind will coincide with one of the symmetries associated with the scattering ellipse. This may be useful in simplifying the analysis of the data.

During the experiment, radar data will be recorded by the new LORAN receiver; and, at the same time, ocean waves will be recorded by the pitch-and-roll buoy. Computer programs for the analysis of the LORAN data have been written, and a preliminary analysis of the data should be completed a few weeks after the data is recorded.

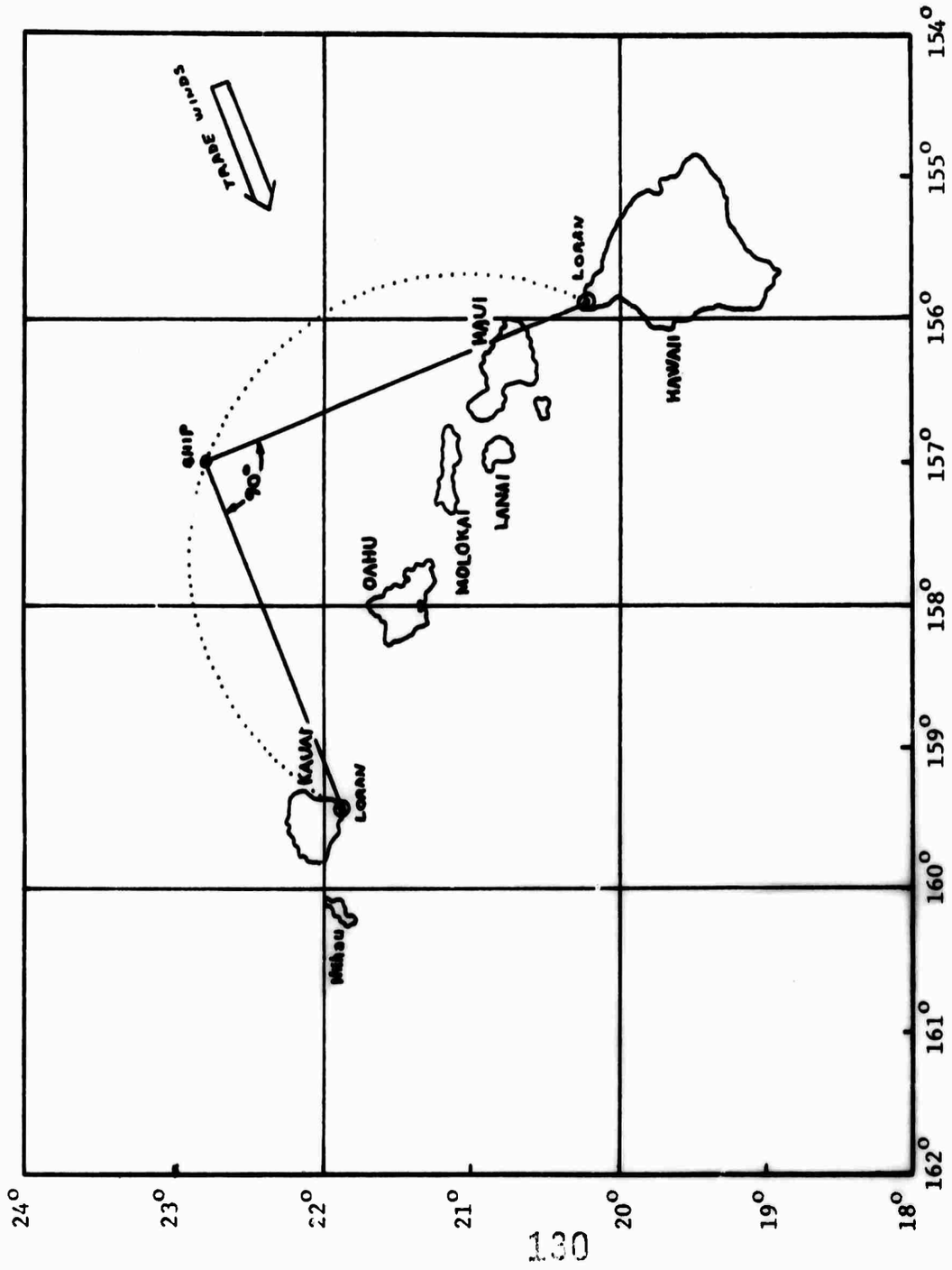

130

Figure 1. Geometry for bistatic experiment using LORAN in a trade-winds region.

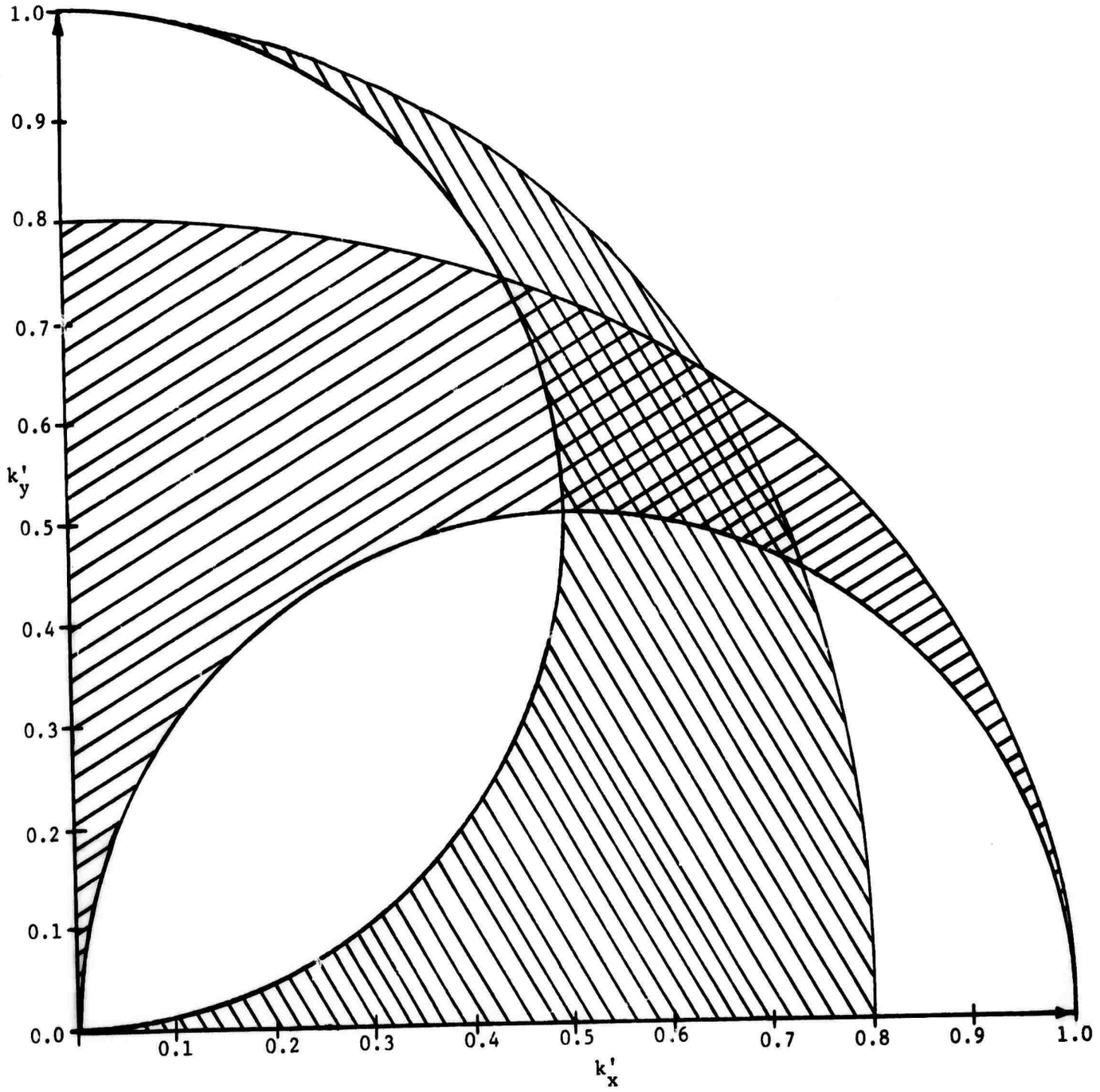

Figure 2. Ocean wave number coverage for bistatic experiment. Shaded areas show those wave vectors (k'_x, k'_y) which scatter radio waves from the transmitters to the receiver, assuming two perpendicular baselines and no scattering from ranges greater than 1.67 baseline units.

IV References

1. Hasselmann, K. 1971 Determination of Ocean Wave Spectra from doppler radio return from the sea surface. Nature Physical Sciences, 229, p. 16-17.

HIGHER ORDER SCATTERING OF RADIO WAVES FROM THE SEA

Robert H. Stewart, Scripps Institution of Oceanography,
University of California, San Diego

The subject of radio scatter from the sea has been studied for several reasons. Scattered radio waves are primarily responsible for the attenuation of radio waves propagating near the sea surface; and, in addition, measurements of the scattered radio field can be used to measure the statistics of ocean waves.

A number of workers, including Barrick, Wait, and Bass have contributed to the theory of radio scattering from the sea, and the reader is refered to Barrick[1,2] for an introduction to the subject. Because of the mathematical difficulty involved in satisfying the boundary conditions at the sea surface, neither the radio nor the ocean wave field has been calculated exactly, and most work has been concerned with the lowest order interaction between the two fields. Recently Hasselmann[3] has considered some aspects of the next higher interaction. In this paper we wish to examine in some detail the processes involved in this interaction.

If the radio and ocean wave fields are expanded in series of plane waves of the form $\exp[i(\underline{k}_j \cdot \underline{x} - \omega_j t)]$, where $\underline{k}$ is the horizontal wave number and ω the frequency, then the field produced by the interaction of these two fields will also be of this form, say $\exp[i(\underline{k}_s \cdot \underline{x} - \omega_s t)]$; and $\underline{k}_s = \Sigma s_j \underline{k}_j$, $\omega_s = \Sigma s_j \omega_j$, where s=+ or -. The lowest order interaction is between an incident radio wave i scattering from an ocean wave o, producing a backscattered wave s. So $\underline{k}_s = \underline{k}_i \pm \underline{k}_o$, and the backscattered wave will have a doppler frequency $\omega_d = \omega_s - \omega_i = \pm\omega_o$. Furthermore, backscatter requires $\underline{k}_s = -\underline{k}_i$, so $\underline{k}_o = \pm 2\underline{k}_i$.

At the next order, an incident radio wave i interacts with two ocean waves 1 and 2 to produce a backscattered radio wave s; and: $\underline{k}_s = \underline{k}_i \pm \underline{k}_1 \pm \underline{k}_2$, $\omega_d = \pm\omega_1 \pm \omega_2$. In this case, the wave number vectors must form a closed polygon as shown in figure 1, and the doppler

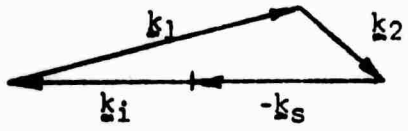

Figure 1. Schematic wavenumber polygon.

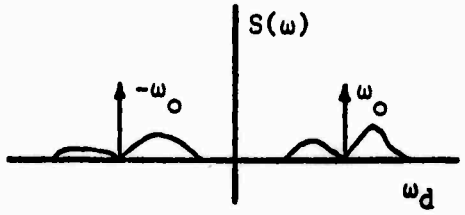

Figure 2. Schematic doppler spectrum.

spectrum is composed of four sidebands adjacent to the two primary lines as shown in figure 2.

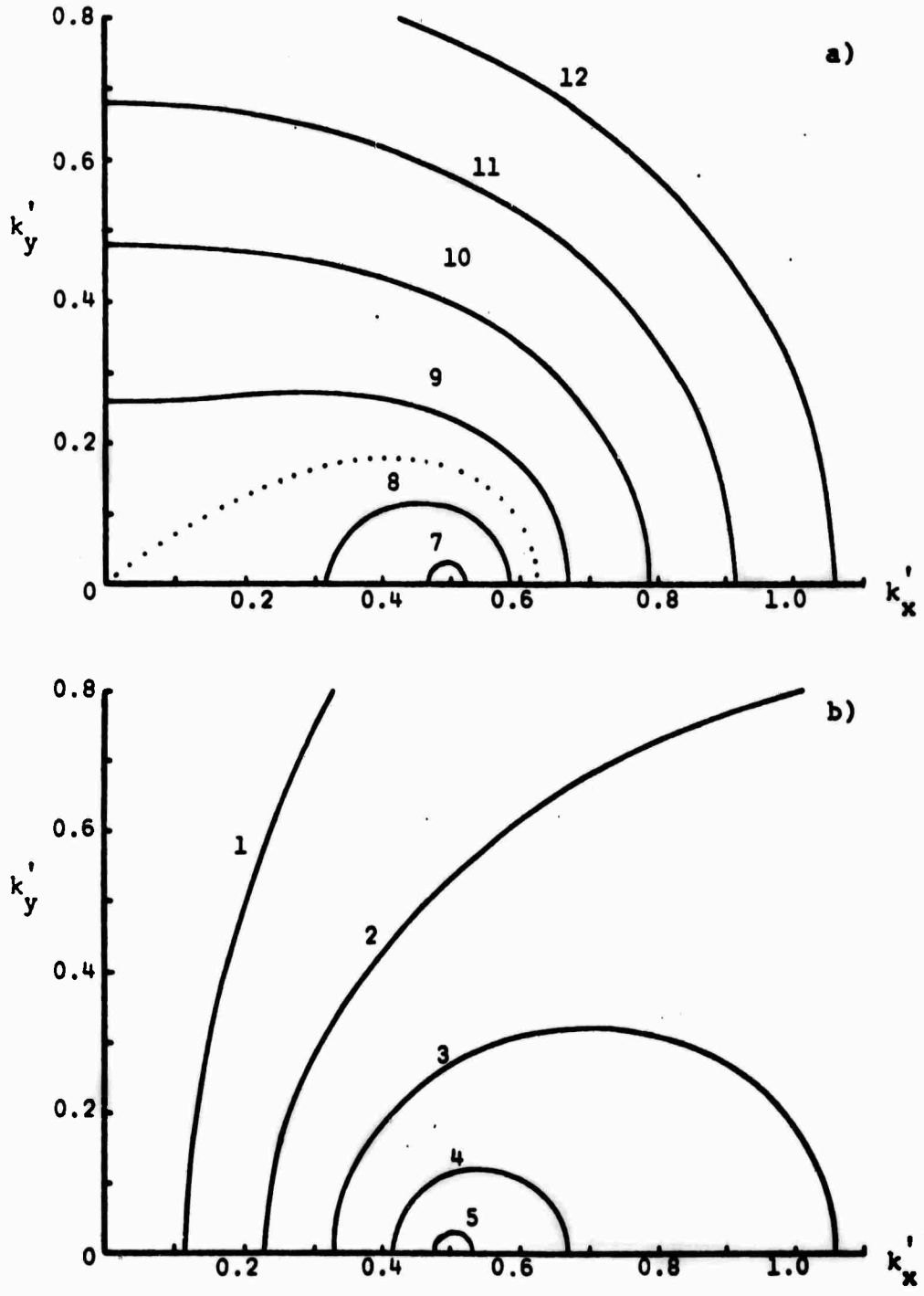

Figure 3. Curves of constant ω' in $\underline{k}$ space. a) $\sqrt{k'_1}+\sqrt{k'_2}=\omega'$; b) $\sqrt{k'_1}-\sqrt{k'_2}=\omega'$; both for $\omega'=n/6$. Values of n are next to the curves.

The introduction of the dispersion relation for ocean waves, $\omega=\sqrt{gk}$ constrains the interaction. All interacting ocean waves producing the same ω_d must lie on the locus $\pm\sqrt{k_1} \pm\sqrt{k_2} = \omega_d$, where $k=|\underline{k}|$. Furthermore, all waves between the curves defined by ω_d and $\omega_d+\delta\omega_d$ contribute to the same doppler band. A number of these curves are shown in figure 3 for equal increments in ω_d given by $\omega'=\omega_d/\omega_o=n/6$

The value of n is given next to each curve; the wavenumbers are scaled by $k'=k/k_o=k/2k_i$, and the curves are symmetric about both axes. Note:1) near $\omega' = \sqrt{2}$ a small change in ω' produces a large proportionate change in $\underline{k}$ space, so many waves can contribute to the doppler band about this frequency; and 2) for $k_1 >> k_2$ the curves are circles centered at (±1/2, 0).

The higher order interactions between conservative fields having a dispersion relation can be written as the sum over all possible cascades of first order interactions[4]. The possible cascades producing figure 2 are shown in figure 4. Here the first order interactions occur at the nodes, and intermediate waves are denoted by $\underline{K}$.

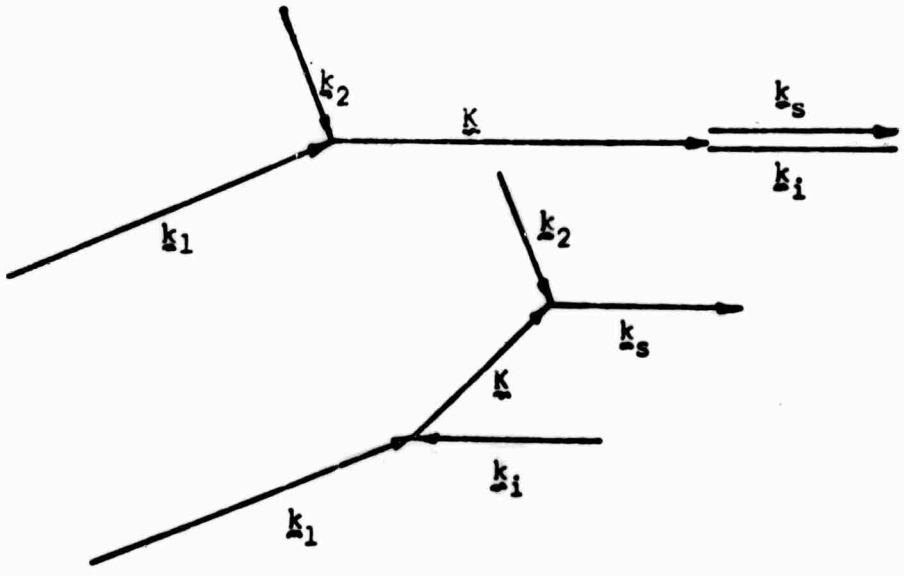

Figure 4. The only two possible cascades of first order interactions producing the interaction shown in figure 2.

In 4a), $\underline{K}$ must be a virtual ocean wave (one which does not obey a dispersion relation). In 4b), $\underline{K}$ can be a real or a virtual radio wave. Of these three processes,4a) is probably the most important.

The total integrated strength of each sideband resulting from this interaction can be estimated easily if: 1) $k_1 >> k_2$, 2) the two dimensional ocean wave spectrum is peaked near k_1, 3) the ocean wave directional spectrum varies as the cosine squared abou' the direction of $\underline{k}_i$ or $\underline{k}_s$, and 4) i is a surface wave. With the first assumption, the virtual ocean wave's spectrum has the form $[F(\underline{k}_1)d\underline{k}_1\ F(\underline{k}_2)d\underline{k}_2\ k_1^2\cos^2\theta]/2\ \delta(\underline{k}\pm\underline{k}_1\pm\underline{k}_2)\ \delta(\omega\pm\omega_1\pm\omega_2)$ + similar terms at $\delta(\omega)$, $\delta(\omega\pm2\omega_1)$, and $\delta(\omega\pm2\omega_2)$. Here θ is the angle between $\underline{k}_1$ and $\underline{k}_2$, and $F(\underline{k})d\underline{k}$ is the two dimensional ocean wave spectrum. With the additional three assumptions the ratio of the power of the integrated second order sideband, E_2, to the power of the first order line, E_1 is $E_2/E_1 = 3\ k_1^2 A/\theta$, where A is the mean square ocean surface elevation. If $k_1 = \pi/m$, $E_2/E_1 = 1$ when the mean wind is 10m/s, assuming the sea can be described by a Pierson-Moskowitz[5] wave spectrum. Under these rather genera.

conditions the second order sidebands can be quite strong. But the simple relationship between the doppler sidebands and the one dimensional ocean wave spectrum proposed by Hasselmann[3] is somewhat modified by the cosine squared weighting function in the second order ocean wave interaction. This will not be important if the ocean waves are primarily in the radio wave direction, but will be important if they are perpendicular.

1. D.E. Barrick (1971 Radio Science 6, p. 517).
2. D.E. Barrick (1971 submitted to IEEE Trans. Ant. Prop.).
3. K. Hasselmann (1971 Nature Phy. Sci. 229, p. 16).
4. K. Hasselmann (1966 Rev. Geophys. 4, p. 1).
5. W.J.Pierson and L.Moskowitz (1964 J. Geophys. Res. 69, p. 5181)